

การเปลี่ยนแปลงระดับน้ำทะเลในอดีตของพื้นที่แหลมโพธิ์ อำเภอยายา จังหวัดสุราษฎร์ธานี



นางสาวสินีนภา พลวิชัย

บทคัดย่อและแฟ้มข้อมูลฉบับเต็มของวิทยานิพนธ์ตั้งแต่ปีการศึกษา 2554 ที่ให้บริการในคลังปัญญาจุฬาฯ (CUIR)
เป็นแฟ้มข้อมูลของนิสิตเจ้าของวิทยานิพนธ์ ที่ส่งผ่านทางบัณฑิตวิทยาลัย

The abstract and full text of theses from the academic year 2011 in Chulalongkorn University Intellectual Repository (CUIR)
are the thesis authors' files submitted through the University Graduate School.

วิทยานิพนธ์นี้เป็นส่วนหนึ่งของการศึกษาตามหลักสูตรปริญญาวิทยาศาสตรมหาบัณฑิต
สาขาวิชาวิทยาศาสตร์สิ่งแวดล้อม (สหสาขาวิชา)
บัณฑิตวิทยาลัย จุฬาลงกรณ์มหาวิทยาลัย
ปีการศึกษา 2560
ลิขสิทธิ์ของจุฬาลงกรณ์มหาวิทยาลัย

PALEO SEA-LEVEL CHANGE OF LAEM PHO, AMPHOE CHAIYA, CHANGWAT SURAT THANI



A Thesis Submitted in Partial Fulfillment of the Requirements
for the Degree of Master of Science Program in Environmental Science

(Interdisciplinary Program)

Graduate School

Chulalongkorn University

Academic Year 2017

Copyright of Chulalongkorn University

Thesis Title PALEO SEA- LEVEL CHANGE OF LAEM PHO,
AMPHOE CHAIYA, CHANGWAT SURAT THANI
By Miss Sinenard Polwichai
Field of Study Environmental Science
Thesis Advisor Professor Montri Choowong, Ph.D.
Thesis Co-Advisor Sumet Phantuwongraj, Ph.D.

Accepted by the Graduate School, Chulalongkorn University in Partial
Fulfillment of the Requirements for the Master's Degree

.....Dean of the Graduate School
(Associate Professor Thumnoon Nhujak, Ph.D.)

THESIS COMMITTEE

.....Chairman
(Associate Professor Srilert Chotpantarat, Ph.D.)

.....Thesis Advisor
(Professor Montri Choowong, Ph.D.)

.....Thesis Co-Advisor
(Sumet Phantuwongraj, Ph.D.)

.....Examiner
(Assistant Professor Penjai Sompongchaiyakul, Ph.D.)

.....External Examiner
(Assistant Professor Krit Won-in, Ph.D.)

สิรินาฏ พลวิชัย : การเปลี่ยนแปลงระดับน้ำทะเลในอดีตของพื้นที่แหลมโพธิ์ อำเภอยะยา จังหวัดสุราษฎร์ธานี (PALEO SEA-LEVEL CHANGE OF LAEM PHO, AMPHOE CHAIYA, CHANGWAT SURAT THANI) อ.ที่ปริกษาวิทยานิพนธ์หลัก: ศ. ดร. มนตรี ชูวงศ์, อ.ที่ปริกษาวิทยานิพนธ์ร่วม: อ. ดร. สุเมธ พันธุ์วงศ์ราช, 172 หน้า.

การศึกษาการเปลี่ยนแปลงระดับน้ำทะเลในอดีตของพื้นที่แหลมโพธิ์มีวัตถุประสงค์เพื่อสำรวจธรณีสัณฐานวิทยาชายฝั่ง ตะกอนวิทยา ของพื้นที่ที่พบหลักฐานการเปลี่ยนแปลงระดับน้ำทะเล และเพื่อวิเคราะห์ประวัติการเปลี่ยนแปลงของระดับน้ำทะเลสมัยโฮโลซีน โดยวิธีการศึกษาเริ่มจากการแปลความหมายภาพถ่ายทางดาวเทียมเพื่อวางแผนเก็บข้อมูลภาคสนามสำรวจลักษณะทางธรณีสัณฐาน และจัดทำแผนที่ธรณีสัณฐานชายฝั่งเพื่อกำหนดจุดเก็บตัวอย่างตะกอนมาศึกษาขนาดและหาอายุโดยวิธีกระตุ้นด้วยแสง

ผลการศึกษา พบว่า พื้นที่ศึกษามีลักษณะที่โดดเด่นของแนวสันทราย และจะงอยที่งอกยาวจากแผ่นดินออกไปในทะเลในทิศตะวันออกเฉียงใต้ ซึ่งสัมพันธ์กับอิทธิพลของกระแสน้ำที่ไหลไปทางทิศตะวันออกเฉียงใต้ โดยแหล่งที่มาของตะกอนนั้นเป็นไปได้ว่ามาจากคลองพุมเรียง ที่ตั้งอยู่ระหว่างหาดทรายเดิมและหาดทรายปัจจุบันของแหลมโพธิ์ นอกจากนี้ ลักษณะการวางตัวของแนวสันทรายในพื้นที่ศึกษานี้ยังแสดงลักษณะเฉพาะตัวที่สามารถแบ่งออกได้เป็น 5 ชุด ซึ่งชุดด้านในสุดของพื้นที่แสดงให้เห็นถึงลักษณะของแนวชายฝั่งโบราณ ซึ่งครอบคลุมพื้นที่ประมาณ 4.5 กิโลเมตรจากชายฝั่งปัจจุบัน จากผลการศึกษาลักษณะทางภูมิประเทศจำนวน 3 แนว แสดงให้เห็นว่าแนวสันทรายมีการสะสมตัวต่อเนื่องออกไปทางทิศตะวันออกเฉียงใต้ ทั้งนี้ หลักฐานทางธรณีสัณฐานชายฝั่งที่แสดงให้เห็นถึงหลักฐานของการเปลี่ยนแปลงระดับน้ำทะเลสามารถแบ่งออกเป็น 3 หน่วย ได้แก่ หาดทรายเก่า ชายหาดปัจจุบัน และ ลากูนเก่า ขนาดตะกอนบริเวณสันทรายโดยเฉลี่ยมีขนาดทรายหยาบถึงทรายปานกลาง ซากดึกดำบรรพ์ทั้งขนาดใหญ่และขนาดเล็ก ได้แก่ หอยสองฝา หอยงาข้าง ฟอแรมมินิเฟอรา และออสตราคอด ในส่วนอายุของตะกอนในพื้นที่ศึกษา ทำให้ทราบว่าบริเวณพื้นที่นี้มีการสะสมตัวของตะกอนอย่างต่อเนื่องเป็นที่ราบแนวสันทรายวางตัวเกือบขนานชายฝั่งโดยมีอายุเก่าสุดคือ $7,170 \pm 460$ ปีมาแล้ว และอายุน้อยที่สุดคือ 110 ปีมาแล้ว จึงทำให้ทราบถึงวิวัฒนาการของชายฝั่งบริเวณอำเภอยะยาว่าเกิดในขณะที่มีการลดระดับของน้ำทะเลในช่วงตอนกลางถึงตอนปลายสมัยโฮโลซีน

สาขาวิชา วิทยาศาสตร์สิ่งแวดล้อม

ลายมือชื่อนิสิต

ปีการศึกษา 2560

ลายมือชื่อ อ.ที่ปรึกษาหลัก

ลายมือชื่อ อ.ที่ปรึกษาร่วม

5787251620 : MAJOR ENVIRONMENTAL SCIENCE

KEYWORDS: SEA-LEVEL CHANGE / BEACH RIDGE / OSL DATING / HOLOCENE

SINENARD POLWICHAJ: PALEO SEA-LEVEL CHANGE OF LAEM PHO, AMPHOE CHAIYA, CHANGWAT SURAT THANI. ADVISOR: PROF. MONTRI CHOOWONG, Ph.D., CO-ADVISOR: SUMET PHANTUWONGRAJ, Ph.D., 172 pp.

The study of beach ridges plains at Laem Pho study area in Amphoe Chaiya, Changwat Surat Thani is aimed to investigate coastal geomorphology and sedimentology to analyze the history of Holocene sea level change. The methodology starts with satellite image interpretation of landform for field survey planning, then, geomorphologic map was done for locating sample collection sites. Grainsize analysis and Optically Stimulated Luminescence (OSL) dating were carried out.

As a result, the study area has dominant landforms of beach ridge plains and sand spit oriented in southeast direction correspondence with southeast longshore current. Source of sediment supply to this coastal plain is possibly come from Phumriang canal locating between former and recent beach ridge plain of Lam Pho. Furthermore, the orientations of beach ridges in this area have individual characteristic and can be classified into 5 series. The innermost beach ridge series can be indicator of paleo-shoreline locating approximately 4.5 km² far from the present shoreline. The three profiles of topography survey indicate the continuation of progradation in eastward direction. Three units of geomorphological landforms as evidences of sea level change consist of old sandy beach, young sandy beach, and old lagoon. Average grain sizes of sand from all beach ridges is coarse- to medium-grained sand. Fossils and microfossils found in beach deposit consist of bivalvia, scaphopoda, foraminiferas, and ostracods. OSL dating of the oldest sand ridge indicate the age of 7,170±460 years BP, whereas, the youngest beach forming sand spit at 110 years ago. All these results indicate that the study area including ridges and swales was formed as beach ridge plain with eastward progradation during the regression from the mid to late Holocene.

Field of Study: Environmental Science Student's Signature

Academic Year: 2017 Advisor's Signature

Co-Advisor's Signature

ACKNOWLEDGEMENTS

This research is supported by the 90th Anniversary of Chulalongkorn University Fund (Ratchadapiseksomphot Endowment Fund) and the Thailand Research Fund (MRG5780008). Your financial support in this research is greatly appreciated. For the initial important persons, I would like to express my very profound gratitude to my research advisor, Professor Montri Choowong and my research co- advisor, Dr. Sumet Phantuwoongraj for their expert guidance and encouragement throughout this long way research. I am blessed for having you as a part of my student's life. Your kindness and cordiality always fulfill my difficult time. Thank you for giving me a chance to use my knowledge to achieve the most effective goal as being a student of Chulalongkorn University.

In addition, I would like to express my thanks to Department of Geology, Faculty of Science, Chulalongkorn University, Bangkok for field equipment and Optically Stimulated Luminescence laboratory and also Assist.Prof. Krit Won-in from Earth science Program, Faculty of Science, Kasetsart University Bangkok, Thailand for providing a gamma ray spectrometer for annual dose calculation.

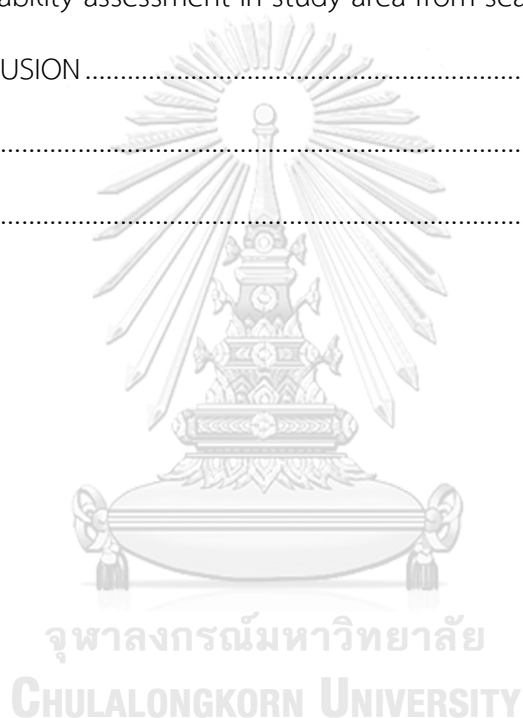
Finally, I would like to thank the members of my family for their mental support and my friends, especially Mr. Peerasit Surakiatchai, Mr. Stapana Kongsan, Mr. Supakorn Takamon, Mr. Theerachet Chaomeepem, Ms. Arunee Karaket, Ms. Chanakarn Ketthong, Ms. Araya Tantiteerakul, Ms. Wallaya Chantara, Ms. Sornsawan Utthakrue, and Ms. Patcharaporn Ngerkerd for their support on the field surveying, laboratory processing, and research writing. Besides, I would like to offer my special thanks to Dr. Assanee Meesook, the most influential person in my life, who although is no longer with us, for building up my mental strength. I would say, I could not have come this far without him. Hopefully, this research will be a part of his dedication and hard work on me along his life.

CONTENTS

	Page
THAI ABSTRACT	iv
ENGLISH ABSTRACT	v
ACKNOWLEDGEMENTS	vi
CONTENTS	vii
LIST OF FIGURES	x
LIST OF TABLES	xviii
CHAPTER 1 INTRODUCTION	21
1.1 Background	21
1.2 Objectives	22
1.3 Scope and output	22
1.4 Description of the study area	23
CHAPTER 2 LITERATURE REVIEWS	30
2.1 Sea-level Change	30
2.1.1 Nature of sea-level changes	30
2.1.2 Causes of sea-level change	35
2.1.3 Quaternary sea-levels	43
2.1.4 Sea-level curve	45
2.2 Coastal evolution	47
2.2.1 Nature of coastal evolution	49
2.3 Literature Reviews	52
CHAPTER 3 METHODOLOGY	58
3.1 Desk study	58

	Page
3.1.1 Satellite Image Interpretation.....	58
3.2 Field Works.....	63
3.2.1 Topographic survey.....	63
3.2.2 Sediment sampling.....	64
3.2.3 Stratigraphic column.....	65
3.3 Laboratory Works.....	69
3.3.1 Sedimentary analysis.....	69
3.3.2 Paleontological analysis.....	73
3.3.3 Age determination by optically stimulated luminescence (OSL).....	74
CHAPTER 4 RESULTS.....	84
4.1 Geomorphological description.....	84
4.2 Topographic survey.....	89
4.3 Lithostratigraphical analysis.....	91
4.3.1 Lithostratigraphical description from coring.....	91
4.4 Sedimentological analysis.....	109
4.4.1 Grain size analysis.....	109
4.5 Age determination by optically stimulated luminescence dating.....	125
4.6 Fossil and microfossil evidence.....	127
4.6.1 Systematic description.....	127
CHAPTER 5 DISCUSSIONS.....	138
5.1 Boundary of paleo-shoreline from satellite image interpretation.....	138
5.2 Stratigraphic correlation.....	139
5.4 Fossils evidence.....	144

	Page
5.5 Ages of sand deposit by optically stimulated luminescence dating.....	144
5.6 sea-level curves.....	146
5.7 Model of coastal geomorphological evolution.....	149
5.8 Sea-level change and vulnerability of the coastal zone	154
5.8.1 Mangrove as an indicator of sea-level changes	155
5.8.2 Vulnerability assessment in study area from sea-level changes	155
CHAPTER 6 CONCLUSION	158
REFERENCES	161
VITA.....	172



LIST OF FIGURES

Figure 2.1 Surface comparison consist of the reference ellipsoid surface (a map of average sea level), the reference geoid surface (a true sea level surface), and the real surface of the Earth (the ground) is the topographic surface.....	31
Figure 2.2 The characteristic of emergent coastlines (relative sea level is falling) and submergent coastlines (relative sea level is rising). A) Emergent coastline B) Submergent coastline.....	34
Figure 2.3 The albedo model, the snow and ice reflects most of the solar radiation back into space, but if there is less ice cover, the ocean and the land warm up causing more ice to melt.....	36
Figure 2.4 The rising of magma at mid-ocean ridges and the latest seafloor moved away from the ridge axis, then the ocean basin is widening and seafloor spreading.....	37
Figure 2.5 Sea level change due to isostatic uplift during glacial and interglacial period.....	38
Figure 2.6 The increasing of glacial ice on the Earth's surface results in the changing form of the crust and sinking. (a) When the ice melts, there is an occur of isostatic rebound and the crust rises to the latest position before glaciation, (b and c) A process of mountain building and mountain erosion.....	40
Figure 2.7 The position of sea surface comparative to a fixed datum close to the sea floor that can point to eustasy and the movement in vertical of the sea floor...	41
Figure 2.8 The hydro-isostasy between ocean and continental. A) The ocean siphoning, water flows from equator to collapsing forebulge areas at higher latitudes. B) The continental levering, water loading at the continental shelf depresses sea floor and then uplift shorelines.....	42
Figure 2.9 A relationship between mean sea level and the geoid.....	43

Figure 2.10 Picture of fossil reefs of the Huon Peninsula in Papua New Guinea which are currently cliff faces rising up to 25 meters above the beach.	44
Figure 2.11 Sea-level curves in Southeast Asia including Malacca Strait (Geyh et al., 1979), Peninsular Malaysia (Tjia, 1987), Singapor (Hesp et al., 1998), Gulf of Thailand (Sinsakul et al., 1985; Choowong et al., 2004; Horton et al., 2005; Nimnate et al., 2015).	47
Figure 2.12 This diagram shows a model of surface temperatures, areas of rising air, winds, and the thermocline (blue surface) in the tropical Pacific during El Niño, normal, and La Niña conditions.	48
Figure 2.13 Mass bleaching of coral in the Great Barrier Reef, Australia.	49
Figure 2.14 The coastal landforms of Durdle Door sea arch is a limestone arch on the Jurassic Coast in Dorset, England that was created by wave.	50
Figure 2.15 The coastal landforms of Beach-dune systems that was created by wind and wave.	51
Figure 2.16 The coastal landforms of the Great barrier reef in Australia that was created by living coral.	51
Figure 3.1 These satellite images mapping were printed out for field work investigation and sediment sampling points identification in field.	58
Figure 3.2 Satellite images showing the study area at Laem Pho, Amphoe Chaiya, Changwat Surat Thani. Satellite image from Google Earth; acquisition period: July 2016.	59
Figure 3.3 Satellite images showing the central part of the study area which exhibited the obviously landform of beach ridges and swales at Laem Pho, Amphoe Chaiya, Changwat Surat Thani. Satellite image from Google Earth; acquisition period: July 2016.	60
Figure 3.4 Satellite images showing the western part of the study area that located in landward direction which around with human settlements at Laem	

Pho, Amphoe Chaiya, Changwat Surat Thani. Satellite image from Google Earth; acquisition period: July 2016..... 61

Figure 3.5 Satellite images showing the topography characteristic of sand spit with beach ridges and swales inside at the southern part of the study area. Satellite image from Google Earth; acquisition period: July 2016..... 62

Figure 3.6 The topographic profile was measured by Total Station SOKKIA SET 630R along transect lines. These pictures consist of a), b), c) The measurement of pole, total station, and tripod respectively before start the topographic survey for calculation with elevation further, d) and e). The topographic profile measurement was done by Instrument man, staff man (rod man), and recorder..... 63

Figure 3.7 The steps of sediment sampling for OSL dating in laboratory which consist of a) Digging an excavation pit at 50x50x50 cubic centimeters, b) Putting pvc tube with end cap at depth 40 centimeters from surface, c) Pvc tube with end cap was put into sediments layer at depth 40 centimeters from surface for sampling sediments for equivalent dose evaluation, and d) Sediments were sampling at depth 40 cm in plastic bag for annual dose calculation..... 65

Figure 3.8 The steps of stratigraphic column for analyzing sediment deposition and paleo-environment which consist of a) Digging an excavation pit at 50x50x50 cubic centimeters, b) Sampling sediments with hand auger, c) After sampling sediments with hand auger, put sediments in the on the plastic sheet for logging description, and d) Description of sediments which include of depth, color, composition, and other evidences. 66

Figure 3.9 In case of sediment samples are clay or very fine to fine grain, and well compaction feature, the sampling will be done by using different tools following these steps; a) Sampling sediments with Gouge auger, b) After sampling sediments with Gouge auger, put Gouge auger on the plastic sheet for logging description, c) Sediments were sampling into plastic bag for study grain size analysis and sediment compositions under a microscope in laboratory. 66

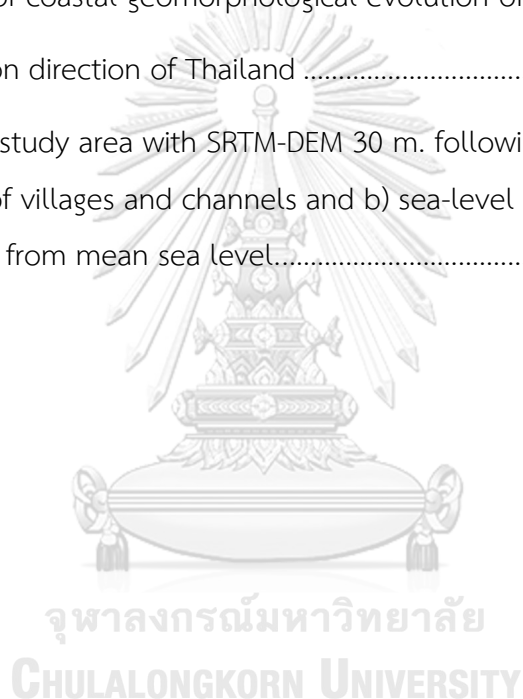
Figure 3.10 Soil texture triangle-classification system based on grain size (United States Department of Agriculture (USDA), 1987).....	68
Figure 3.11 Grain-size analysis by sieving method following a) Drying sediment samples in the oven at temperature 70°C about 6-8 hours, b) Taking sieve stacks to mechanical shaker and shakes for 10 minutes, and c) Tapping sediments out of each sieve stacks for weight calculation.	70
Figure 3.12 Sediment compositions analysis in laboratory room. a) Using a binocular microscope for classifying sediment compositions. b) Sediments sample under the microscope.	71
Figure 3.13 This chart showing the grain-size classification detail which consist of phi sizes, millimeter diameters, size classifications, and American Society for Testing and Materials and Tyler sieve sizes.	71
Figure 3.14 Comparison charts for visual estimation of roundness and sphericity of sediments (modified after Hryciw et al., 2016).....	72
Figure 3.15 Comparison charts for visual estimation of coarse fragments (modified after Terry and Chilingar, 1955).....	72
Figure 3.16 The study of fossil identification under microscope following a), b) Taking sediments which abundant of fossil to sort sediment out and bring only fossil to study, and c) The picture of fossil was prepared for species identification under microscope.....	73
Figure 3.17 The study of fossil identification by scanning electron microscope (SEM) following a) Microfossils that were sort out under microscope for study by scanning electron microscope (SEM) were arrayed on the stub before put into the scanning electron microscope (SEM), b) Putting the stub that cover with microfossils into scanning electron microscope (SEM), and c) The picture of microfossil by scanning electron microscope (SEM) was prepared for species identification.	74

Figure 3.18 The flow chart of methodology for age determination. (Modified after Pailoplee, 2004)	77
Figure 3.19 The steps for annual dose calculation by gamma ray spectrometer following a) Gamma ray spectrometer, b) Sediment samples in plastic boxes are prepared for putting in gamma ray spectrometer, and c) Putting the box into gamma ray spectrometer and start calculation.....	79
Figure 3.20 The steps for water content analysis following a) and b) Weighting wet and dry sediments (after baked in the oven) in beakers for water content calculation, and c) The table shows weight percent of sediments from water content calculation.....	79
Figure 3.21 The steps for preparing sediment samples for annual dose calculation following a) Sediment samples in plastic bags from fieldwork, b) Drying all of sediment samples in the oven, and c) After sediments were dried, then sieving sediments with sieve shaker and containing sediment over 20 mesh in plastic box.	81
Figure 3.22 The steps for equivalent dose evaluation following a) Sieving sediments with mesh no.20 in red light in laboratory, b) Dilute HCl and HF for etching plagioclase minerals, organic matter, carbonate and clay particles.	81
Figure 3.23 The steps for equivalent dose evaluation following a) An isodynamic separator and b) Putting sediment samples into an isodynamic separator for separating heavy minerals and magnetic minerals.	82
Figure 3.24 The steps for equivalent dose evaluation following a) Cleaning sample trays, b) Putting sediment samples in each of trays and then put trays onto the circle carousel, c) A Risø TL/OSL reader are ready for putting the circle carousel on, and d) Closing and start running a Risø TL/OSL reader for equivalent dose evaluation.	82
Figure 3.25 A Risø TL/OSL reader for equivalent dose evaluation.	83

Figure 3.26 This drawing picture shows the mechanism inside a Risø TL/OSL reader that redrawn from Risø National Laboratory. (Modified after Preusser et al., 2008).....	83
Figure 4.1 The coastal geomorphic map of Amphoe Chaiya where Laem Pho study area is located (red star).....	84
Figure 4.2 Geomorphological of study area from satellite image and the different color star are boundary of study locations.....	85
Figure 4.3 Old sandy beach in the study area.	86
Figure 4.4 Young sandy beach in the study area.....	87
Figure 4.5 Old lagoon in the study area.....	89
Figure 4.6 This linear graph showing topographic profile from topographic survey measuring of line 1.....	90
Figure 4.7 This linear graph showing topographic profile from topographic survey measuring of line 2.....	90
Figure 4.8 This linear graph showing topographic profile from topographic survey measuring of line 3.....	90
Figure 4.9 Lithostratigraphic locations from coring in each of geomorphological units on satellite image.....	91
Figure 4.10 The stratigraphic correlation from station LP 3-1-1 to 3-1-4.....	107
Figure 4.11 The stratigraphic correlation from station LP 3-2-1 to 3-2-3.....	108
Figure 4.12 The stratigraphic correlation from station LP 3-3-1 to 3-3-8.....	108
Figure 4.13 Locations of sediment sampling for studying grain size analysis in sediment from series A to E of beach ridge series.	111
Figure 4.15 Bar graph of composition of sediment sampling from series A to E of beach ridge series. This bar graph shows the major composition of sediment sample from all of series is quartz.	123

Figure 4.16 Bar graph of composition of sediment sampling from series A to E of beach ridge series. This bar graph shows the minor composition of sediment sample from all of series are feldspar and organic matter. Bioclasts are dominant only in series C and D.....	124
Figure 4.17 Age results from OSL dating in each of sampling locations with different star colors for different beach ridge series.....	126
Figure 4.18 Foraminifera: (1 - 3) <i>Ammonia pauciloculata</i> (Phleger and Parker, 1951); (4,5) <i>Ammonia ketienziensis</i> (Ishizaki, 1943); (6 - 9) <i>Ammonia beccarii</i> (Linné, 1758).....	133
Figure 4.19 Foraminifera: (1 - 6) <i>Elphidium hispidulum</i> (Cushman, 1936b); (7) <i>Elphidium macellum</i> (Fichtel and Moll, 1798); (8 - 12) <i>Elphidium advenum</i> - lateral (Haynes, 1973).	134
Figure 4.20 Foraminifera: (1 - 6) <i>Elphidium limpidum</i> (Ho, Hu et Wang, 1965); (7) <i>Miliolina</i> (<i>Quinqueloculina</i>) <i>bogdanowiczi</i> (Serova, 1955) and (8) <i>Nodosaria intermittens</i> (Roemer, 1838).	135
Figure 4.21 Foraminifera: (1 - 9) <i>Asterorotalia pullchella</i> (d'Orbigny, 1839) (Synonym: <i>Asterorotalia trispinosa</i> (Thalman, 1933)).....	136
Figure 4.22 Mollusk: (1) <i>Carditella pallida</i> (E. A. Smith, 1881) and.....	136
Figure 4.23 Ostracod: (1) <i>Cyprideis ruggierii</i> . (Decima, 1964); (2) <i>Keijella reticulata</i> (Whatley & Zhao (Yi-Chun), 1988); (3) <i>Keijella</i> sp. (Sars, 1866); (4) <i>Callistocythere canaliculata</i> (Reuss, 1850); and (5) <i>Palmoconcha guttata</i> (Norman, 1865).	137
Figure 5.1 Geomorphology of study area from satellite image and the red dash line shows paleo-shoreline boundary.....	139
Figure 5.2 Frequency of typhoons recorded at Cha-am and Kui Buri (modified after Williams et al. 2016). Red square indicate age of beach ridge from Laem Pho.)	146
Figure 5.3 The summary of sea-level curves in Southeast Asia including Malacca Strait (Geyh et al., 1979), Peninsular Malaysia (Tjia, 1987), Singapor (Hesp et al.,	

1998), Gulf of Thailand (Sinsakul et al., 1985; Choowong et al., 2004; Horton et al., 2005; Nimnate et al., 2015).	148
Figure 5.4 Sea-level envelop at Laem Pho study area from the data only in series B, C, and D (series A is lack of topographic profile data and series E is recent beach).	149
Figure 5.5 Geomorphological of study area from satellite image with the dash lines of beach ridges orientations in each of series.	153
Figure 5.6 Model of coastal geomorphological evolution of Laem Pho study area.	153
Figure 5.7 Monsoon direction of Thailand	154
Figure 5.8 Map of study area with SRTM-DEM 30 m. following: a) study area showing location of villages and channels and b) sea-level rises showing flood area at 1-4 meters from mean sea level.....	157



LIST OF TABLES

Table 3.1 USDA soil-separates classifications (Soil Survey Division Staff, 1993).....	69
Table 4.1 The lithological log of beach ridge at station LP 3-1-1.....	92
Table 4.2 The lithological log of beach ridge at station LP 3-1-2.....	93
Table 4.3 The lithological log of beach ridge at station LP 3-1-3.....	94
Table 4.4 The lithological log of beach ridge at station LP 3-1-4.....	95
Table 4.5 The lithological log of beach ridge at station LP 3-2-1.....	96
Table 4.6 The lithological log of beach ridge at station LP 3-2-2.....	97
Table 4.7 The lithological log of beach ridge at station LP 3-2-3.....	98
Table 4.8 The lithological log of beach ridge at station LP 3-3-1.....	99
Table 4.9 The lithological log of beach ridge at station LP 3-3-2.....	100
Table 4.10 The lithological log of beach ridge at station LP 3-3-3.....	101
Table 4.11 The lithological log of beach ridge at station LP 3-3-4.....	102
Table 4.12 The lithological log of beach ridge at station LP 3-3-5.....	103
Table 4.13 The lithological log of beach ridge at station LP 3-3-6.....	104
Table 4.14 The lithological log of beach ridge at station LP 3-3-7.....	105
Table 4.15 The lithological log of beach ridge at station LP 3-3-8.....	106
Table 4.16 Result of grain size analysis of sediment sampling from series A of beach ridge series.....	111
Table 4.17 Result of grain size analysis of sediment sampling from series B of beach ridge series.....	112
Table 4.18 Result of grain size analysis of sediment sampling from series C of beach ridge series.....	112

Table 4.19 Result of grain size analysis of sediment sampling from series D of beach ridge series	112
Table 4.20 Result of grain size analysis of sediment sampling from series E of beach ridge series	113
Table 4.21 Summary of grain size parameters from series A to E of beach ridge series	117
Table 4.22 Summary of result of grain size analysis of sediment sampling from series E of beach ridge series	118
Table 4.23 Bar chart of grain size analysis from series A to E of beach ridge series. This bar graph shows the average mean grain size values of sediment sample from series A to E.	119
Table 4.24 Bar chart of grain size analysis from series A to E of beach ridge series. This bar graph shows the average standard deviation (sorting) values of sediment sample from series A to E.....	119
Table 4.25 Bar chart of grain size analysis from series A to E of beach ridge series. This bar graph shows the average kurtosis values of sediment sample from series A to E.....	120
Table 4.26 Bar chart of grain size analysis from series A to E of beach ridge series. This bar graph shows the average skewness values of sediment sample from series A to E.	120
Table 4.27 Result of composition of sediment sampling from series A of beach ridge series.	122
Table 4.28 Result of composition of sediment sampling from series B of beach ridge series.	122
Table 4.29 Result of composition of sediment sampling from series C of beach ridge series.	122

Table 4.30 Result of composition of sediment sampling from series D of beach ridge series.	123
Table 4.31 Result of composition of sediment sampling from series E of beach ridge series.	123
Table 4.32 Results of sampling at series A of beach ridge series from OSL dating... 125	
Table 4.33 Results of sampling at series B of beach ridge series from OSL dating... 125	
Table 4.34 Results of sampling at series C of beach ridge series from OSL dating... 125	
Table 4.35 Results of sampling at series D of beach ridge series from OSL dating... 126	



CHAPTER 1

INTRODUCTION

1.1 Background

Climate change becomes a main cause of many environmental problems. Geologically, climate change has been occurred for a long time throughout geological time span. Over the last 50 years, human activities release tons of carbon dioxide (CO₂) into the atmosphere causing the increase of global temperature. The global temperature has changed and affected in living, environment, and social and economy around the world. According to the warming of the climate system that circulated global temperature, there is significant evidence such as an increase of ocean temperatures that melting the ice sheet and release water to the ocean then the global sea-levels are rising. Paleo-sea-level change has been recognized since late Pleistocene to middle Holocene worldwide. Sea-level change has caused significantly inland flooding and left behind many landform evidences. In general, this change has close relationship with global climate change that made up from the physical factors such as wind, wave, tide and longshore current. The sea-level change can be observed by geomorphological evidence left behind around the coastal zone. Sediment deposition by coastal process is the important key to solve the history of paleo-sea-level change because the sediment, itself, can be recorded by different process of deposition during marine transgression and regression. Early researches in Thailand regarding sea-level change hypothesized that sea-level rising in the Gulf of Thailand (GoT) is caused by the global warming and also the change in direction of ocean circulation, the reduction of sediment supplies to coastal system. Most previous research has paid attention to explain the evolution of the coast based mostly upon sedimentological evidences recorded in coastal landforms and relationship among those coastal landforms.

This thesis area is located in Changwat Surat Thani where such coastal landforms as swamp, lagoon, beach ridge plain and sand spit were dominated. Tidal channel with mangrove forest and bird-foot tidal delta of Tapi River are also found. These coastal landforms are of local sea-level change evidence. All those landforms and their deposition can be generally recognized as far as 13 kilometers inland. Additional physical evidences of sea-level change are also expected to be found from this area in order to help understanding the history of coastal evolution.

1.2 Objectives

1. To investigate coastal geomorphology, sedimentology from the area where the evidence of sea-level changes was found at Laem Pho, Amphoe Chaiya, Changwat Surat Thani.
2. To analyze the history of Holocene sea-level change.
3. To evaluate environmental change in the study area

1.3 Scope and output

1. Scope

The scope of this study is concerned with the analysis in the coastal geomorphology and coastal stratigraphy only where they can be inferred as evidences of the Holocene shoreline. All data will relate to coastal geomorphology and its change during the maximum transgression to the regression at present mean sea-level. The scope of study area is approximately 70 square kilometers.

2. Output

The output of this study is to anticipate how the sea-level change related to the evolution of coastal geomorphology in Laem Pho area, Amphoe Chaiya, Changwat Surat Thani.

1.4 Description of the study area

This part presents and describes overall environment setting of the study area in ascending order; general topography, geology, and climate.

1. General topography

Changwat Surat Thani is located in the southern part of Thailand (Figure 1.1). The area covers approximately 13,000 square kilometers which composed of both low basins and high plateaus with forested mountains. Surat Thani borders the Gulf of Thailand to the north and east, Chumphon to the north, Nakhon Si Thammarat and Krabi to the south, Phang-Nga and Ranong to the west and Nakhon Si Thammarat to the east. Changwat Surat Thani is the largest province of the South located 685 kilometers from Bangkok. The study area is confined to the northern portion of the Surat Thani Province, bounded by latitude $9^{\circ} 8' 23''$ N and longitude $99^{\circ} 19' 50''$ E. The UTM data is on WGS-84 base map Zone 47P. The study area is on latitude $9^{\circ} 23' 12''$ N and longitude $99^{\circ} 12' 0''$ E with base map zone 47P 521959 1037608.

The topography of study area can be divided into four parts, coastal plain, alluvial plain, upland area, and high mountain area. The high-mountain area is in the southwest part of study area, namely “Khao Luong” mountain and the southeast part, namely “Khao Sok” mountain. These mountains are about 1,200 m high. The upland area consists of undulating landform and isolated hills. The undulating area, which covers the largest part of study area, has an elevation between 20 and 100 meters above mean sea-level. It is mostly covered by rubber tree plantations. The coastal area is composed of delta and beach sand. It is broad and flat with elevations little higher than the sea-level, in some cases even lower and extend up to 5 kilometers from coastal to the inland area. Sand beaches are situated along the northern and eastern seaside. The river delta in the west of Surat Thani city is built up by the Tape River. The present-day main river mouth is located northeast of Surat Thani city. The

delta is formed in the shape of bird's foot. The elevation of this area is fairly low, between -1 to +5 meters (Tatong et al., 2001).

2. Regional Geology

Regional geological setting of Changwat Surat Thani consists of sedimentary, metamorphic, and igneous rocks which can be described as follows:

Sedimentary and metamorphic rocks;

1) Ordovician rocks are alternatively called the Thung Song Formation. It is found in a very small area close to the granite body in the north-west of Surat Thani and south-east of study area. Thus rocks were partly metamorphosed by granitic intrusion. The rocks are also strongly folded and faulted. These rocks are closely associated with and lie unconformably above the Pre-Cambrian high-grade metamorphic rocks in Shan-Thai Terrane. The Thung Song Formation is a thick sequence of tropical limestone dolomites and calcareous shale (Khawdee, 2008).

2) Silurian-Devonian-Carboniferous rocks are alternatively called of Huai Prick Formation. It is found in a small area nearby the granite body in the granitic intrusion. The formation is composed of sandstone, mudstone, slate, quartzite, schist, and phyllitic shale. Limestone lenses can be found in this formation. The rocks have thin to thick beds of light brown to greening grey color. Some tentaculites, crinoids, and gastropods fossils have been found which indicate an age ranging from Devonian to Permo-Carboniferous (Chaimanee, 2001).

3) Permian rocks are known as Ratburi Limestone or Ratburi Group. The Permian rocks occur as isolated hills in the southwestern and eastern part of the study area. The rocks are composed of limestone and dolomitic limestone. They are gray to dark gray in color and usually appear in thick to massive beds. In some areas, especially near faults, the limestone was transformed to dolomite. The rocks are intercalated with dark gray shale. Lenticular chert is found locally including fossils of;

Fusulinida; Schwagerina sp., Minojapanella sp.

Caralia; Waagenophyllum sp.

Smaller foraminifera; Pachyphloia sp. , Eotuberitina sp. , Tetratarsis sp., Agalhammina sp., Geinitijina sp., Nankinella sp.

Brachiopoda; Chonetacean

The fossils date from the middle to the upper Permian (Tatong et al, 2001).

4) Triassic rocks are named Saibon Formation. It has been recognized in the south of Amphoe Phunphin in a cluster of mountains. The rocks contain sandstone, siltstone, limestone lenses and conglomerate. The sandstone is maroon to brownish-red in color and medium to coarse grained. The rocks generally appear in thick to massive beds with cross bedding in some parts. The siltstone is yellowish-brown in color. It is thinly bedded and contains carbonaceous layers. The light gray limestone lenses have a thickness of around 3 to 5 meters. Bivalves and foraminifera have been found in this rock. The conglomerate contains pebbles of limestone in a matrix of red sand (Khawdee, 2008).

5) Jurassic rocks are named Lam Thap Formation (Trang Group). The rocks occur in a large area between Amphoe Chaiya and Amphoe Tha Chang as isolated hills in the southeastern part of the study area. They contain arkosic sandstone and siltstone. The sandstone is fine to coarse grained and thick-bedded showing small-scale trough cross-bedding. The rock is alternated by conglomerate and quartzitic sandstone and is light gray to light brown in color (Tatong et al., 2001).

6) Jurassic-Cretaceous rocks are named Phunphin Formation (Trang Group). The rocks comprise mainly arkosic sandstone. They were recognized in a small area near Amphoe Phunphin. The arkosic sandstone is red to purple in color, fine to medium grained containing mica. The rocks are poorly cemented and have beds

ranging from 0.5 to 2 meters' thickness. They are intercalated with shale, which is purple in color and thinly bedded. Cross-bedding, which was formed in troughs, has been observed in this rock unit (Tatong et al., 2001).

7) Tertiary rocks are known as Krabi Group has been identified in an undulating area in the western part of the study area. They are generally composed of semi-consolidated mudstone, siltstone, sandstone, marlstone, and fossiliferous and argillaceous limestone. Lignite and gypsum are often found. The lignite is usually interbedded with clay, in a so-called 'lignitic zone'. The lignitic zone varies greatly in thickness ranging from 6.2 to 43.3 meters. The lignite within the zone generally consists of multiple seams. Each seam has a thickness ranging from 0.15 to 4.20 meters. (Tatong et al., 2001)

8) Quaternary sediments, according to their depositional environment, can be divided principally into three environments, continental, deltaic, and coastal (Chaimanee, 2001):

a) The sediments of continental environment are comprised of colluvium (Qc), terrace (Qt), fluvial sediment (Qf), alluvial floodplain (Qa), and alluvial swampy (Qs) sequences. They cover large areas especially along the main rivers.

-The colluvial sequence (Qc) is usually found in the areas nearby mountains and composed of gravel, sand, and clay. It is normally red in color. Sometimes laterite and hardpan can be recognized. The sequence is expected to form the oldest sequence in the quaternary sediments.

-The terrace sequence (Qt) consists of clayey sand and gravel layers, friable to loose, and white in color with abundant mottles and concretions. The sand layers consist of very coarse-grained sand, which is poorly sorted. The sequence occurs in the southwestern part of the study area, between the colluvial sequence and colluvial floodplain sequence and overlies the colluvial sequence.

-The fluvial sequence (Qf) is composed of sand and intercalated gravel layers. The sequence is loose to friable and yellow to white in color with abundant mottle. It has been seen in large areas in the southeast of the study area, where surrounded by the colluvial sequence. The layers are poorly sorted and overlay on the colluvial sequence.

-The alluvial floodplain sequence (Qa) consists of silty clay layers, which are alternated by sand layers. The clay is stiff to friable and poorly sorted. The sequence is white to light gray in color with abundant mottles. It is found along the main rivers and overlies the fluvial sequence.

b) The sediments of deltaic environment can be classified into 4 sequences, delta plain alluvial sediments (Qdpa), delta plain poorly drained march sequence (Qdpm2), delta plain well-drained marsh sequence (Qdpm1), and delta front (Qdf) sequence.

-The delta plain - alluvial sequence (Qdpa) is composed of silty clay and clayey sand, white in color and with a firm to friable consistency. There are abundant mottles. It occupies both sides of the Phum Duang River and extends up to the southern part of Amphoe Tha Chang.

-The delta plain – poorly drained march sequence (Qdpm2) is formed by peaty clay, which is dark brown to brownish gray in color. It is soft to firm and has abundant plant remains. In the lower part of the sequence generally a peat layer is found. The sequence occurs in the southern part of Amphoe Tha Chang.

- The delta plain – well- drained march sequence (Qdpm1) consists mainly of silty clay, which is gray in color and soft. Jarosite mineral traces occur in the upper part of the sequence, and fine-grained sand lenses have been observed in the lower part. It occurs in the western part of the Surat Thani city area.

-The delta front sequence (Qdf) consists usually of silty sand, which is fine grained and greenish gray in color. The sequence contains abundant shell fragments. The sequence occurs at the outer margin of the delta, near the sea.

c) The sediments of coastal environment occur mainly along the shoreline, where fluvial influence is low. The sediments in coastal areas of Surat Thani are also influenced by sea-level change which has been widespread recognition in the Southeast Asia. The sea-level reached a peak at 5 meters above present mean sea-level around 6,000 years BP (Sinsakul, S. , 2000). It regressed and then reached a new peak at about 2.5 meters at 4,000 years BP. The coastal sediments can be classified into tidal flat (Qtf), beach sand ridge (Qb), and lagoon sequence (Ql).

-The tidal flat sequence (Qtf) is composed principally of silty clay, which is firm to soft and yellowish to light greenish gray in color. There are moderately to abundant plant remains and fine-grained sand lamina. The sequence is confined to low-lying areas near the sea.

-The beach sand ridge sequence (Qb) consists chiefly of sand, which is loose, medium to coarse-grained, and yellowish-gray to light greenish-gray in color. There are slightly to abundant shell fragments. The beach sand ridges are found as elongated strips inside the tidal flat area and were formed during the Holocene marine ingressión.

- The lagoonal sequence (Ql) is mostly composed of silty clay, which is soft and dark brown to dark gray in color. There are abundant plant remains and fine-grained sand lenses. The sequence can be found behind beach sand ridges.

Igneous rocks

Igneous rocks are recognized only at one place in a small area, in the southeastern part of the study area, named after Khao Luang Mountain. The Khao Luang granite is described as light gray to pinkish brown in color and of equigranular texture. The rocks comprise essential minerals, potassium feldspar, plagioclase, quartz, and biotite-muscovite.

3. Climate

The study area is situated on peninsular Thailand within the Gulf of Thailand side. It is influenced by southwest and northeast monsoons. The summer season lasts from January to April. The highest average temperature in April is up to 31° C. The annual average temperature is 26° C. The monsoon season begins in May and ends in December. It can be divided into 2 periods. The first period is between May and October. During this time the area is influenced by southwest monsoon bringing high humidity from its passage over India Ocean before reaching land. The second wet period is between November and December when the area is influenced by the northeast monsoon, which passes Gulf of Thailand. (Khawdee, 2008)

CHAPTER 2

LITERATURE REVIEWS

The previous studies such as the changing of sea-level in Thailand and vicinity, and the dating method for determining age of beach deposits and so on will be described in this section. Moreover, the overall environmental setting of Laem Pho where located in Amphoe Chaiya, Changwat Surat Thani, Southern of Thailand will be presented in this chapter.

2.1 Sea-level Change

The sea-level has been fluctuating for long periods of time and normally caused of ice ages and other global events in nowadays. Various reasons can motivate the changes which can be categorized into two patterns including “eustatic change” for global sea-level and “isostatic change” for local sea-level. However, it depends on the effect root that is a global effect or a local effect on sea-level.

2.1.1 Nature of sea-level changes

According to the interconnection of the oceans, the fluctuation of sea-level has been transmitted through the oceans around the world. Although this case is a general rule, some complex effects encouraged to the sea-level behavior and created the global fluctuations. Since the water that occupies in ocean basins can easily deform, the sea surface is a potentiometric surface which always deposits horizontally with regard to the local gravity field except where is roughly deformed by winds and flows. The local gravity field at any place encloses the field that was generated by the earth, and modified by the depth of water along with the characteristics of nearby rock masses or ice sheets. Therefore, surface of the sea lies in a complicated and specific configuration of highs (such as over the North Atlantic) and lows (such as over the equatorial Indian Ocean) (Williams, M. et al., 1998).

Moreover, it showed that the maximum elevation was different approximately 200 meters. The three-dimensional form of the rough surface is named as the geoid that is similar to an ellipsoid, the ordinary geometric figure which has been frequently displayed as the shape of the solid earth. Global sea-level fluctuations have changed in the particular form of the geoid. Besides, the magnitude of the change at any area relies on the relative that it lies high or low on the geoid surface (Figure 2.1). In addition, the geoid perturbation could motivate a significant sea-level variation and a quantitative analysis of the possible effect's size (Williams et al., 1998).

Accordingly, water was added to the oceans by glacial melting or was taken from them by global cooling phases that provided a major notional worldwide sea-level fluctuation mechanism, which referred to the land locally produced either transgression or regression. When sea-level changed because the water volume in the ocean basin has varied, it was described as “eustatic change” (Williams et al., 1998).

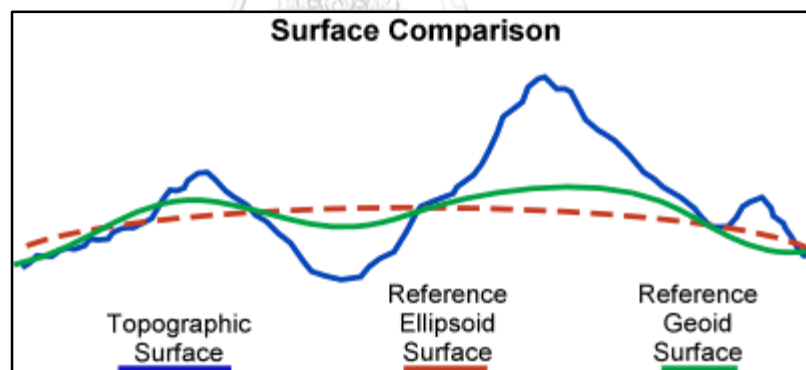


Figure 2.1 Surface comparison consist of the reference ellipsoid surface (a map of average sea level), the reference geoid surface (a true sea level surface), and the real surface of the Earth (the ground) is the topographic surface.

(Source: <https://www.unavco.org/education/resources/tutorials-and-handouts/tutorials/geoid-gps-receivers.html>)

The records of sea-level changes showed that the past sea-levels around the continent margins were more variable by the tectonic movement of the land. The measurement could be effective by studying the elevation of the line where water

and land meet, however an obvious fall of sea-level could be prevented by old beach deposits or sea caves that caused by the land rising. An ordinary cause of elevation change of the land was isostatic rearrangement that operated by the changing in crust loading, moreover, it resulted that the crust was supported by highly viscous and deformable mantle below. An increasing of the crust loading lead to slow subsidence of the land, in addition the removal of the load results in a similarly slow static rebound or recovery (Williams et al., 1998).

So, this is related to the study of Quaternary sea-level changes, which resulted from the growth and melting of land ice. The alteration of ice mass borne by the continents caused the isostatic subsidence or uplift, therefore the evidence of the old shorelines and other coastal index has been changed especially near glaciated areas. In addition, the differentiation of water mass in the oceans motivated a similar effect by the load varying that is borne by the rock of the sea floor. Nevertheless, the essential skill and plentiful knowledge were needed to be applied to solve the result distortion of sea-level changes records (Williams et al., 1998).

The main article in Quaternary sea-level changes studies has been a study of sea-level history. There were many environmental processes that have been controlled or enforced by sea-level including climatic and environmental significance. Furthermore, sea-level was being one of the main determinants of coastland geomorphology and coastline evolution. The coastal zone evolution has represented in terms of human settlement and development of cultures (Williams et al., 1998).

The previous study suggested that the postglacial sea-level had slowly risen since 6,000 BC permitted the origin of sediment accumulation in Nile delta region, then lead to the agricultural supporting and the development of the Predynastic settlements. Sea-level has modulated the major of nutrients fluxes in the ocean. Sea-level has also controlled the area boundary of dry land and through the agency of carbonic acid corrosion; the differentiation in exposed land may exert the global

carbon cycle and the climate greenhouse effect controls. Moreover, the relationship among sea-level with the marine sediment bodies collection, hydrocarbon reservoirs, and other marine resources is significantly correlate to create a main focus on stratigraphic and geological work. The variation of sea-level history presented there are various controls on the relation between sea-level and the different histories of sea-level against the land that have been created regionally under the dominant power of a specific control or group controls (Williams et al., 1998).

Some landscapes were created on the coastland around the world when the sea placed higher or lower than the land, particularly during Quaternary times. Since the beach deposits or coastal stranded above high tide level, it can be indicated to an emerged coastline that the sea was originally at higher level, whereas the drowned valley mouths indicated to a submerged coastland where the valleys were excavated by their rivers when the sea placed at lower level. Although a marine transgression occurred when sea-level increased to attack the land, a marine regression occurred when sea-level downed to reveal the past sea floors as a land area (British Geological Survey, 2016).

In addition, the relation of sea-level had often risen and fallen over geological time. It presented that some coastal areas have been tectonically long stable, and appeared obvious indications of the continued instability significantly earthquakes and volcanic activities. When the sea-level has remained close relative to the land as long as it can recognize coastline characters, some of these were above sea-level or emerged, and some are below or submerged (Figure 2.2). Moreover, many of the coastlands in the world in past 6,000 years have been recognized as the sea at its present relative level. Sea-level depends on the water volume in the oceans which can be defined by the balance of water evaporation and water precipitation due to the hydrological cycle and the crustal depression's size and shape containing seawater.

Moreover, the data of mean sea-level can be measured through upward and downward movements of relative sea-level (Bird, 2008).

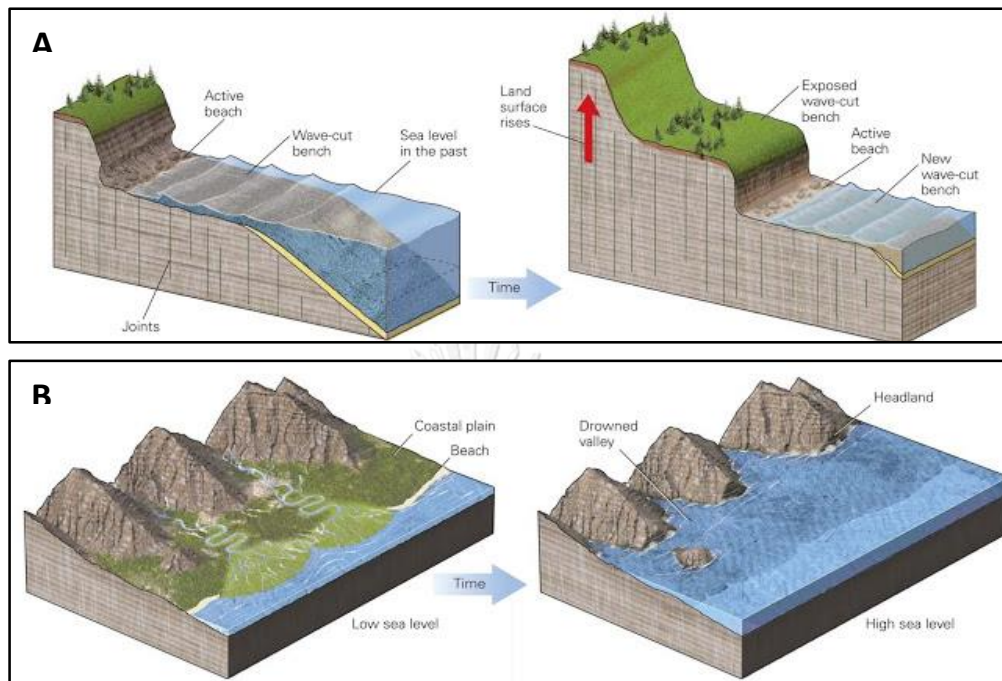


Figure 2.2 The characteristic of emergent coastlines (relative sea level is falling) and submergent coastlines (relative sea level is rising). A) Emergent coastline B) Submergent coastline

(Source: <http://geologylearn.blogspot.com/2015/12/causes-of-coastal-variability.html>)

The previous studies showed that lots of sea water was stored in ice sheets and glaciers during the last ice age, and it found that the average of sea-level in the past was lower than now more than 130 meters. However, the changes of sea-level have related to the growth and melting of ice sheets that quickly occurred while the rises and falls of sea-level have more slowly occurred. Moreover, these gradual changes have produced the vastly thick of sedimentary rocks that have been recorded in the long history of geological time (British Geological Survey, 2016).

2.1.2 Causes of sea-level change

There are various reasons that are the causes of the changes of sea-level in the different time. The increasing of present sea-level is the result of not only the melting of the land ice but also the warming and expanding of the water in oceans. When the ice at sea based has melted, it has had no direct effect on sea-level because it would be a part of the ocean system. Since the density of ice has been less than water, then it replaced a balance of water mass and led to the floating of ice. Therefore, the sea-level has no increase when ice melts (British Geological Survey, 2016).

Nevertheless, the indirect effect on Arctic ice melting is the Albedo changes, that albedo is the ability of the surface to reflect sunlight (Figure 2.3). For example, ice and snow have good surface to reflect the sun's warming ray. As the ice in Arctic melts, the warming of polar region will increase more quickly causes the ocean can adsorb the heat energy from the sun. Therefore, the heating resulted in the melting of Arctic ice and also higher warming which is the classic feedback in climate. According to the changes of the water amount that stored in the oceans or the changes in ocean basins' geometry that converts the capacity of the ocean volume that can contain water, there is the eustatic sea-level change takes place. When the amount of water that collected in the ice caps affects to the sea-level change, it named glacial-eustasy. The previous data indicated that the land areas were covered with thick of ice layers during glacial periods. The gravity of the ice resulted in the lowing of the surface of the earth's crust. However, the melting ice and the earth's crust can rebound at the end of the glacial periods, which is known as an isostatic sea-level change. It caused a relative that the rising of the land is not the volume of the increasing water. The changes of sea water's temperature have encouraged the sea water changes due to the expanding of sea water at higher temperatures. Since the climate is warmer, the

oceans will adsorb the heat ead to the rising of their volume and also increases of sea-levels (British Geological Survey, 2016).

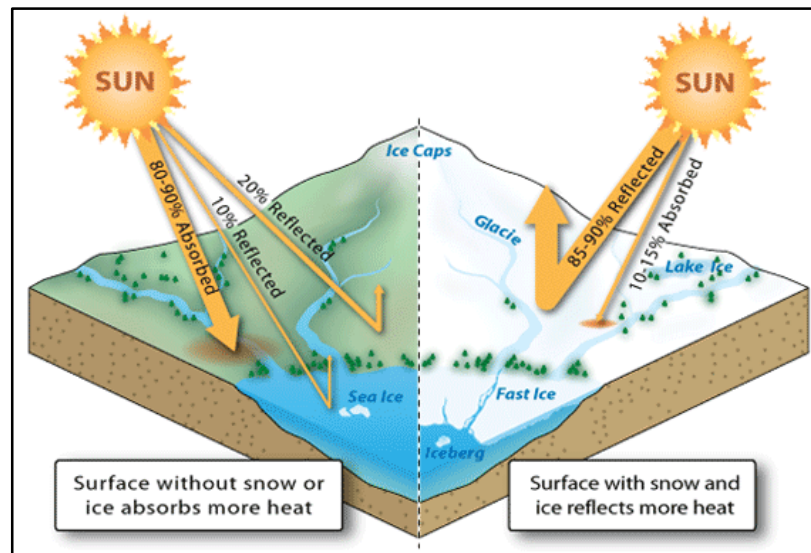


Figure 2.3 The albedo model, the snow and ice reflects most of the solar radiation back into space, but if there is less ice cover, the ocean and the land warm up causing more ice to melt.

(Source:<https://www.skymetweather.com/content/climate-change/climate-change-arctic-ice-may-disappear-by-2040-alarm-scientists/>)

According to Williams et al. (1998), there are many processes can cause sea-level changes. Some of the mechanisms resulted in slowly effect, whereas some showed immediately action. There are some of the most mechanisms and investigation is recognized as the timing and size of the effects on sea-level during the Quaternary such as;

- Tectonism and changes in gauge sea-level

The most fluctuations in sea-level are the results of the changes of the ocean basins capacity. The main factor that causes the changes is character of the activity along the mid-ocean ridge system which estimates the globe. Among the ridges, the volcanic activities lead to the warmth and youthfulness of the oceanic crust, thus

the rock stand isostatic high. Then, sea floor distribution carries the new rock away from the ridges in rate centimeter per year and it causes the sea floor subsidence (Williams et al., 1998).

Therefore, the oceanic ridges's characteristic is determined by thermal isostatic processes (Figure 2.4). The character of the oceanic ridges that formed a board arch can define the depth of the ocean floor under the water surface or the geoid. The sediment's thickness has covered the sea floor near the continents's margins but away from the actually frame zones. The depth of the ocean has a close relative with the age of the rocks forming the sea floor. Moreover, the rate of the sea floor diffusion and reflection increased the heat distribution to the ridge system, carrying the new crustal rock away from the ridge more rapidly. These change the shape and dimensions of the ridge system, so the ocean volume increases and the sea-level will be also displaced upwards. Therefore, the changes of oceanic ridge volume are able to generate the largest fluctuations in sea-level (Williams et al., 1998).

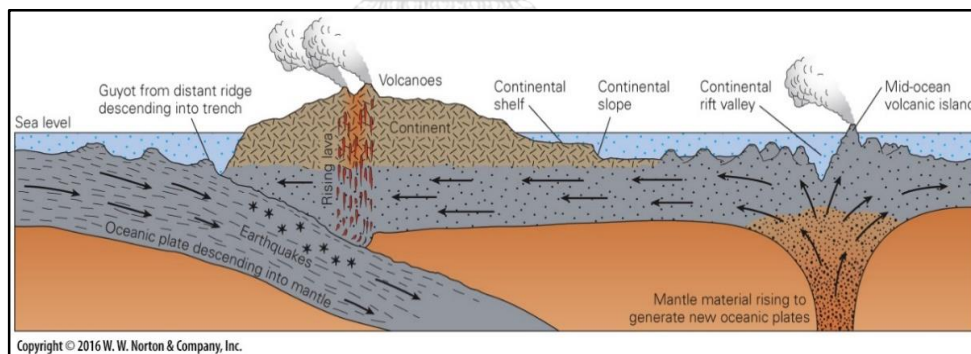


Figure 2.4 The rising of magma at mid-ocean ridges and the latest seafloor moved away from the ridge axis, then the ocean basin is widening and seafloor spreading. (Source: http://www.geo.hunter.cuny.edu/tbw/Iceland.Field.Trip/Lectures/2.plate.tectonics/plate_tectonics.htm)

- Quaternary ice growth and decay glacio-eustatic control of sea-level

The growth and melting of land ice produces the significant cause of sea-level fluctuation in the Quaternary which is the classic mechanism for creating of eustatic changes in sea-level (Figure 2.5). The evaporation of the water in the ocean takes place in the low latitudes where the water is warm, however it results in sea-level decreasing when the water is stored as land ice in high latitude. According to the developing of glacial conditions, sea-level decreases very slowly. Although the sea-level fluctuations relate to several steps of interruptions that are more rapid with sea-level increasing, the amount of eustatic dropping is around 120 - 150 meters below present sea-level at the last glacial maximum (Williams et al., 1998).

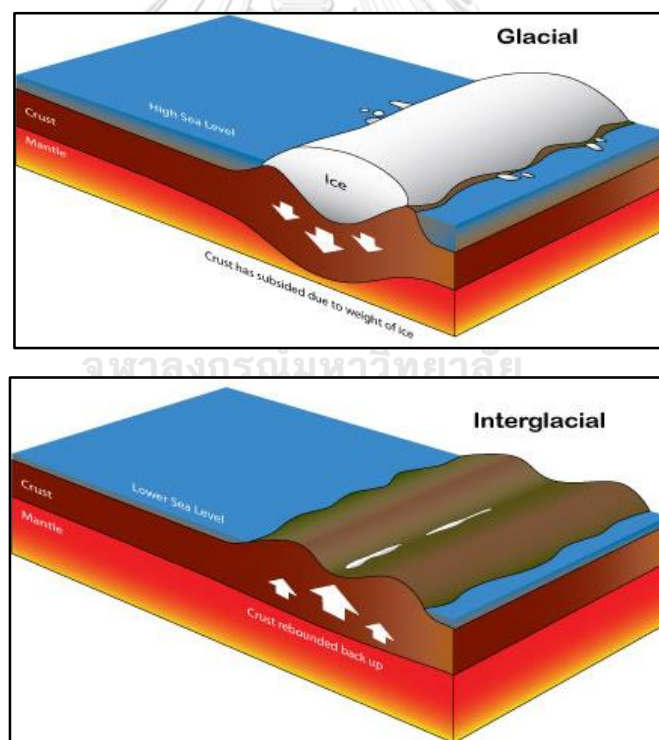


Figure 2.5 Sea level change due to isostatic uplift during glacial and interglacial period.

(Source: <http://www.bgs.ac.uk/discoveringGeology/climateChange/general/coastal>)

- Isostatic and sea-level changes

The glacio- eustatic fluctuations are the connection of the redistribution of mass among the ocean basins and the continents. When the ice loaded, the continents drop but the oceanic crust rises. Then, the deglaciation causes the unloaded land raises with isostatic and the ocean floors subside. This is why the history of sea-level is very complicated. As the ice is the only part of the north and south of the continents, then the crust would displace material in the under mantle which is greatly viscous, in subsiding or rising. The timescale over the subsidence or risen of continents is different from it over the act by oceanic crust as the amount of vertical movements are related (Williams et al., 1998).

Moreover, the several of thermal characteristic of the mantle under the continents is also involved. Therefore, the trace of sea-level that printed on the land would be a complicated recoding at different rates. Moreover, the interesting control is supported by the tectonic motivation of the mantle flow from the ocean to continent. The reward movement of displaced material in the mantle relates to the isostatic subsidence and uplift of continents and ocean basins. Nevertheless, land ice expands and melts to originate isostatic subsidence and uplift too quickly for the flowing of the viscous mantle to keep pace (Figure 2.6). Therefore, when the ice loaded continents subsided, it creates deformation of the mantle and the interference is slowly transmitted because of the viscous flow of the mantle. The doubly readjusting of the earth between the glacial and non-glacial conditions is required as the large transfer of material volume in the late Quaternary (Williams et al., 1998).

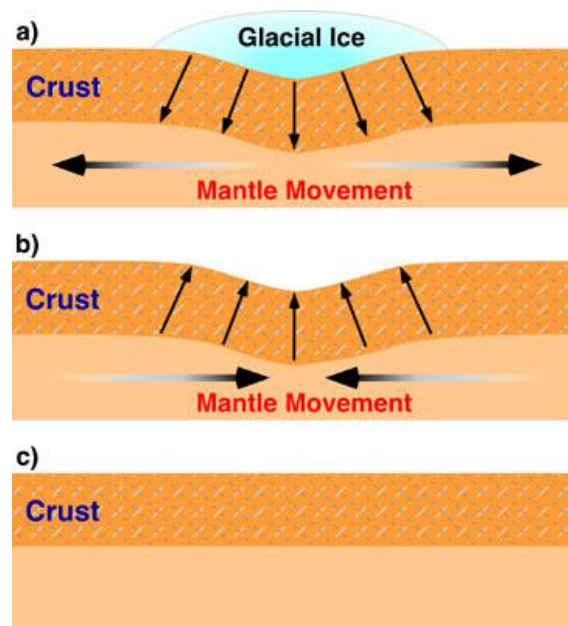


Figure 2.6 The increasing of glacial ice on the Earth's surface results in the changing form of the crust and sinking. (a) When the ice melts, there is an occur of isostatic rebound and the crust rises to the latest position before glaciation, (b and c) A process of mountain building and mountain erosion.

(Source: <http://www.physicalgeography.net/fundamentals/10h.html>)

- Changing water loads and their effects

The local and regional changes process which related to sea-level is hydro-isostasy (Figure 2.8). The eustatic rise results in marine transgression producing additional load of water that be loaded on the continental shelf which hold a decreased water load during glacial stages (Figure 2.7). The shelf is a continental crust curves under the variable load which is the largest on the outer shelf where the depth of water is highest and lowest near the shoreline. This causes the minor changes in the relative sea-level along the continental borders. Therefore, the amount of flexure will relate to the rock's rigidity, moreover the load of water which covers the continental shelf will rely on the shelf width. The variation of geographic will guarantee that the eustatic sea-level fluctuations are recorded by field evidence at various elevations. Nevertheless, the eustatic sea-level increasing is related to the up-warping

of continental borders that the nearby sea floor is curved down under the heavier water load resulting in the postglacial transgression. Although in the case of the mid Holocene the uplift coastline characters of the far field oceans were not necessary to be recorded a higher measure sea-level, the uplift coastline features are to be expected. Therefore, the after hydro-isostatic stagger and elevation of the physical evidence that traced a previous position of the coast are reflected (Williams et al., 1998).

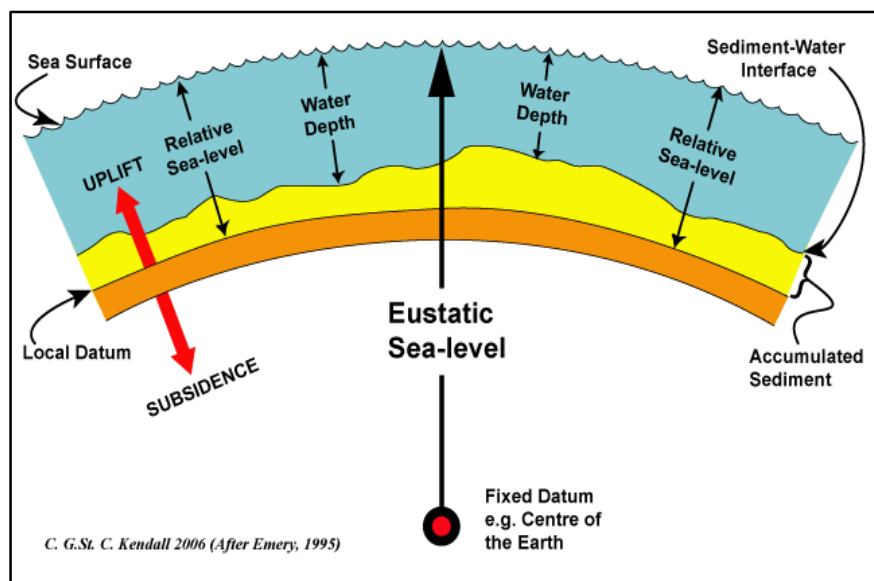


Figure 2.7 The position of sea surface comparative to a fixed datum close to the sea floor that can point to eustasy and the movement in vertical of the sea floor. (Source:<http://www.sepmstrata.org/Terminology.aspx?id=relative%20sea%20level> (#)

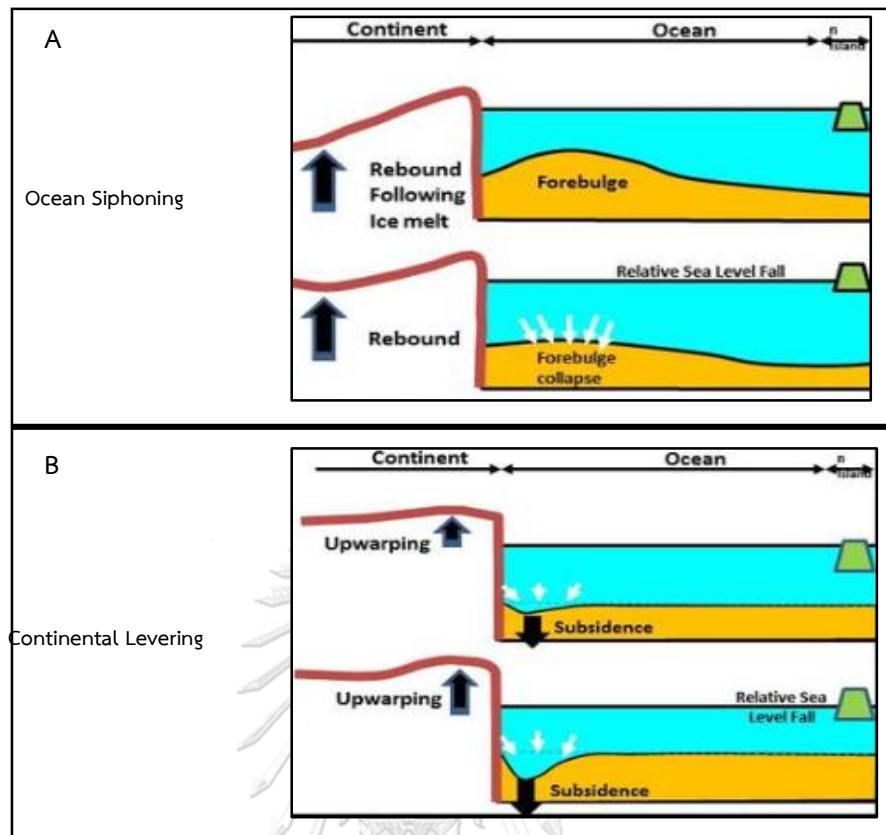


Figure 2.8 The hydro-isostasy between ocean and continental. A) The ocean siphoning, water flows from equator to collapsing forebulge areas at higher latitudes. B) The continental levering, water loading at the continental shelf depresses sea floor and then uplift shorelines.

(Source: <http://www.easttexasgeo.com/changes-in-latitudes-changes-in-attitudes-latitudinal-effects-on-sequence-stratigraphy/h58yq20rt9jy98xbxjovnt5amuvwsx>)

- The geoid gravitational controls on sea-level

The falling of relative sea-level during deglaciation that known as land emergence caused of isostatic rebound of the crust. The component of the relative sea-level decreasing, that was observed close to the area where loaded by glacial ice, was the result of the geoid perturbation (Figure 2.9). The land emergence's record did not present the actual rate of isostatic rise of the land because the meltwater flowed

into the ocean and caused the corresponding eustatic rise. However, the isostatic is responsible to the cold discharge sites around the enormous ice sheet. Although the large volume of meltwater returned to the oceans, the deglaciation area was connected with rapid sea-level fall (Williams et al., 1998).

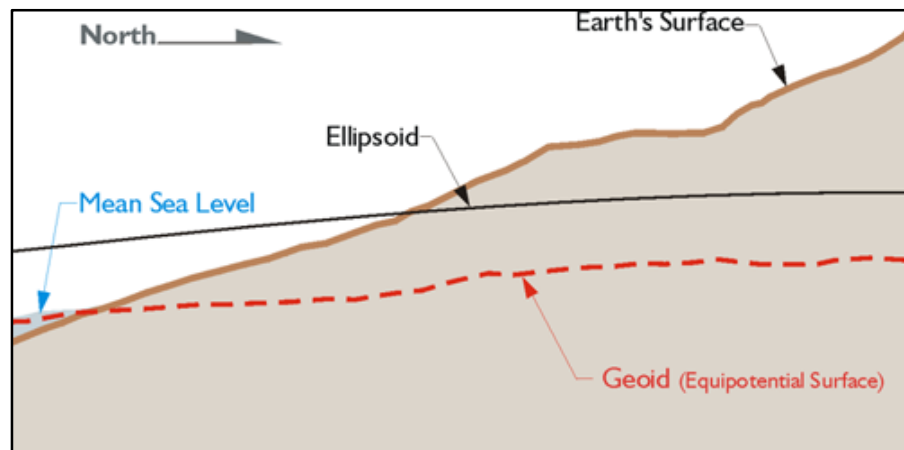


Figure 2.9 A relationship between mean sea level and the geoid.

(Source: <https://www.e-education.psu.edu/geog862/node/1820>)

2.1.3 Quaternary sea-levels

The sea-level record is a part of the upper Quaternary around the last 400 ka, moreover, there were a few locations where can be recorded. The old evidence was dated by uranium disequilibrium techniques, while the radiocarbon was applied in the recent 40 ka. According to previous discussion of the sea-level controls, the tectonics or isostasy of somewhere has had the effects on the evidence elevation, for example the record that derived from fossil coral reefs founded in a landing-like which line above the shoreline of the Huon Penninsula in Papua New Guinea (Figure 2.10). This area places in the conflict zone among the Pacific and Indo-Australian lithospheric plates and be controlled by tectonic influence. The result showed the stable raise of a fault-bounded block of land as a mean rate at 0.5 - 3 millimeters per year. As this raise relates to the principal ongoing plate tectonic processes, it has not changed largely during the late quaternary (Williams et al., 1998).

The fringing coral reef crowd can be encouraged by the present Huon coast. Although the coral crowds have continued elevated and suffer exposure, they did not display. The condition during a glacial boundary was that meltwater have returned to ocean basins then produced a worldwide transgression. The increasing of sea-level that took place in a rate of millimeters per year was effectively pursued with the rising Huon Peninsula, along with the coral crowds can expand in larger size. The fossil of coral reefs has run up to 700 meters and showed the order of glacial boundaries, which the crest of each reef dating from the peak of a postglacial transgression. The decreasing of sea-level was opposite to the coral expansion, moreover the record of the rise of the lowest stands of the oceans during glacial time did not derive from Huon Peninsular. The sea-level history can be traced by these reefs from their present elevation over the past sea-level cause of the stable increasing. The data showed the level of the sea at the time when coral was glowing. Moreover, the dating of the coral fractions was permitted to create a full chronology (Williams et al., 1998).



Figure 2.10 Picture of fossil reefs of the Huon Peninsula in Papua New Guinea which are currently cliff faces rising up to 25 meters above the beach.

(Source: <https://www.flickr.com/photos/coralcoe/6387028641/>)

2.1.4 Sea-level curve

Sea-level curve records are the effective tool for understanding many sea-level data from many researchers from Southeast Asia region (Figure 2.11). Sea-level curve records have developed at first by Geyh et al. (1979) from the studied of Malacca Strait released that the curve indicates a maximum mid-Holocene sea-level of +5 meters which showing a smoothly falling sea-level but they could not determine whether sea-level fell smoothly or in an oscillatory trend.

While the curve by Sinsakul, S. et al. (1985) which studied the Gulf of Thailand showed that sea-level rose until about 6,000 years BP and reached a height of about +4 meters, then there was in a regressive trend until 4,700 years BP, at 4,000 years BP sea-level rose again to an elevation of +2.5 meters and from 3,700 to 2,700 years BP, there was a regressive phase that the depositions along this period are below present mean sea-level, after that the transgression started again at 2,700 years BP and reached +2 meters at 2,500 years BP, the last regression period occurred till the present sea-level was reached about 1,500 years BP. As the similar trend as the studied of Thai-Malay Peninsula by Tjia (1987) and Tjia and Fujii (1992) which showed the 3 rebound phases in the curves during the Mid to Late Holocene with highstands at 6, 4, and 2.7 ka and two sea-level highstand at approximately 4,500 and 2,500 years BP. The first high sea-level was up to 3-4 metres above present sea-level (Sinsakul, S. , 1992). Although, the curve by Sinsakul et al. (1985) represents a complex sea-level history, it is a basis for the present investigation of the Holocene period in Thailand.

Nevertheless, the studied of Singapore sea-level curve by Hesp, P. A. et al. (1998) plotted against the Geyh et al. (1979), Sinsakul et al. (1985), Tjia (1987) and Tjia and Fujii (1992). A rapid post glacial marine transgression rising to present mean sea-level at 6,500 BP, sea-level rose to approximately 3 meters. Then around 2,000 to 1,000 years BP, sea-level was reached to present sea-level.

After that Choowong et al. (2004) proposed a revised sea-level envelope for the Gulf of Thailand which corresponded well with the sea-level curves subsequently constructed for the Thai-Malay Peninsula by (Horton et al., 2005). The curves show an upward trend of rising Holocene sea-level to a Mid-Holocene highstand, then sea-level slightly fall to the present. The average rate of sea-level rise at Thai-Malay peninsula is approximately 5 millimeters per years, while the sea-level fall from highstand was at approximately 1.1 millimeters per years and no evidence of second highstand (Horton et al., 2005). After that Nimnate et al. (2015) presented additional sea-level curve for the Gulf of Thailand, the area of study at Pak Nam Chumphon which locates northern of Lam Pho study area. They studied the evidence of sea-level from osl dating of former beach ridge plains together with the other geological evidence such as the occurrence of sea notches in different level and bio-erosion found at the wall of limestone. After studied, the results released that the highest level of transgression approximately 4-5 meters at last 7,600 years BP.

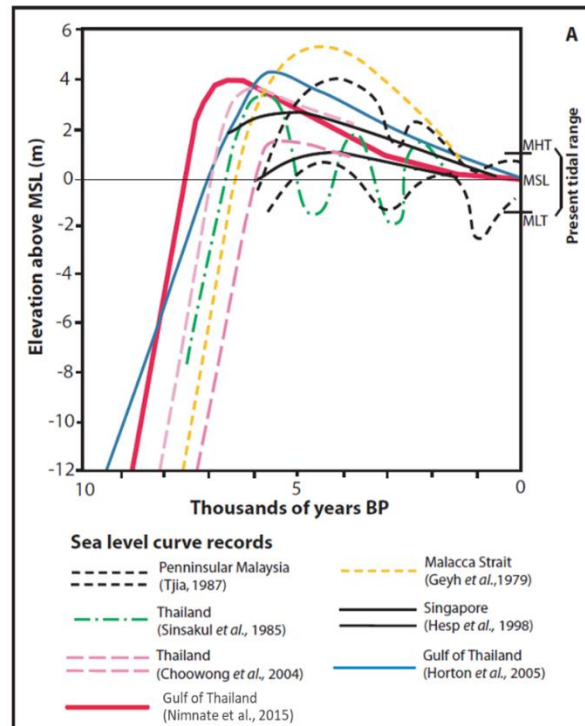


Figure 2.11 Sea-level curves in Southeast Asia including Malacca Strait (Geyh et al., 1979), Peninsular Malaysia (Tjia, 1987), Singapore (Hesp et al., 1998), Gulf of Thailand (Sinsakul et al., 1985; Choowong et al., 2004; Horton et al., 2005; Nimnate et al., 2015).

2.2 Coastal evolution

Coasts are dynamic systems that be the difference of form and process which can named morphodynamics at the various time and space scales relating geomorphological and oceanographical factors. The short-term interferences such as storm affected to the coastlands which can return to the pre-interference morphology, refer to ordinary morphodynamic equilibrium (Nicholls et al., 2007).

The additional pressures have been used as human activities that be able to occupy over natural processes. Several coastlands were continued improvement toward a dynamic equilibrium that often applies at various states to change wave energy and sediment supply. The coastlines reacted to change the external conditions

to the system, for example storm. The natural variation of the coastlands made it hard to identify the climate change impacts (Nicholls et al, 2007).

For example, mostly shorelines in the world presented the recent erosion's evidence, whereas the important driver is not sea-level increasing. The coastline had a rapid fluctuation of the interface between land and sea, where many populations have been living. Moreover, the shorelines have been under the danger from a diversity of natural and anthropogenic impacts such as the climate and sea-level fluctuations. The changes of coastline can be a result of the relation of climate fluctuations including ocean and atmosphere. The frequent and intense of The El Niño Southern Oscillation (ENSO) events in the Indo-Pacific regions showed the relative with the occurring of coral bleaching and death (Figure 2.12 and 2.13). These might change as a component of climate change, and turn into larger extensive according to the global warming (Nicholls et al, 2007).

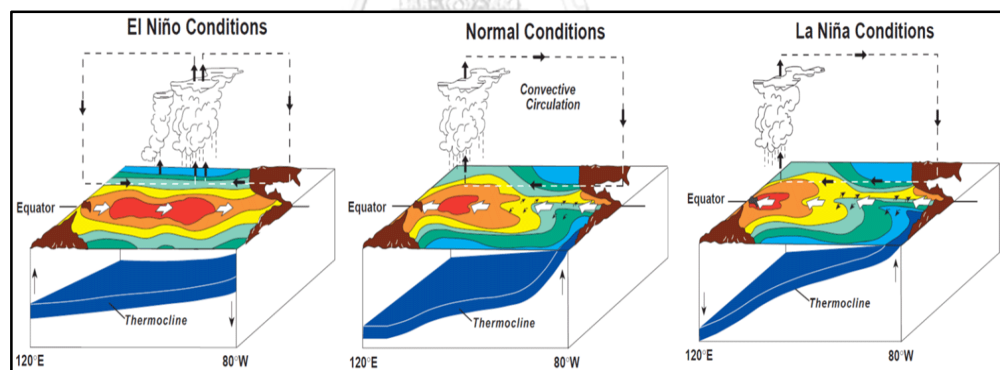


Figure 2.12 This diagram shows a model of surface temperatures, areas of rising air, winds, and the thermocline (blue surface) in the tropical Pacific during El Niño, normal, and La Niña conditions.

(Source:<http://www.reefresilience.org/coral-reefs/stressors/climate-and-ocean-change/el-nino-southern-oscillation/>)



Figure 2.13 Mass bleaching of coral in the Great Barrier Reef, Australia.

(Source: <https://phys.org/news/2016-10-corals-die-great-barrier-reef.html>)

In addition, the dynamic system of the coastal was frequently presented the complexation as non-linear morphological change. The deposition, erosion, and transport of sediment have related with time-lags, moreover the moderate transport processes of supply and removal of sediment resulted in the morphological evolution of sedimentary coastlines. A coastline might apply the equilibrium in where the processes were balance. Nevertheless, the morphodynamic change was frequently induced by the external factors, such as storms to take from the equilibrium state. The sediment transport got the effect from climate change and sea-level rise (Nicholls et al, 2007).

2.2.1 Nature of coastal evolution

The forming of the coastal landforms has been influenced by the range of morphogenic factors. The climate factors have encouraged the wave and wind system which can shape the coastal characters; moreover, they also influenced the weathering processes involving decay and decompose of the coastal rock from tropical to arctic and from wet to dry environments. Climate have conditioned the coastal plants and animals which have created their characters range from mangrove swamps

to the shorelines, coral reefs to sand dunes, and the organism that attack on the surface of the rock. The oceanographic factors, such as sea temperature and salinity, have encouraged the coastal processes included the effects of rise and fall currents and tidal currents. Then, these factors were determined by climate and the ocean currents' patterns. The data of ancient coastlands that was established by the past fluctuations, have continually influenced the evolution of exist coastlands. Furthermore, the evolution of coastline in the historical times has been changed by the effects of plenty human activities on the coastlands and the hinterland (Williams et al, 1998).

Therefore, the morphogenic systems can define the coastal landform evolution though there were various factors encouraged the processes that acted on the shore. The coastal landforms can be created by the energy such as wind, current, and living organisms along with the materials such as water, rock, and sediment (Figure 2.14, 2.15, and 2.16). Moreover, they also become a factor that influenced the changes. However, these are able to study as the responsible to various processes which act over specific periods (Williams et al, 1998).



Figure 2.14 The coastal landforms of Durdle Door sea arch is a limestone arch on the Jurassic Coast in Dorset, England that was created by wave.

(Source: https://fr.wikipedia.org/wiki/Durdle_Door)



Figure 2.15 The coastal landforms of Beach-dune systems that was created by wind and wave.

(Source: <http://www.snh.org.uk/publications/online/heritagemanagement/erosion/2.2.shtml>)



Figure 2.16 The coastal landforms of the Great barrier reef in Australia that was created by living coral.

(Source: https://www.huffingtonpost.com/2013/12/04/coral-reef-breeding_n_4388094.html)

2.3 Literature Reviews

The studied of sea-level changes through the last glacial cycle by Lambeck and Chappell (2001) presented that during the Quaternary period, the sea-level change was originally an effect of the cyclic growth and decay of ice sheets, resulting in a complex spatial and temporal pattern. In addition, inclusive models of sea-level change enable the migration of coastlines for predicting glacial cycles. The increase of sea-level from the last glacial maximum on the tectonically stable Sunda Shelf in Southeast Asia has been derived from a siliciclastic system. The sea-level reconstructions are confirmed through the record on coral reefs. Furthermore, the rise of sea-level was as much as 16 meters within 300 years (14.6 to 14.3 thousand years ago) (Hanebuth, 2000).

Moreover, from the studied of (Rabineau et al., 2006) mentioned that paleo sea-level reconsidered from direct observation of paleoshoreline position during Glacial Maxima (for the last 500 ka) showed that according to the drastic climate changes that characterized the cooling trend in the last few million years of Earth history brought about variegation of eustatic sea-level which had gigantic impact on ecology and geology of continental margins. The shoreline positions can be observed for a local measurement of Relative Sea-level. This measurement needs to be corrected from the effect of tectonic and thermal subsidence, compaction, sediment loading and glacio-hydro isostasy. Therefore, the reconstruction of a sea-level curve is not an easy task to back in time.

During the Late Pleistocene glaciation, there was a dropping of sea-level all over the world. In Southeast Asia, particularly in the Gulf of Thailand, there was an evidence of sea-level dropped more than 50 meters, also as a present of Sunda shelf as a continental (Bisward, 1973). In the end of Late Pleistocene, the climate is warm and wet, so the ice mass melted and cause sea-level rise and transgression worldwide.

After Middle Holocene, sea-level retreated backward and caused the progradation of coastal area (Chaimanee, 2002).

From the studied of Choowong (2002) released that the isostatic models and Holocene relative changes in sea-level from the coastal lowland area in the Gulf of Thailand, the research composed of three steps, including systematic geomorphological classification of the coast, the identification of lithofacies base on field coring data and radiocarbon dating, and the establishment of geological models to show spatial and stratigraphical relationships between the morphology and lithofacies. The evolution of the coastal lowland area in the Gulf of Thailand was directly influenced by both eustatic and isostatic changes in sea-level, particularly during the Holocene epoch.

Sinsakul, S. et al. (2002) studied the coastal changes of the Gulf of Thailand. They presented the deposition of marine sediments in inland areas that was a result from sea-level changes during 9,000-1,000 year BP. and they characterized these deposits by coastal geomorphology of sand dunes, beach sands, lagoons, marsh and tidal flats vegetated with mangrove forest. The dynamic environment can be observed around these coastal areas also.

Woodroffe and Horton (2005) studied Holocene sea-level changes in the Indo-Pacific, they explained that there are many locations of the Holocene sea-level reconstructions in the Indo-Pacific region and the nature of Holocene sea-level change is widely similar in all locations.

In addition, the studied sea-level change in the Gulf of Thailand from GPS-corrected tide gauge data and multi-satellite altimetry by Trisirisatayawong et al. (2011) which focused on the sea-level changes that have been affected from the global climate change. The average rate of sea-level rise around the Gulf of Thailand is 3-5 millimeters per year which is higher than the global average rate by 1.8 ± 0.2

millimeters per year as well as Indonesia. In addition, the studied of sea-level change and vertical motion from satellite altimetry, tide gauges and GPS in the Indonesian region by Fenoglio-Marc et al. (2012) that was the same survey and the average rate of sea-level is higher than a global average mean sea-level rise approximately 4 millimeters per year. Along with at the Malacca Strait and the east coast of Thai-Malay peninsula by Luu et al. (2005) which mentioned that geocentric sea-level rise rates are approximately 4.4 ± 3.1 and 4.6 ± 2.5 millimeters per year, respectively. In the common period 1993–2009, geocentric sea-level rise rates along the Malaysian coast are similar, and can be compared with the global trend.

Chaimanee (2001) studied coastal evolution of the Greater Surat Thani city area, Southern Thailand. According to the studied of Quaternary sediments by paleogeography and facies relationship in the basin base on C-14 dating results of Quaternary sediments in the study area, there are three main of depositional environments included Delta, Coastal, and Continental environment. Furthermore, the main depositional environment during Quaternary sediments is non-marine or fluvial environment which has partially marine incursion. In the late Pleistocene which was believed that it is a cause of global sea-level fall, in Southeast Asia especially in the Gulf of Thailand the sea-level dropped more than 50 meters and effected to Sunda shelf emerged as a continent. When the late Pleistocene was over, the climate turned to warm and humid. As well as the melting of ice mass affected to the sea-level rise around the world and had an impact of sea water inundating throughout the coastal plain of Thailand. In Surat Thani city area, there is an experience of transgression into upland areas as far as Kian Sa town with approximately 35 kilometers from the present shoreline. The results from C-14 dating showed that the arriving time of transgression into Surat Thani coast at about 8,000 years BP. According to the rapid sea-level rise during Early Holocene possible effected some parts of the vertical transgression sequence have been eroded. The transgression has a maximum height at more than 5 meters about 5,000 years BP. At the end of Mid Holocene, the sea started backward

to the ocean and the coast was prograded. So the coastal plain of Surat Thani area had developed about 5,000 years BP. by forming the tidal flat and beach ridge along the Surat Thani coastland and the Chaiya coastland and forming the fluvial delta plain at Phunphin area. Because of an influx of upland sediments into the sea, the coastal plain has prograded rapidly. As far as about 1,000 years BP., the sediments supplied to the sea decreased and affected to the fluvial dominant delta transforming into the tide-dominant data. The Surat Thani and Chaiya coasts have possible been in still-stand phase since that time with the mudflat and beach barrier forming respectively.

Silapanth (2005) studied, Geoarchaeology of Thungsetthi, Tambon Nayang, Amphoe Cha-Am, Changwat Phetchaburi. The studied showed that this research area has a historical significance and because the present of archaeological evidence which was believed that the Thungsetthi used to be an ancient communication networks between Southern and Central regions of Thailand. The studied involved geomorphology, sedimentology, and archaeology. The landscape changed in the Mid Holocene and the propagation of the land in eastward direction can be referred to the Mid Holocene marine regression. The results also showed that Thungsetthi had been located on a beach ridge and barriers and surrounded with the paleo-channels connecting to paleo-shoreline. After the mid Holocene regression that is a cause of the morphological changing in this area i.e. a change in direction of paleo-channels, and a change has been continuing to the present. The archaeological evidence in this area can related to other major Dvaravati communities in Central Thailand and can interpret that this area used to be a significant communication with other communities along this Holocene beach barrier.

According to the seasonal coastal change along the Prachuap Khiri Khan areas which is a connecting area next to Phetchaburi, has a study of seasonal shoreline changes of the Prachuap Khiri Khan coast by Songmuang (2005), the study areas are Pranburi truncated beach ridges plain, Prachuap Khiri Khan Bay, and Wanakorn beach

ridge plain released and they are also difference in morphology. The study of geomorphology, aerial photography in each of time, along with the measurement of coastline, beach, and shorefaces vertically and horizontally can refer to a change of sedimentation in seasonal time. The study released that there was an equilibrium or balance of annual sediment gain and loss from the shorefaces in Prachuap Khiri Khan Bay. In the shoreface profiles of Pranburi and Wanakorn areas showed the similarity of an annual depositional rate of shoreface sand that have larger number than erosion. Moreover, the shoreface slope relied on the volume of sediment gain and loss from the coast. From Songmuang (2005)'s studied concluded that the major cause of the coastal changes in this area is on the seasonal monsoon storms and the annual sedimentary cycles are very important key to erosion and deposition process along the individual shoreline area.

The study of coastal change along southern peninsular coast of the Gulf of Thailand from Prachuap Khiri Khan to Nakhon Si Thammarat that have gotten a tropical storm both in the past and present time which is a cause of washover deposits by Phantu Wongraj, S. (2012) that studied sedimentological characteristics of storm-induced washover deposits along the coastal zone of Changwat Prachuap Khiri Khan to Nakhon Si Thammarat, Thailand. The study was about the modern and ancient storm surge washover deposits that can be generated by several storm surge events along the southern coast of the Gulf of Thailand. The study areas composed of the areas that got an effect from modern storm surges including Prachuap Khiri Khan, Chumphon, Surat Thani, and Nakhon Si Thammarat. Washover deposits can be characterized into three types including, perched fan, washover terrace, and sheetwash lineations. Moreover, these depositional patterns were found far inland from shoreline within a distance 100 meters for modern deposit and 400 meters for ancient deposit. Phantu Wongraj (2012) concluded that there was storm surge washover that was affected from an attack of Typhoon 19 times in 8,000 years ago, showing the frequency of an occurrence of Typhoon in Southeast Asia in Mid Holocene which has a warm

climate or can identify the sensitivity of areas which have a changing due to a Mid Holocene sea-level highstand. After an initial discovering of a possibility to relate between warm climates and a frequency attack of Typhoon have a gigantic effect to the social. These may be an effect of climate change that is continuing to present day accordingly Williams, H. et al. (2016) that studied about geological records of Holocene Typhoon strikes on the Gulf of Thailand coast. At least the studies of coastal change along the Gulf of Thailand at Chumphon which was a study of evidence of Holocene sea-level regression from Chumphon coast of the Gulf of Thailand by Nimnate et al. (2015) released that the beach ridge plains located as far as 10 kilometers inland at Chumphon estuary area which was an evidence of the paleo sea-level change. The old beach ridges can comprise into 3 sets including inner beach ridge plains that deposition by south to north longshore currents, while middle and outer ridges were formed by north to south currents and all of them deposited in Holocene. Marine fossils were found in the former tidal deposit that can identify to intertidal and mangrove environments.

CHAPTER 3

METHODOLOGY

3.1 Desk study

3.1.1 Satellite Image Interpretation

Satellite image interpretation was done for making geomorphological map before Field work. The satellite image data using in this study, from Google Earth software, were acquired in 2016 by Quick Bird Satellite with 0.6m resolution. The images were geo-referenced to Universal Transverse Mercator (UTM) coordinate system zone 47 N with datum WGS84. Subsequently, the rectified satellite images were input to ArcMap 10.2.2 software for created satellite image map. The interpretation of satellite images was aiming to identify the geomorphology of the area especially beach ridges and swales for making geomorphological map. The satellite image map also uses for mark the specific sites for the field work and sediment sampling area (Figure 3.1, 3.2, 3.3, 3.4, and 3.5).



Figure 3.1 These satellite images mapping were printed out for field work investigation and sediment sampling points identification in field.



Figure 3.2 Satellite images showing the study area at Laem Pho, Amphoe Chaiya, Changwat Surat Thani. Satellite image from Google Earth; acquisition period: July 2016.



Figure 3.3 Satellite images showing the central part of the study area which exhibited the obviously landform of beach ridges and swales at Laem Pho, Amphoe Chaiya, Changwat Surat Thani. Satellite image from Google Earth; acquisition period: July 2016.



Figure 3.4 Satellite images showing the western part of the study area that located in landward direction which around with human settlements at Laem Pho, Amphoe Chaiya, Changwat Surat Thani. Satellite image from Google Earth; acquisition period: July 2016.



Figure 3.5 Satellite images showing the topography characteristic of sand spit with beach ridges and swales inside at the southern part of the study area. Satellite image from Google Earth; acquisition period: July 2016.

3.2 Field Works

3.2.1 Topographic survey

Detail field work study, including topographic survey by Total Station SOKKIA SET 630R, was performed after geomorphological map was made. Topographic survey was carry out for identification various features and elevations of the land which released the result as a value of distance and height (Figure 3.6). The aim of topographic survey is to analyze survey data between the natural and man-made features of the land, following their elevations.



Figure 3.6 The topographic profile was measured by Total Station SOKKIA SET 630R along transect lines. These pictures consist of a), b), c) The measurement of pole, total station, and tripod respectively before start the topographic survey for calculation with elevation further, d) and e). The topographic profile measurement was done by Instrument man, staff man (rod man), and recorder.

3.2.2 Sediment sampling

According to sea-level change over the geological time, sediment is the important evidence for understanding how the history recorded. Sediment composition and stratigraphic record can describe themselves for timing of deposit and paleo-environment of their areas. Sediments samples were collected for laboratory analysis which including grain-size analysis, stratigraphic column, paleontological analysis, and age determination. Sediment sampling for age dating, Optically Stimulated Luminescence dating (OSL dating) method, were collected at the specified beach ridges, selected from satellite image map, for determining the deposition time of beach ridges.

The method starts from digging an excavation pit at 50x50x50 cubic centimeters and then collect the sediments at depth 40 centimeters. Samples sampling for age determination can separate into 2 parts; the Equivalent dose and the Annual dose. The Equivalent dose needs to prevent from sunlight in filed and all kind of light except the red light in laboratory is allowed. Therefore, sediments were sampling by putting plastic tubes with end-caps and tightly seal with duct tape. After that, pull it out carefully. For Annual dose and sieve analysis, sediments were sampling approximately 900 grams at the same depth in plastic bag. For subsurface stratigraphy, sediment logging was carry out by hand auger which aiming for interpret the deposition environment of sediments at each selected area. Furthermore, paleontological analysis also performed if there are fossil evidences in sediment sample (Figure 3.7).



Figure 3.7 The steps of sediment sampling for OSL dating in laboratory which consist of a) Digging an excavation pit at 50x50x50 cubic centimeters, b) Putting pvc tube with end cap at depth 40 centimeters from surface, c) Pvc tube with end cap was put into sediments layer at depth 40 centimeters from surface for sampling sediments for equivalent dose evaluation, and d) Sediments were sampling at depth 40 cm in plastic bag for annual dose calculation.

3.2.3 Stratigraphic column

To analyze paleo-environment of the study area, sediment deposition needs to be studied in detailed through stratigraphic column. Firstly, a test pit which size approximately 50x50x50 cubic centimeters was excavated by shovel, then a hand auger or a gouge auger was used for drilling into the subsurface part of the test pit for collecting the sediments below. Subsequently, we remove the sediment from a hand auger and put down on a plastic sheet for the sediment description. Finally, the samples were packed in the plastic bag for the sedimentary analysis at laboratory of department of geology, faculty of science, Chulalongkorn University (Figure 3.8 and 3.9).



Figure 3.8 The steps of stratigraphic column for analyzing sediment deposition and paleo-environment which consist of a) Digging an excavation pit at 50x50x50 cubic centimeters, b) Sampling sediments with hand auger, c) After sampling sediments with hand auger, put sediments in the on the plastic sheet for logging description, and d) Description of sediments which include of depth, color, composition, and other evidences.

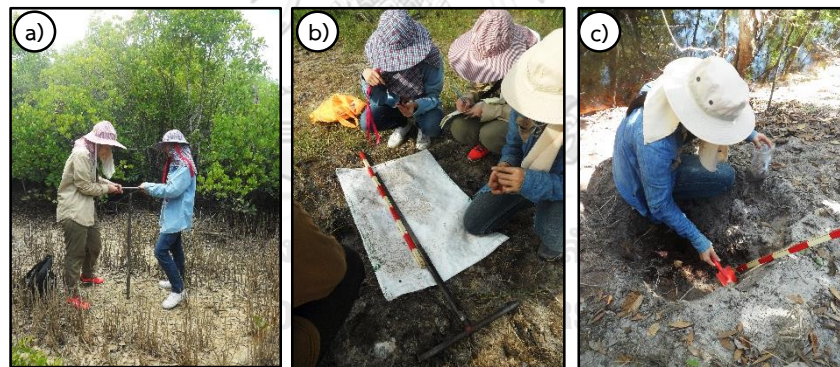


Figure 3.9 In case of sediment samples are clay or very fine to fine grain, and well compaction feature, the sampling will be done by using different tools following these steps; a) Sampling sediments with Gouge auger, b) After sampling sediments with Gouge auger, put Gouge auger on the plastic sheet for logging description, c) Sediments were sampling into plastic bag for study grain size analysis and sediment compositions under a microscope in laboratory.

Soil classification for stratigraphic column

Stratigraphic column in field work needs to classify the sediments texture follow soil classification system. In this study, the description of sediment texture is classified base on USDA soil taxonomy which was developed by the United State Department of Agriculture.

USDA textural soil classification

Most of the soil classification systems developed for engineering purposes are based on particle size distribution, soil liquidity, and soil plasticity. However, one of the most widely used soil classification systems, the USDA textural classification, which the USDA adopted in 1938 (United States Department of Agriculture (USDA), 1987). Textural classification of soil in the USDA system is simple because it is based on only particle size distribution. The USDA system was developed for agricultural purposes. It has some engineering application by providing a relatively easy method for general field classification of soils. However, “loamy” is not an engineering term, so there should be avoided when discussing the engineering properties of a soil (Wisconsin Department of Transportation, 2017). Many textural classification systems were developed to specifics needs. In agriculture, textural classification is used to determine crop suitability and to evaluate the soil’s response to environmental and management conditions like drought or calcium requirements. In water resources engineering, it can be used to determine how much water will infiltrate through a given soil. Because of its relative simplicity compared with other classification systems (USCS, AASHTO, etc.), so the USDA system is widely used around the world (García-Gaines and Frankenstein, 2015).

The primary classifications following:

- **Sand:** particle sizes from 2.0 to 0.05 mm in diameter
- **Silt:** particles sizes from 0.05 to 0.002 mm in diameter

- **Clay:** particles smaller than 0.002 mm in diameter

USDA system divided into 12 classes which displayed on the USDA triangle, showing in Figure 3.10.

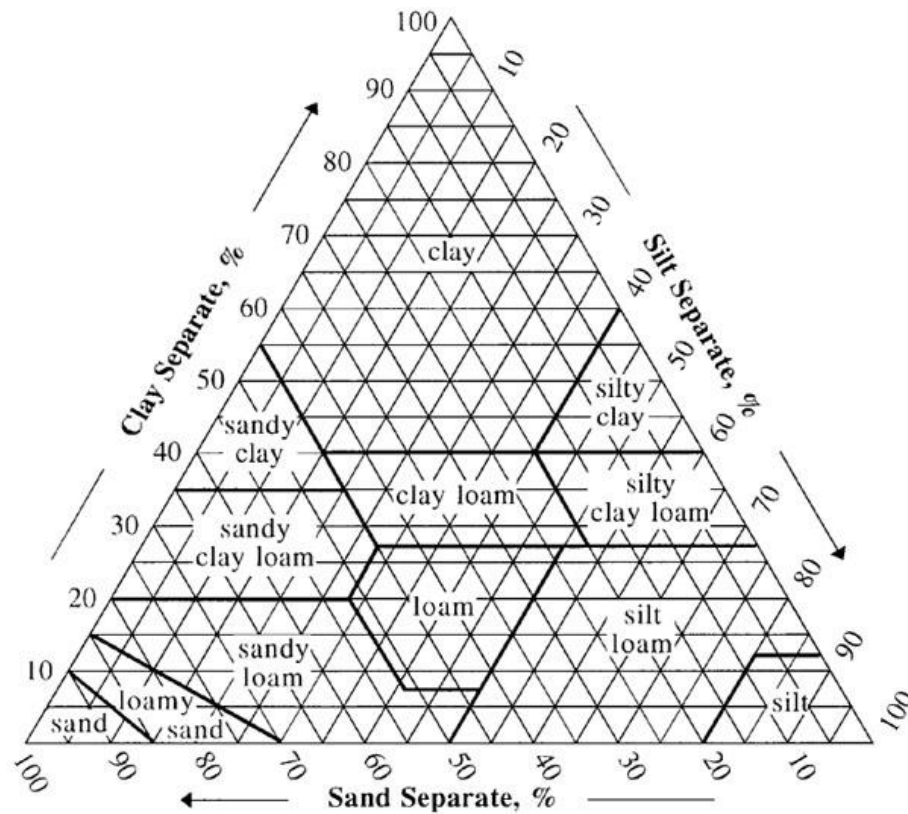


Figure 3.10 Soil texture triangle-classification system based on grain size (*United States Department of Agriculture (USDA), 1987*)

In all textural classification systems, further refinements are used to identify the different between sands and gravels. In the USDA system, sand has five subcategories depending on particles diameters as showing in Table 3.1.

Name of Soil Separate	Diameter Limits (mm)
Very fine sand	0.05–0.10
Fine sand	0.10–0.25
Medium sand	0.25–0.50
Coarse sand	0.50–1.00
Very coarse sand	1.00–2.00

Table 3.1 USDA soil-separates classifications (Soil Survey Division Staff, 1993)

3.3 Laboratory Works

In this section, we divided into 3 categories consist of sedimentary analysis, Paleontological analysis, and Age determination by optically stimulated luminescence (OSL).

3.3.1 Sedimentary analysis

For sedimentary analysis, after collecting samples by gouge auger and hand auger, sediment samples were brought to the laboratory for analyze in term of grain-size analysis, sediment compositions, roundness, and sphericity.

Grain-size analysis is important because of the grains size of mineral in sediments has varies. Generally, sediment grains were usually classified their sizes with their diameter and can be compared with Wentworth scale. Then the particle size distribution will release the texture of sediments that show the outstanding results in class of sandy, silty, clayey, or others. Sieve analysis experiment starts with the steps below (Figure 3.11, 3.12, 3.13, 3.14, and 3.15).

1) Drying sediment samples which collected in plastic bag from fieldwork into the oven at temperature 70°C about 6-8 hours for release water between grains.

2) Then weighting sediment samples approximately 400 grams and brought them to sieve stacks at mesh no. 10, 18, 35, 60, 120, 230, and pan. Checking the cleanness of the sieve stacks before putting the sediment samples in for prevention them from other samples contaminated.

3) Taking all sediment samples to sieve in sieve stacks no.10 on top that was assembled with all selected sieves number with pan on the bottom. Then close the cap over them, takes them to mechanical shaker and shakes for 10 minutes.

4) Finally, take all of sieve stacks out of mechanical shaker, tap sediments out of each sieve stacks, and weight the sediment samples in each of sieve stacks that retained soil and record in weight table. After finished in sieve analysis experiment part, the record in weight table was used for calculation in the moment method that was used to calculate the statistic parameters in differentiating the type of sediment deposition following Phantuwongraj, S. (2006).

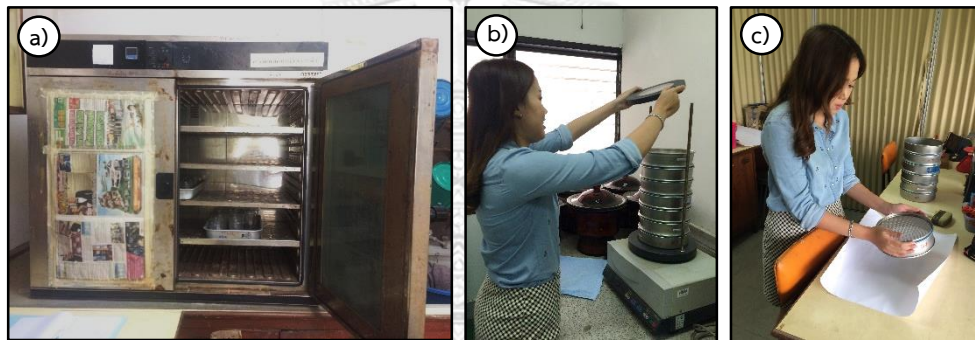


Figure 3.11 Grain- size analysis by sieving method following a) Drying sediment samples in the oven at temperature 70°C about 6-8 hours, b) Taking sieve stacks to mechanical shaker and shakes for 10 minutes, and c) Tapping sediments out of each sieve stacks for weight calculation.



Figure 3.12 Sediment compositions analysis in laboratory room. a) Using a binocular microscope for classifying sediment compositions. b) Sediments sample under the microscope.

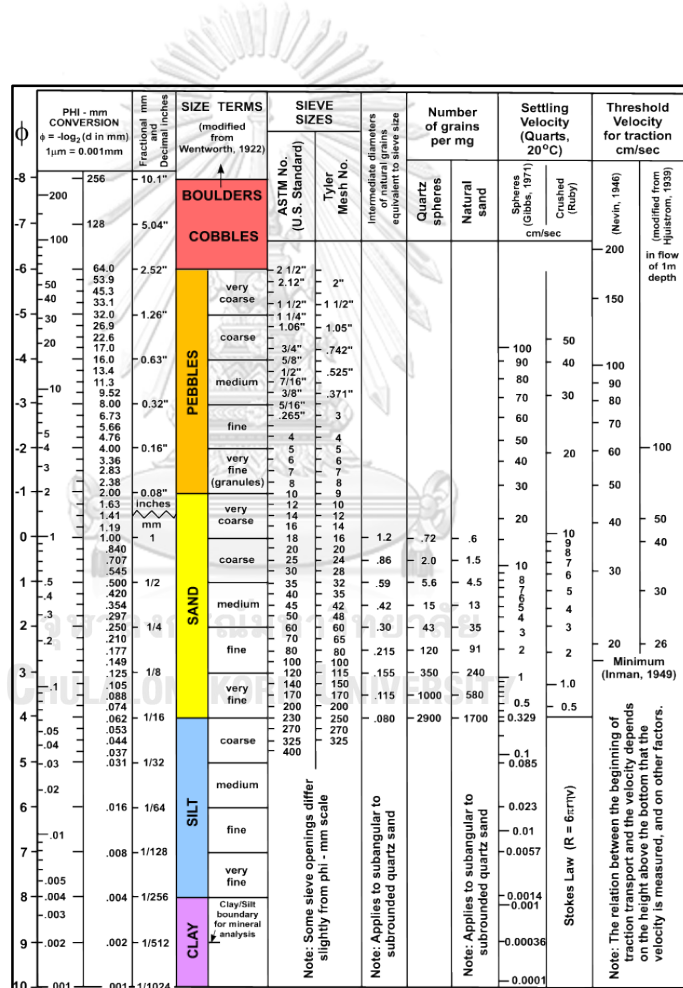


Figure 3.13 This chart showing the grain-size classification detail which consist of phi sizes, millimeter diameters, size classifications, and American Society for Testing and Materials and Tyler sieve sizes.

(Source: <https://pubs.usgs.gov/of/2000/of00-358/graphics/chapter1/c1f9chrt.gif>)

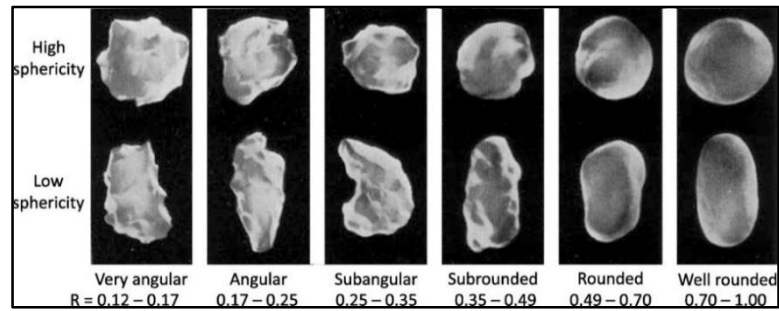


Figure 3.14 Comparison charts for visual estimation of roundness and sphericity of sediments (modified after Hryciw et al., 2016).

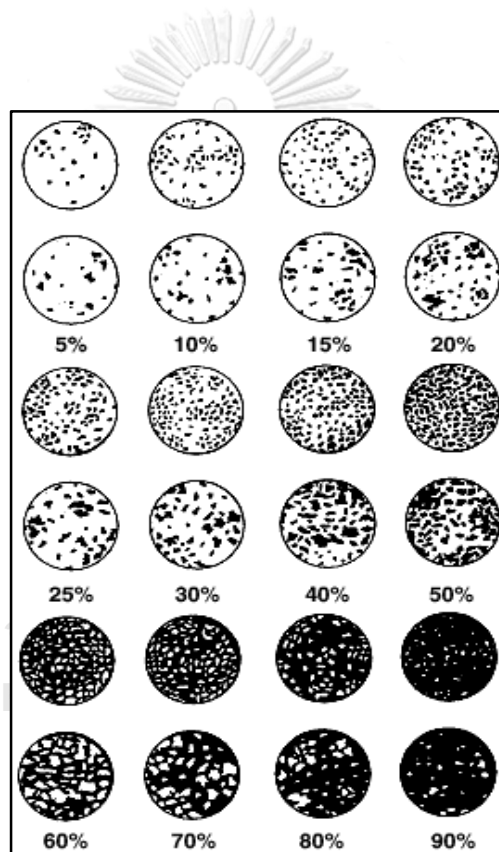


Figure 3.15 Comparison charts for visual estimation of coarse fragments (modified after Terry and Chilingar, 1955).

3.3.2 Paleontological analysis

The evidences of marine fossil that were found in sediment samples are the important indicators for indicating the paleo-environment of the area. Fossil evidence can use for interpret the deposition environment or source of the sediments. Moreover, the study in detailed under microscope and scanning electron microscope (SEM) can be used to identify the species of fossils which can reveal the more specific data about their habitat area.

Firstly, the procedure starts with the selection of sediment sample that has abundant of fossil approximately 100 grams, after it was dried by the oven at 70°C for 24 hours, then sieving with mesh no. 18, 35, and 60 to sort mineral grains out and bring fossil remain to identify species under microscope and scanning electron microscope (SEM) for microfossil further (Figure 3.15 and 3.16).

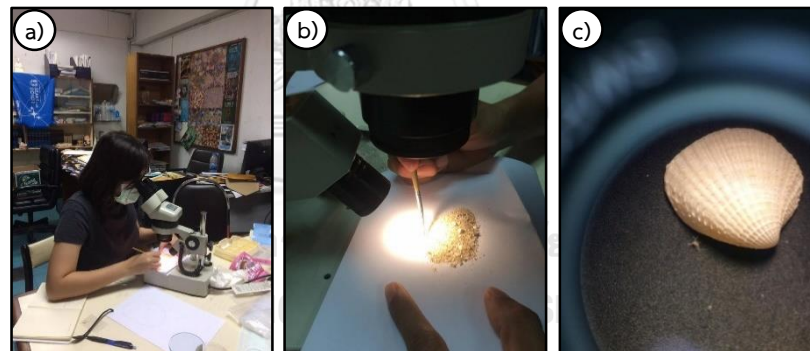


Figure 3.16 The study of fossil identification under microscope following a), b) Taking sediments which abundant of fossil to sort sediment out and bring only fossil to study, and c) The picture of fossil was prepared for species identification under microscope.



Figure 3.17 The study of fossil identification by scanning electron microscope (SEM) following a) Microfossils that were sort out under microscope for study by scanning electron microscope (SEM) were arrayed on the stub before put into the scanning electron microscope (SEM), b) Putting the stub that cover with microfossils into scanning electron microscope (SEM), and c) The picture of microfossil by scanning electron microscope (SEM) was prepared for species identification.

3.3.3 Age determination by optically stimulated luminescence (OSL)

Luminescence dating is well known method for studying in Quaternary research such as paleo-climate, archaeology, evolution of landform, and Quaternary materials. Age determination is a part of luminescence dating method for Quaternary research that can solve the age of sediment in the past for understanding paleo-climate and evolution of landform and it can clearly identify the environment and timing when analyze together with fossil identification. The evaluation of the paleo-time in sediment can be done by using luminescence techniques by Preusser et al. (2008) and these methods used principle of optically and thermally sensitive light or luminescence signal. Especially, quartz and feldspar are mineral grains which mostly used for evaluation. The principle of these techniques are upon the period after mineral grains was last exposed to daylight or heated up to 100°C and absorbed the energy. When mineral grains exposure to light or are heated, the luminescence signal in grains is erased, then it is completely removed. After that mineral grains are sealed from daylight and remain at normal temperatures, the luminescence signal

accumulates again, and being induced by naturally occurring radioactivity. The amount of energy that was absorbed per mass of mineral is $1 \text{ J kg}^{-1} = 1 \text{ Gy}$ (Gray).

The luminescence method that was used in this research is optically stimulated luminescence dating (OSL dating), which uses a principle of determining the age of burial of quartz or feldspar bearing sediments based on the radiation and excitation in crystal lattices, and stems from the real condition which has an imperfect in a crystal lattice, in addition they must have the ability to reserve the ionizing energy (Aitken, M.J, 1998; Botter-Jensen et al., 2003; Lian, 2007). This luminescence method consists of 2 significant parameters for calculation. The first parameter is equivalent dose determination (ED) and the other part is annual dose calculation (AD). The OSL radiation in sediments comes from alpha, beta, and gamma radiation that emitted during the decay of ^{235}U , ^{238}U , ^{232}Th , ^{40}K , and ^{87}Rb , and their daughter products, in the mineral grains and their surroundings, and from cosmic rays. The radiation is absorbed by the crystal lattice on sediment burial, and over time, excites electrons causing them to migrate within the crystal and become stored in “traps” resulting from crystal lattice defects. This energy is then released as photons in visible wavelengths which called “luminescence” on photon irradiation either by exposure to sunlight or artificial light, or by heating at approximately 500°C resetting the clock. In conditions of restricted laboratory, the sample was collected under light-restricted conditions, controlled exposure of the sample to photons yields a luminescence response which is the equivalent dose (ED), the intensity of which is a function of the dose rate within the sediment, and the length of time the sample was exposed to the background radiation.

The main component of an OSL laboratory is the reader machine. This device facilitates the determination of equivalent dose (ED), and the creation of a luminescence growth curve, which plots the relation between luminescence intensity and laboratory dose rates (beta dose), for a particular sample aliquot that containing approximately 100 grains per sample. The first exposing of the sample aliquot is for

getting a quantity of photons in term of blue wavelength and determining the luminescence that occurs in response. The sample is irradiated with increasing radiation levels (beta), and re-exposed to determine the luminescence which occurs at each irradiation level. Then the equivalent dose (ED) is determined by applying a regression to the data, and determining the radiation dose that corresponds to the initial luminescence signal. Additionally, the age determination is calculated by the equivalent dose (ED) divided by the annual dose (AD) which is measured on the surrounding sediments following this equation:

$$\text{Age (kyr)} = \text{Equivalent Dose (Gy)} / \text{Annual Dose (Gy/kyr)}$$

Where;

Equivalent Dose (Unit in Gy): The total accumulated dose that received by irradiation from natural radioactivity and preserve this record through time. In the case of sediments, residual intensity from the bleaching experiment is considered.

Annual dose (Unit in Gy/kyr): Irradiation dose per year from natural radioactivity. Annual dose is calculated from the chemical data of radiogenic elements (which consist of Uranium, Thorium, and Potassium) and cosmic ray evaluation.

In order to identify the age, there must have two parameters which are the environmental dose rate (Annual dose; AD) and the laboratory dose of radiation (Equivalent dose; ED) which gives the same intensity of luminescence as did in AD. The equivalent dose (ED) is divided by the dose rate yields time. Despite the fundamental concept is straight-forward, there are many caveats that must be accounted for stemming from partial bleaching of grains during burial, mixing of grains by bioturbation, and soil formation processes which alter the dose rate over time (Bateman et al., 2006). The treatment preparation of sediment samples for OSL analysis which include

of the method for annual dose (AD) calculation and equivalent dose (ED) determination following these steps below (Figure 3.17).

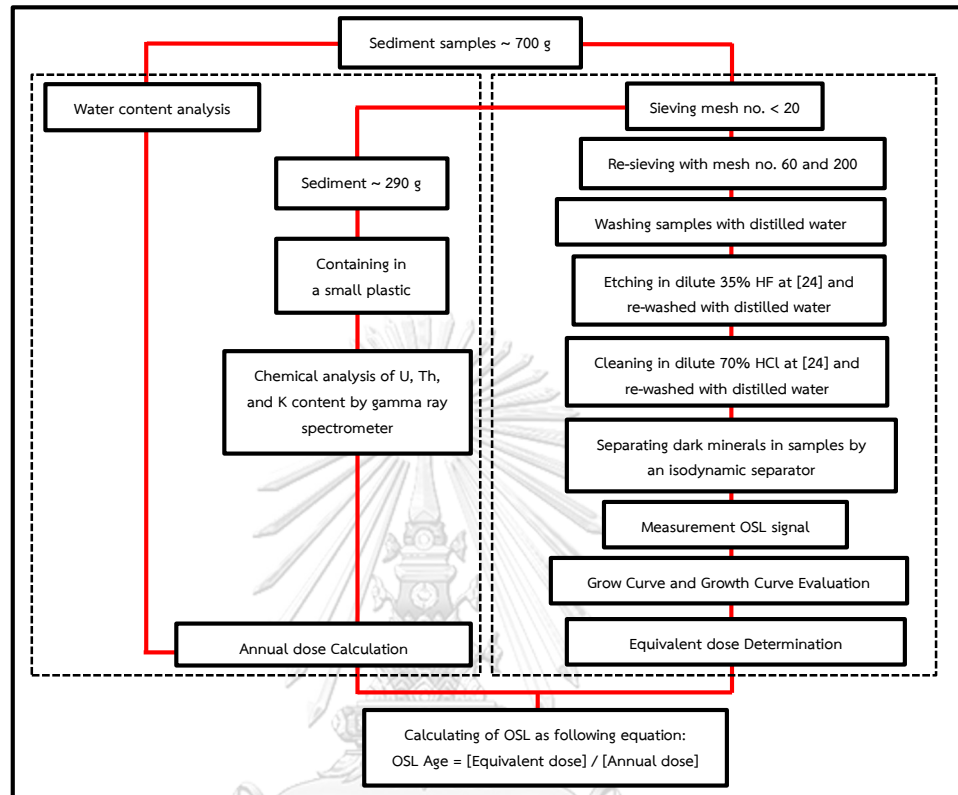


Figure 3.18 The flow chart of methodology for age determination. (Modified after Pailoplee, 2004)

- Annual dose calculation (AD)

For annual dose calculation (AD) which use a principle of ionizing radiation from their radioactive contents together with a small fraction of cosmic ray (Aitken, M. J. , 1985). The radioactive elements which conduct to annual dose rate consist of Uranium (U), Thorium (Th), and Potassium (K_2O). Uranium (U) and Thorium (Th) have a result of decay in α , β and γ radiation, while Potassium (K_2O) has a result of decay in β and γ radiation. Annual dose calculation consists of 2 steps below.

1) Calculation of water content in sediment grains

Water content analysis is a significant parameter for annual dose determination. This is a calculation of the quantity of surface moisture that was preserved around sediment grains. In addition, this is the first step which must be done first after back from field work due to moisture surface in sediment grains is easy evaporation.

Firstly, weighing beakers and note in the table before putting sediment in, then putting sediment samples from fieldwork approximately 45 grams in beakers 100 milliliters and weighing them and note in the table. After that dry them in the oven at 70 °C for 24 hours and weight them again and note. So, there are the weight of beakers, wet sample, and dried sample for water content calculation which be ready for annual dose determination further (Figure 3.18). The formula of water content analysis for each samples is following:

$$\text{Water content (\%)} = \frac{(\text{Weight of wet sample} - \text{Weight of dried sample})}{\text{Weight of dried sample}} \times 100$$

2) Measurement of U, Th and K contents and evaluation of cosmic ray component by gamma ray spectrometer

Firstly, dry the sediment samples from the plastic bags that were picked from fieldwork at 80°C for 7-8 hours, then sieving sediment samples with mesh no.20 and containing them approximately 290 grams in plastic boxes. Taking plastic boxes with sediment samples to calculate with Gamma Ray Spectrometer (Figure 3.19 and 3.20).



Figure 3.19 The steps for annual dose calculation by gamma ray spectrometer following a) Gamma ray spectrometer, b) Sediment samples in plastic boxes are prepared for putting in gamma ray spectrometer, and c) Putting the box into gamma ray spectrometer and start calculation.

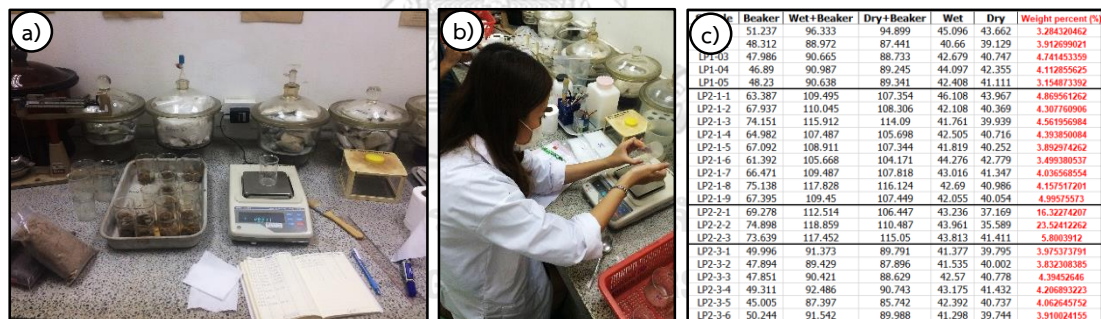


Figure 3.20 The steps for water content analysis following a) and b) Weighting wet and dry sediments (after baked in the oven) in beakers for water content calculation, and c) The table shows weight percent of sediments from water content calculation.

- Equivalent Dose Determination

For equivalent dose determination (ED) which must be done under dark-room in red light conditions consist of 4 steps below (Figure 3.21, 3.22, 3.23, 3.24, and 3.25).

1) Sieving sediments (which were sampling in pvc tubes with endcap to prevent from sunlight in field and any kinds of lights but red light in laboratory is allowed because it does not disturb the samples) with mesh no.20 in the water for getting rid of sediments in grain-size up to very coarse sand and organic materials.

2) Re-sieving in the water again with mesh no.60 and 200 for making sure that will get the purify sediment samples and using the sediment under mesh no.60 and above 200 to washing several times with distilled water.

3) Taking them to etch in dilute 35% of HF at 24% concentration. and leaving until 15 minutes for dissolved the plagioclase minerals, clay particles, and to remove the outermost rind of the quartz grain then re-washed with distilled water, after that leaving in dilute 70% HCl at 24% concentration and 15 minutes leaving for eliminating organic materials and carbonates and re-washed with distilled water till they are clean. Then drying them in the oven for 24 hours.

4) After that taking them to separate heavy minerals and magnetic minerals with an isodynamic separator for getting only concentrate quartz sands in the appropriate size before OSL signal measurement and grow curve and growth curve evaluation. Finally, equivalent dose determination will be done by a Risø TL/OSL reader.

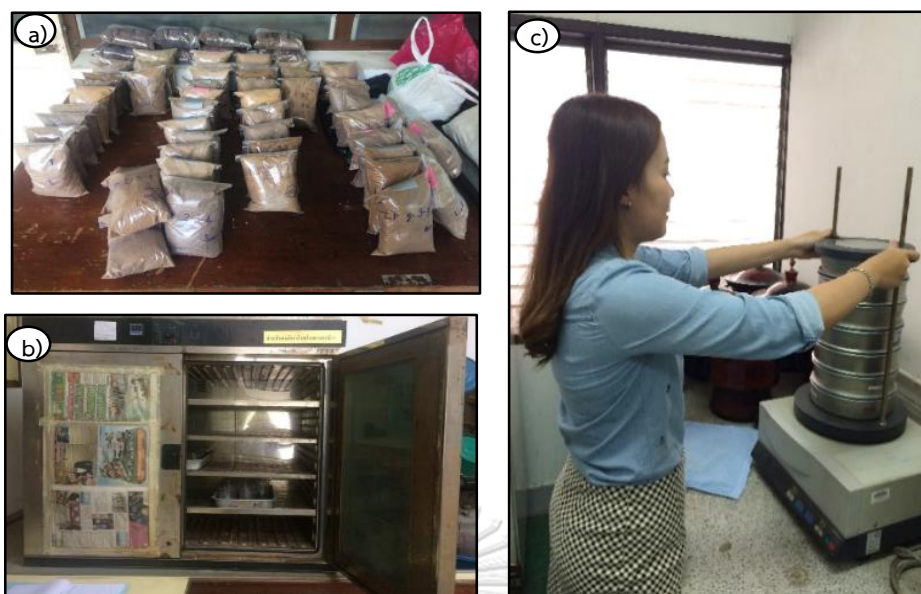


Figure 3.21 The steps for preparing sediment samples for annual dose calculation following a) Sediment samples in plastic bags from fieldwork, b) Drying all of sediment samples in the oven, and c) After sediments were dried, then sieving sediments with sieve shaker and containing sediment over 20 mesh in plastic box.

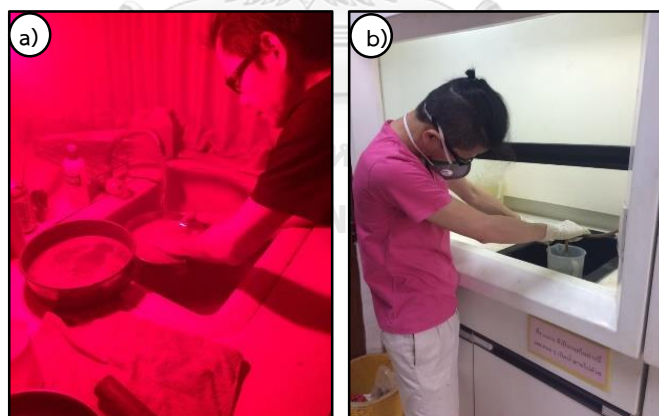


Figure 3.22 The steps for equivalent dose evaluation following a) Sieving sediments with mesh no.20 in red light in laboratory, b) Dilute HCl and HF for etching plagioclase minerals, organic matter, carbonate and clay particles.

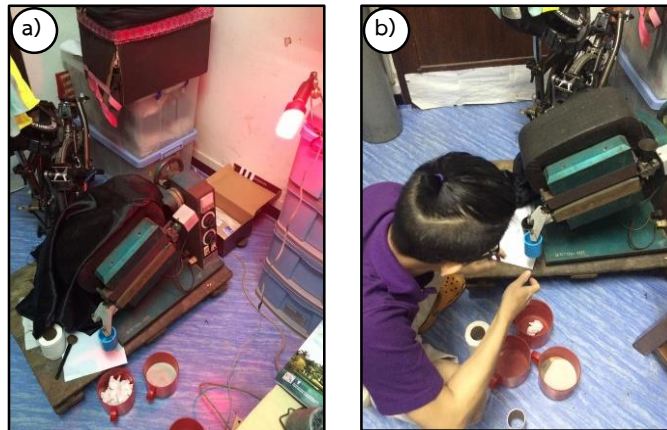


Figure 3.23 The steps for equivalent dose evaluation following a) An isodynamic separator and b) Putting sediment samples into an isodynamic separator for separating heavy minerals and magnetic minerals.

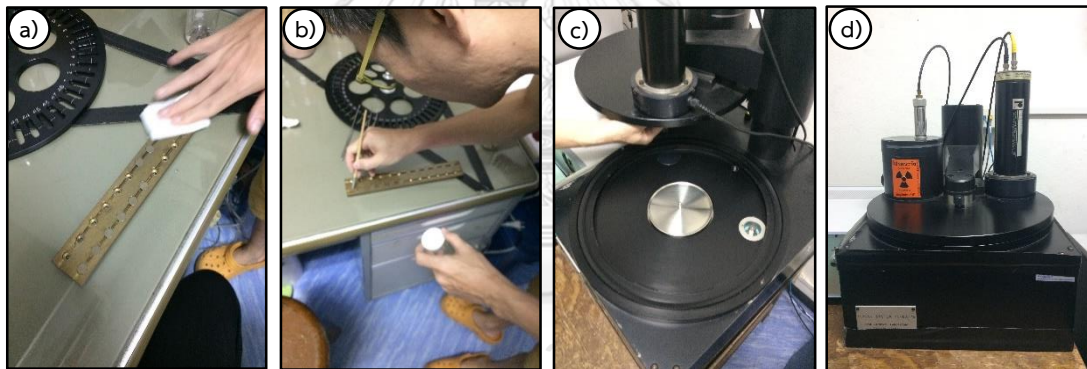


Figure 3.24 The steps for equivalent dose evaluation following a) Cleaning sample trays, b) Putting sediment samples in each of trays and then put trays onto the circle carousel, c) A Risø TL/OSL reader are ready for putting the circle carousel on, and d) Closing and start running a Risø TL/OSL reader for equivalent dose evaluation.



Figure 3.25 A Risø TL/OSL reader for equivalent dose evaluation.

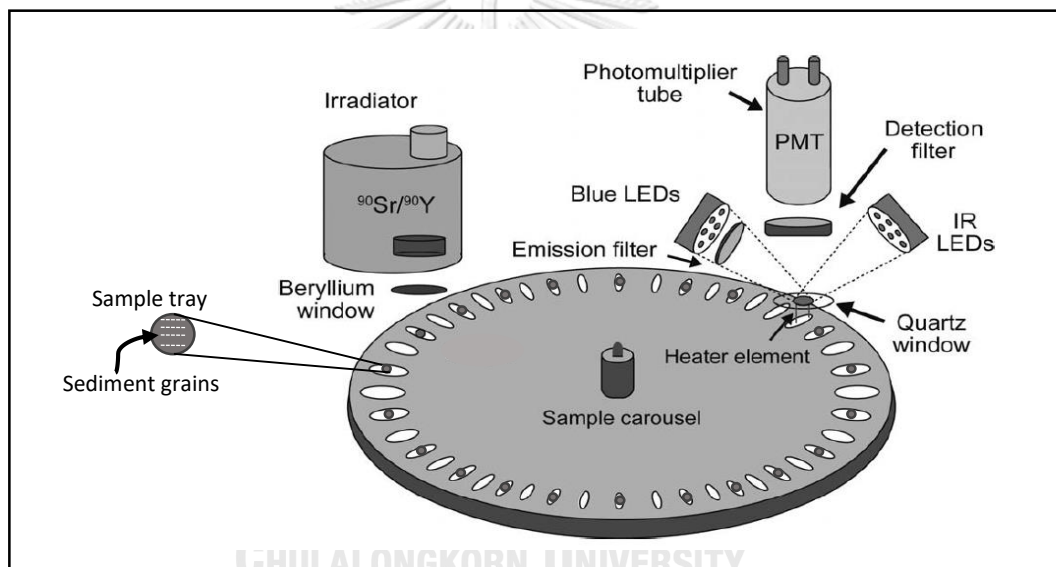


Figure 3.26 This drawing picture shows the mechanism inside a Risø TL/OSL reader that redrawn from Risø National Laboratory. (Modified after Preusser et al., 2008)

CHAPTER 4

RESULTS

4.1 Geomorphological description

Geomorphological description of Laem Pho study area was firstly done by the interpretation of satellite image that clearly show characteristics of each morphology. After satellite interpretation, field survey was conducted to study stratigraphic record from coring. Stratigraphic record from coring is the best tool to describe depositional environment and to recheck with geomorphological interpretation. After field survey, some locations may be changed or modified from the first interpretation. Geomorphological units in Laem Pho study area were divided into 3 units which consist of old sandy beach, young sandy beach, and old lagoon (Figure 4.1 and 4.2).

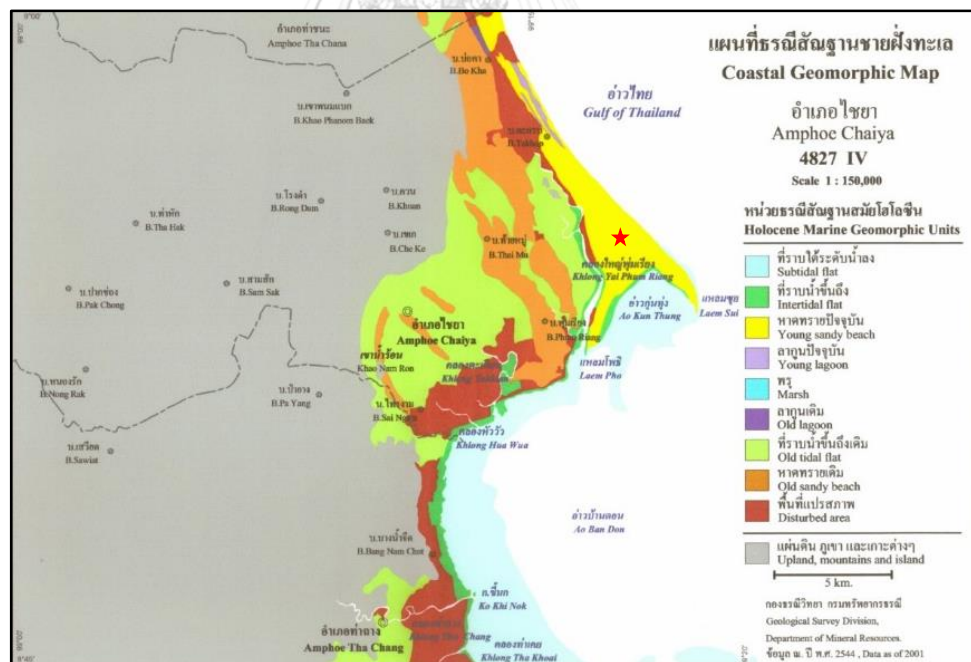


Figure 4.1 The coastal geomorphic map of Amphoe Chaiya where Laem Pho study area is located (red star).

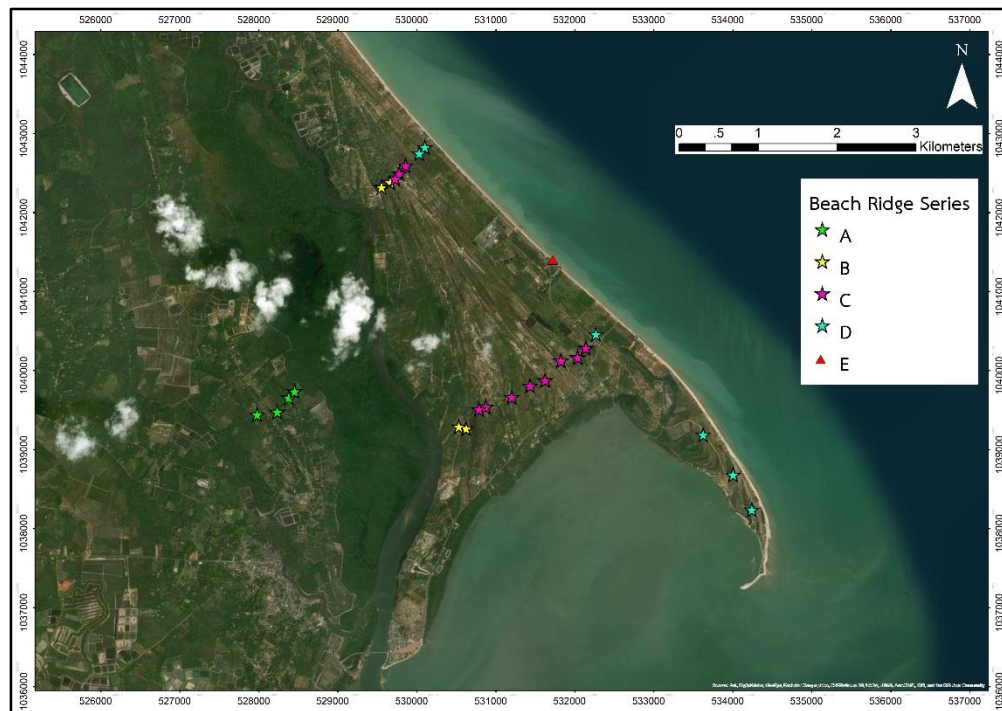


Figure 4.2 Geomorphological of study area from satellite image and the different color star are boundary of study locations.

Old sandy beaches

Beach ridges are dominant landforms in this study area. They are dominantly composed of sand or sediment both from longshore transportation and reworked from underlying material. Beach ridges are generally formed during high wave conditions and/or elevated water levels such as storm surges, or by the combination of wave and aeolian deposition (Hesp, P., 2005; Otvos, 2000). Beach ridges usually define as relict, semi-parallel, multiple wave and wind-built landforms which occurred in the intertidal and supratidal zones. The direction form is parallel or perpendicular to the shoreline upon the shoreline current and wave direction. The height of ridge is usually up to high tide level. The forming of costal barriers is as mainland beaches in marine transgression phase and in a pattern of beach ridges and lagoons in regression phase. Behind one beach ridge, there may be a higher ridge running parallel and formed when wave height was higher which is called swale or runnel that usually found between two ridges. In addition, beach ridges may consist of relict strand plain ridges and wind-

blown eolian sand on top. The rising of water level can submerge beach ridges causing of erosion then become less distinct.

Laem Pho study area has gigantic beach ridge plains together with swales which are dominant landforms in the central part of the study area (Figure 4.3). Beach ridges can be separated into 3 series of orientation as inner ridges, middle ridges, and outer ridge. Especially, middle and outer ridges are the indication of paleo-shoreline showing sediments transportation and deposition from north to south direction. Each beach ridge is divided by wet, dry, and vegetation swale, or old lagoon.



Figure 4.3 Old sandy beach in the study area.

Young sandy beaches

Young sandy beaches are located along shoreline and formed by deposition of particles which have been carried by water currents from other areas. Materials to form beach may be partly transported alongshore from the place that shore erosion occurred, and from the land via canals.

Lame Pho study area, young beach is located between the old sandy beaches eastward to the present shoreline (Figure 4.4). There are partly barrier beaches which consist of modern sand spit and dunes. The height of beaches is varying between 0.5-2 meters and sediments are composed of quartz sand and marine fauna that brought up to deposit on beach by wave current in monsoon season. Young beach ridges include sand bars that are forming in front of beaches. At the study area, the formation of modern sand spit growing to the south indicates the south direction of longshore current.

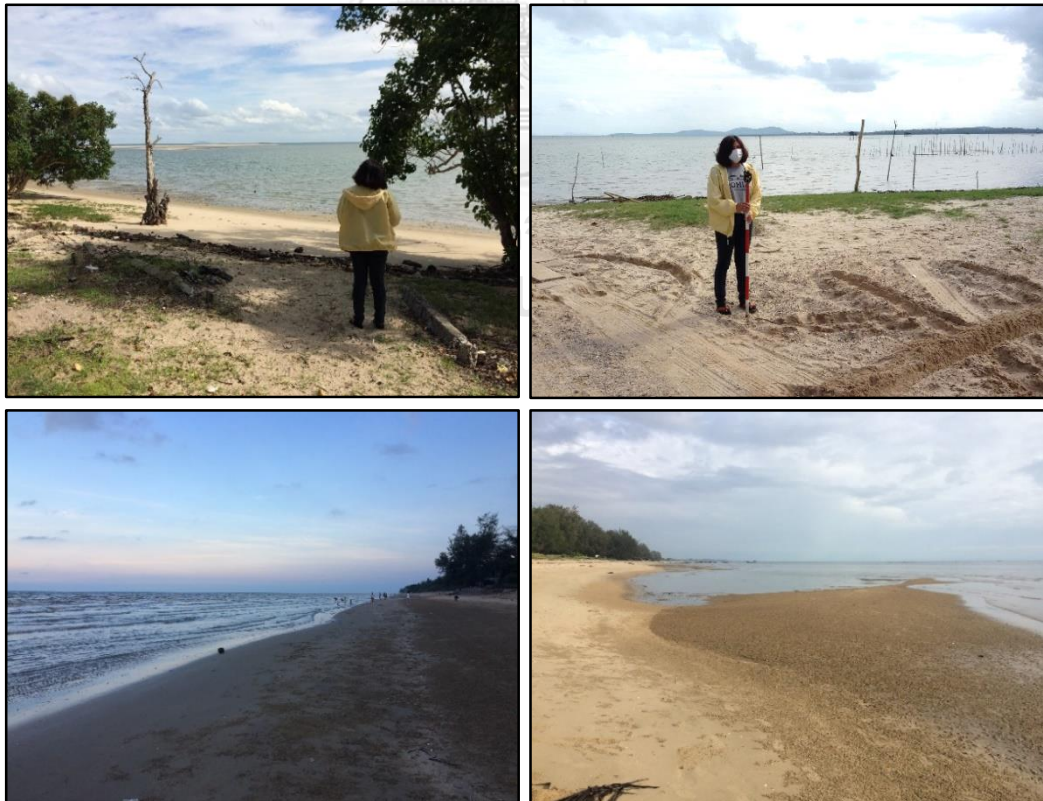


Figure 4.4 Young sandy beach in the study area.

Old Lagoon

A lagoon is a shallow body of water behind beaches or barrier beaches which can be separated from a larger body of water by barrier islands, parallel to the shoreline, connect to the sea through a channel or seepage through a barrier. Besides, the large lagoon probably has an evidence of tidal flat and marsh. The development of barrier- lagoon morphology occurs along coasts with a small tidal range. There is fine-grained sediment that supplied to lagoons as suspended materials in seawater through the past of barrier. There is abundant of organic material from vegetation along shores of the lagoon. In tropical zone, there are systems of trees with aerial root (mangroves) at the

shallow border of the lagoon. Swale is kind of old lagoon that develops after regression and located between 2 ridges (Chaimanee, 2001). The morphologic feature of swale is “a long narrow, generally shallow, trough like, elongate depression between two beach ridges, aligned roughly parallel with the coastline” (Bates and Jackson, 1980).

Laem Pho study area, sediment deposition is mostly sand interbedded with marine clay, and has an evidence of organic matter and marine fossil. There are wet, dry and vegetated swales in this area. In present day, old lagoons are shallow and deposit with sediments which can called dry swales are used for palm tree plantation, vegetated swale and wet swales become shrimp farm or water pond for agriculture (Figure 4.5).



Figure 4.5 Old lagoon in the study area.

4.2 Topographic survey

From a result of remote sensing interpretation, geomorphological landforms in this area from the west to the east include tidal channel, former beach ridge plain (beach ridge and swale) and modern sand spit. There are 3 lines of topography survey measurement. The topography survey of line 1 indicated that maximum elevation of beach ridge plain is about 4 meters above present mean sea-level. The elevation relief of beach ridge and swale on beach ridge plain is less than 1 meters (Figure 4.6). The topography survey of line 2 indicated that maximum elevation of beach ridge plain is almost 2 meters above present mean sea-level. The elevation relief of beach ridge and swale on beach ridge plain is less than 1 meters (Figure 4.7). The topography survey of line 3 indicated that maximum elevation of beach ridge plain is almost 4 meters above present mean sea-level. The elevation relief of beach ridge and swale on beach ridge plain is almost -1 meters (Figure 4.8). They indicate the continuation of progradation in eastward direction (landward).

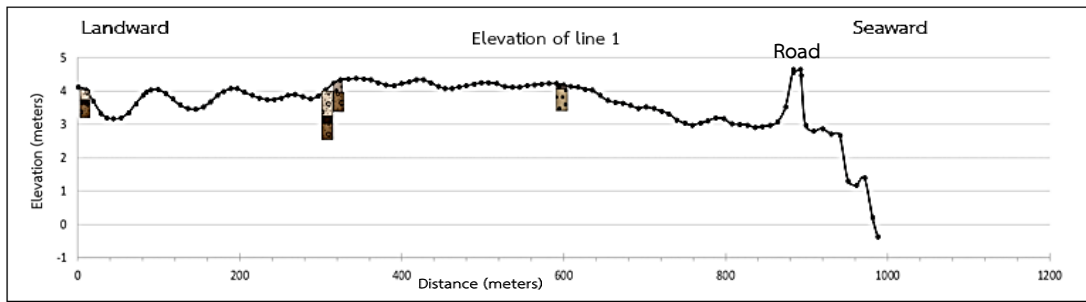


Figure 4.6 This linear graph showing topographic profile from topographic survey measuring of line 1.

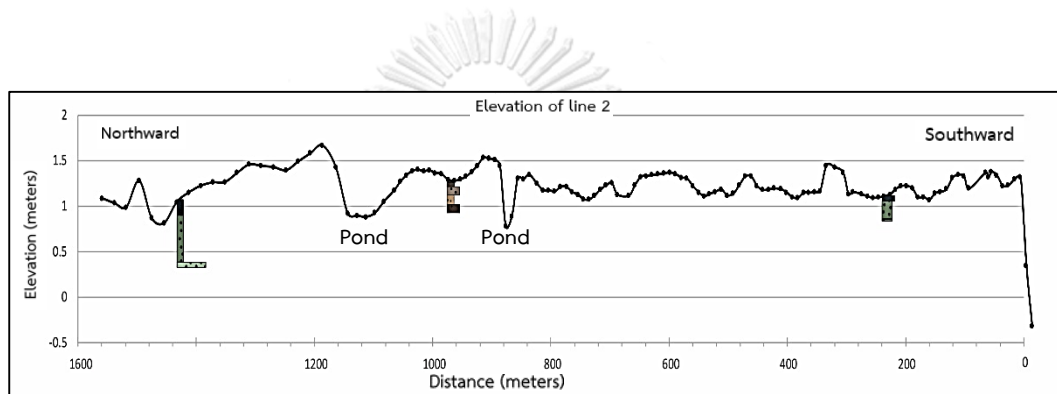


Figure 4.7 This linear graph showing topographic profile from topographic survey measuring of line 2.

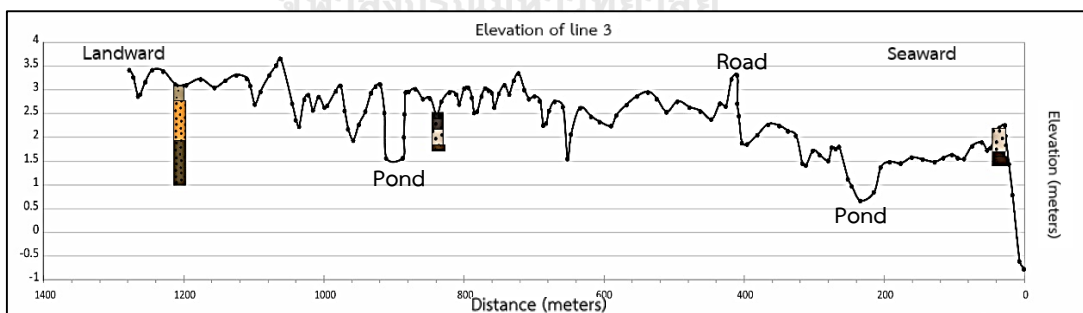


Figure 4.8 This linear graph showing topographic profile from topographic survey measuring of line 3.

4.3 Lithostratigraphical analysis

4.3.1 Lithostratigraphical description from coring

Core description is widely used to characterize the features and depositional environments of sediments (Lason et al., 1997). These processes are benefit for explanation paleo-depositional environment. The interpretation is on sediments recorded and other evidences appear along each cores. The group of description is upon categories of landform classification before. Lithostratigraphical description in this study consists of 15 cores that can represent characteristics of sediments in each of landform (Figure 4.9).

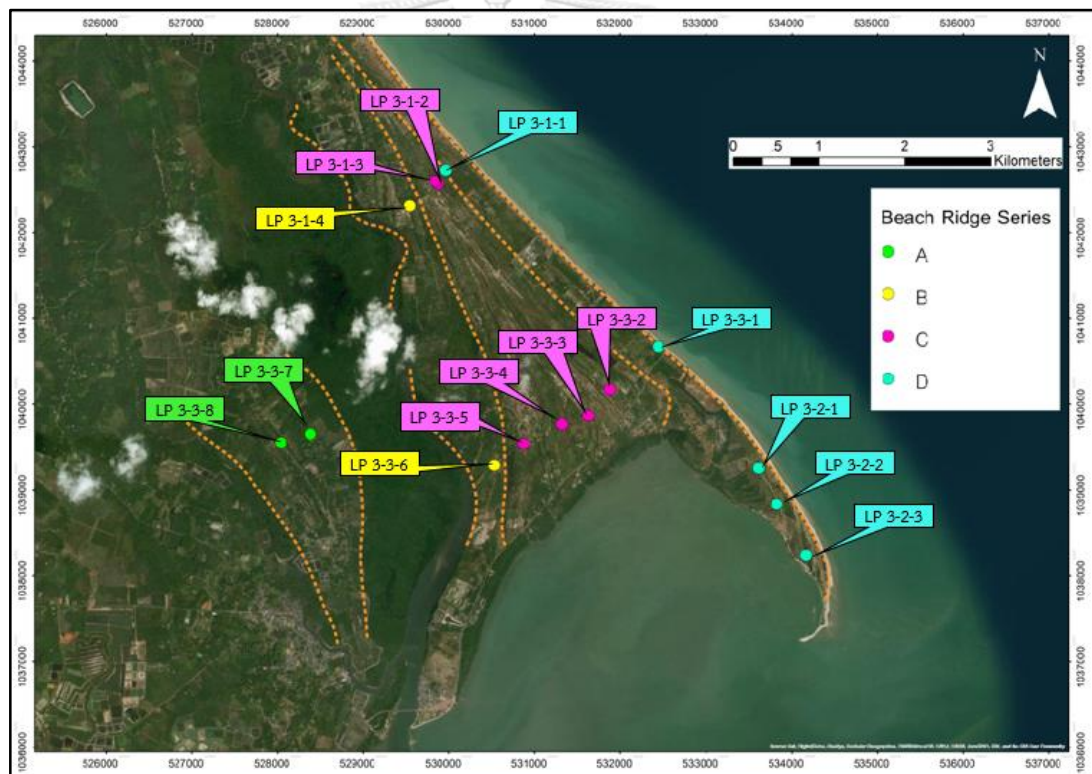


Figure 4.9 Lithostratigraphic locations from coring in each of geomorphological units on satellite image.

Station: LP 3-1-1 UTM grid of 529541 E 1042309 N

There are classified into 3 lithological layers which consist of 0-30 cm is very coarse to coarse sand in gray color with organic topsoil and rootlets, 30-45 cm is very coarse to coarse sand in very dark brown color, and 45-85 cm is very coarse to coarse sand in brown color. All of layer contact is gradational contact. This depositional environment is a characteristic of beach ridge deposit (Table 4.1).

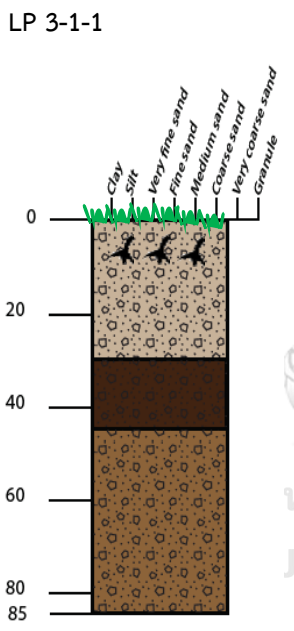
Lithology	Layer contact	Thickness (cm)	Description
		30	Organic topsoil and rootlets at 0 - 10 cm; gray; very coarse to coarse sand
	Gradational contact	15	Very dark brown; very coarse to coarse sand
	Gradational contact	40	Brown; very coarse to coarse sand

Table 4.1 The lithological log of beach ridge at station LP 3-1-1.

Station: LP 3-1-2 UTM grid of 529872 E 1042570 N

There are classified into 3 lithological layers which consist of 0-70 cm is very coarse to coarse sand in gray color with organic topsoil and rootlets, 70-90 cm is very coarse to coarse sand in very dark brown color, and 90-135 cm is very coarse to coarse sand in brown color. All of layer contact is gradational contact. This depositional environment is a characteristic of beach ridge deposit (Table 4.2).

Lithology	Layer contact	Thickness (cm)	Description
	Gradational contact Gradational contact	70 20 45	Organic topsoil and rootlets at 0-10 cm; light gray; very coarse to coarse sand Very dark brown; very coarse to coarse sand Brown; very coarse to coarse sand

Table 4.2 The lithological log of beach ridge at station LP 3-1-2.

Station: LP 3-1-3 UTM grid of 529841 E 1042599 N

There are classified into 3 lithological layers which consist of 0-30 cm is coarse sand in gray color with organic topsoil and rootlets, 30-90 cm is coarse to very coarse to coarse sand in brown color, and 90-95 cm is coarse sand in very dark brown color. All of layer contact is gradational contact. This depositional environment is a characteristic of beach ridge deposit (Table 4.3).

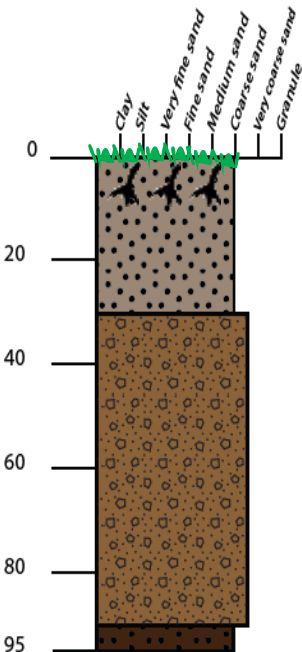
Lithology	Layer contact	Thickness (cm)	Description
<p>LP 3-1-3</p> 	<p>Gradational contact</p> <p>Gradational contact</p>	<p>30</p> <p>60</p> <p>5</p>	<p>Organic topsoil and rootlets at 0-10 cm; gray; coarse sand</p> <p>Brown; very coarse to coarse sand</p> <p>Very dark brown; coarse sand</p>

Table 4.3 The lithological log of beach ridge at station LP 3-1-3.

Station: LP 3-2-2 at UTM grid of 533826 E 1038835 N

There are classified into 4 lithological layers which consist of 0-10 cm is sandy loam which has a range of sand size in fine sand in dark gray color with organic topsoil and rootlets, 10-30 cm is medium to fine sand in gray color, 30-50 cm is sandy loam which has a range of sand size in fine sand in brown color, 50-70 cm is sandy loam which has a range of sand size in medium to fine sand in dark gray color. All of layer contact is gradational contact. This depositional environment is a characteristic of swale deposit (Table 4.6).

Lithology	Layer contact	Thickness (cm)	Description
	Gradational contact	10	Organic topsoil and rootlets at 0 - 5 cm; dark gray; sandy loam
	Gradational contact	20	Gray; medium to fine sand
	Gradational contact	20	Light brown; sandy loam
	Gradational contact	20	Dark gray; sandy loam

Table 4.6 The lithological log of beach ridge at station LP 3-2-2.

Station: LP 3-2-3 at UTM grid of 533617 E 1039253 N

There are classified into 6 lithological layers which consist of 0-10 cm is sandy loam which has a range of sand size in coarse to medium sand in gray color with organic topsoil and rootlets at 0 – 5 cm, 10-45 cm is coarse to medium sand in light gray color, and 45-60 cm is sandy loam which has a range of sand size in medium to coarse sand in gray color, 60-.90 cm is sandy loam which has a range of sand size in coarse to medium sand in bluish gray, 90-93 cm is sandy loam in black color with rootlet and organic matter, 93-113 cm is sandy loam which has a range of sand size in medium sand in dark bluish gray with shell and peat fragments. All of layer contact is gradational contact. This depositional environment is a characteristic of swale deposit.

Lithology	Layer contact	Thickness (cm)	Description
	Gradational contact	10	Organic topsoil and rootlets at 0 - 5 cm; dark gray; sandy loam
	Gradational contact	35	Light gray; coarse to medium sand
	Gradational contact	15	Gray; sandy loam
	Gradational contact	30	Greenish gray; sandy loam
	Gradational contact	3	Black; sandy loam; organic matter; rootlets
	Gradational contact	20	Dark bluish gray; sandy loam; shell and peat fragments

Table 4.7 The lithological log of beach ridge at station LP 3-2-3.

Station: LP 3-3-1 at UTM grid of 532446 E 1040672 N

There are classified into 3 lithological layers which consist of 0-30 cm is fine sand in light brownish gray color with organic topsoil and rootlets, 30-110 cm is medium to fine sand in yellowish brown color, and 110-200 cm is medium to fine sand in grayish color with bioclasts and shell fragments. All of layer contact is gradational contact. This depositional environment is a characteristic of beach ridge deposit (Table 4.8).

Lithology	Layer contact	Thickness (cm)	Description
<p>LP 3-3-1</p>	<p>Gradational contact</p> <p>Gradational contact</p>	<p>30</p> <p>80</p> <p>90</p>	<p>Organic topsoil and rootlets at 0 - 10 cm; light brownish gray; fine sand</p> <p>Yellowish brown; medium to fine sand</p> <p>Grayish brown; medium to fine sand; bioclasts; shell fragments</p>

Table 4.8 The lithological log of beach ridge at station LP 3-3-1.

Station: LP 3-3-2 at UTM grid of 531877 E 1040173 N

There are classified into 5 lithological layers which consist of 0-15 cm is coarse to medium sand in very dark gray color with organic topsoil and rootlets, 15-35 cm is coarse to medium sand in dark gray color, 35-75 cm is coarse to medium sand in light gray color, 75-85 cm is very coarse to coarse sand in dark brown color and 85-90 cm is very coarse to coarse sand in very dark brown color. All of layer contact is gradational contact. This depositional environment is a characteristic of beach ridge deposit (Table 4.9).

Lithology	Layer contact	Thickness (cm)	Description
		15	Organic topsoil and rootlets at 0 – 5 cm; very dark gray; coarse to medium sand
	Gradational contact	20	Dark gray; coarse to medium sand
	Gradational contact	40	Light gray; coarse to medium sand
	Gradational contact	10	Dark brown; very coarse to coarse sand
Gradational contact	5	Very dark brown; very coarse to coarse sand	

Table 4.9 The lithological log of beach ridge at station LP 3-3-2.

Station: LP 3-3-3 at UTM grid of 531319 E 1039764 N

There are classified into 3 lithological layers which consist of 0-90 cm is coarse to medium sand in light gray color with organic topsoil and rootlets, 90-100 cm is very coarse to coarse sand in gray color, and 100- 130 cm is very coarse to coarse sand in very dark brown color. All of layer contact is gradational contact. This depositional environment is a characteristic of beach ridge deposit (Table 4.10).

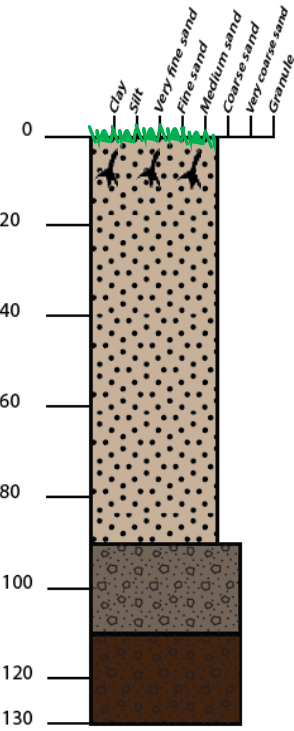
Lithology	Layer contact	Thickness (cm)	Description
<p>LP 3-3-3</p> 	<p>Gradational contact</p>	<p>90</p> <p>10</p> <p>20</p>	<p>Organic topsoil and rootlets at 0 – 10 cm; light gray; coarse to medium to sand</p> <p>Gray; very coarse to coarse sand</p> <p>Very dark brown; very coarse to coarse sand</p>

Table 4.10 The lithological log of beach ridge at station LP 3-3-3.

Station: LP 3-3-4 at UTM grid of 531625 E 1039865 N

There are classified into 3 lithological layers which consist of 0-100 cm is coarse to medium sand in light gray color with organic topsoil and rootlets, 100-120 cm is coarse to medium sand in very dark brown color, and 120-160 cm is very coarse to medium sand in very dark brown color. All of layer contact is gradational contact. This depositional environment is a characteristic of beach ridge deposit (Table 4.11).

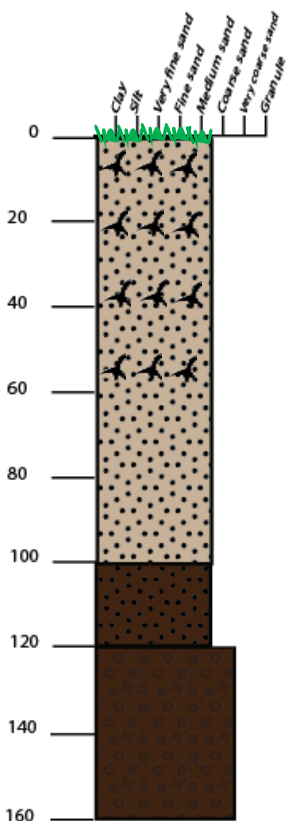
Lithology	Layer contact	Thickness (cm)	Description
	<p>Gradational contact</p> <p>Gradational contact</p>	<p>100</p> <p>20</p> <p>40</p>	<p>Organic topsoil at 0 – 10 cm and rootlets at 0 - 60 cm; light gray; coarse to medium sand</p> <p>Very dark brown; coarse to medium sand</p> <p>Very dark brown; very coarse to medium sand</p>

Table 4.11 The lithological log of beach ridge at station LP 3-3-4.

Station: LP 3-3-5 at UTM grid of 530869 E 1039539 N

There are classified into 3 lithological layers which consist of 0-90 cm is medium sand in light gray color with organic topsoil and rootlets, 90-120 cm is very coarse to coarse sand in very dark brown color, and 120-150 cm is very coarse to coarse sand in strong brown color. All of layer contact is gradational contact. This depositional environment is a characteristic of beach ridge deposit (Table 4.12).

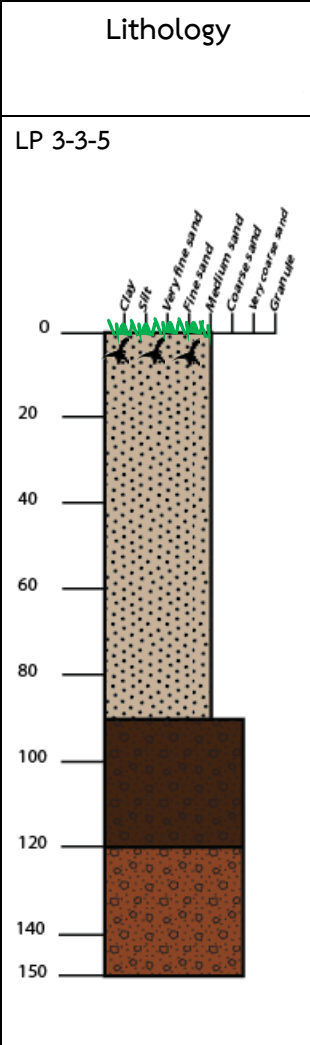
Lithology	Layer contact	Thickness (cm)	Description
	<p>Gradational contact</p> <p>Gradational contact</p>	<p>90</p> <p>30</p> <p>30</p>	<p>Organic topsoil and rootlets at 0 – 10 cm; light gray; medium sand</p> <p>Very dark brown; very coarse to coarse sand</p> <p>Strong brown; very coarse to coarse sand</p>

Table 4.12 The lithological log of beach ridge at station LP 3-3-5.

Station: LP 3-3-6 at UTM grid of 530529 E 1039288 N

There are classified into 4 lithological layers which consist of 0-60 cm is medium sand in light gray color with organic topsoil and rootlets at 0 – 20 cm, 60-150 cm is very coarse to coarse sand in light brown color, 150-180 cm is very coarse to coarse sand in strong brown color, 180-200 cm is very coarse to coarse sand in very dark brown color, and 200-240 cm is very coarse to coarse sand in brown color. All of layer contact is gradational contact. This depositional environment is a characteristic of beach ridge deposit (Table 4.13).

Lithology	Layer contact	Thickness (cm)	Description
<p>LP 3-3-6</p> <p>0 20 40 60 80 100 120 140 160 180 200 220 240</p> <p>Clay Silt Very fine sand Fine sand Medium sand Coarse sand Very coarse sand Granule</p>	<p>Gradational contact</p> <p>Gradational contact</p> <p>Gradational contact</p> <p>Gradational contact</p>	<p>60</p> <p>90</p> <p>30</p> <p>20</p> <p>40</p>	<p>Organic topsoil and rootlets at 0 – 20 cm; light gray; medium sand; rootlets</p> <p>Light brown; very coarse to coarse sand</p> <p>Strong brown; very coarse to coarse sand</p> <p>Very dark brown; very coarse to coarse sand</p> <p>Brown; very coarse to coarse sand</p>

Table 4.13 The lithological log of beach ridge at station LP 3-3-6.

Station: LP 3-3-7 at UTM grid of 528383 E 1039653 N

There are classified into 5 lithological layers which consist of 0-105 cm is medium to fine sand in gray color with organic topsoil and rootlets at 0 – 10 cm, 105-145 cm is very coarse to coarse sand in very dark brown color, 145-175 cm is very coarse to coarse sand in brown color, 175-195 cm is very coarse sand in brown color, and 195-205 cm is coarse sand in brown color. All of layer contact is gradational contact. This depositional environment is a characteristic of beach ridge deposit.

Lithology	Layer contact	Thickness (cm)	Description
		105	Organic topsoil at 0 – 10 cm; gray; medium to fine sand
	Gradational contact	40	Very dark brown; very coarse to coarse sand
	Gradational contact	30	Brown; very coarse to coarse sand
	Gradational contact	20	Brown; very coarse sand
	Gradational contact	10	Brown; coarse sand

Table 4.14 The lithological log of beach ridge at station LP 3-3-7.

Station: LP 3-3-8 at UTM grid of 528040 E 1039551 N

There are classified into 4 lithological layers which consist of 0-40 cm is fine sand in gray color with organic topsoil and rootlets at 0 – 10 cm, 40-90 cm is fine sand in brown color, 90-110 cm is medium sand in very dark brown color, and 110-170 cm is very coarse sand in very dark brown color. All of layer contact is gradational contact. This depositional environment is a characteristic of beach ridge deposit (Table 4.15).

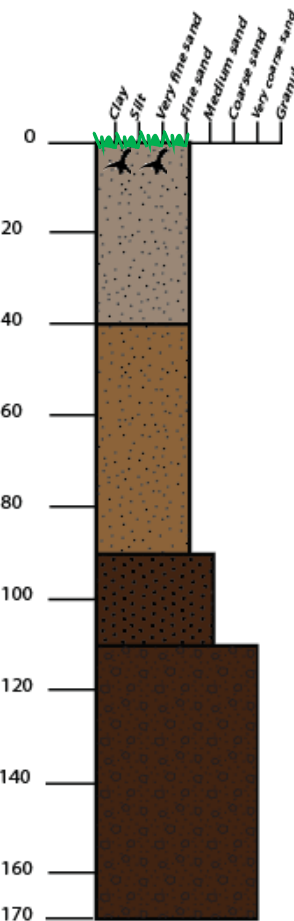
Lithology	Layer contact	Thickness (cm)	Description
<p>LP 3-3-8</p> 	<p>Gradational contact</p> <p>Gradational contact</p> <p>Gradational contact</p>	<p>40</p> <p>50</p> <p>20</p> <p>60</p>	<p>Organic topsoil at 0 – 10 cm; gray; fine sand</p> <p>Brown; fine sand</p> <p>Very dark brown; medium sand</p> <p>Very dark brown; very coarse sand</p>

Table 4.15 The lithological log of beach ridge at station LP 3-3-8.

4.3.2 Lithostratigraphical correlation

Stratigraphic correlation is the important tool for analysis the relationship between sediment strata at different localities by comparing the sediment type and characteristic of, grain size, color, texture, and composition both in vertical and lateral change to understand the paleo-depositional environment of study area.

In Lame Pho study area, after data collect from coring, the stratigraphy of each borehole show the dominant deposition of sand which grain size ranging from very coarse sand to fine sand (Figure 4.10, 4.11, and 4.12). The key bed that outstanding found in mostly boreholes is the sequence of very dark brown sand which present at station LP 3-1-1 to 3-1-3 and LP 3-3-2 to 3-3-8.

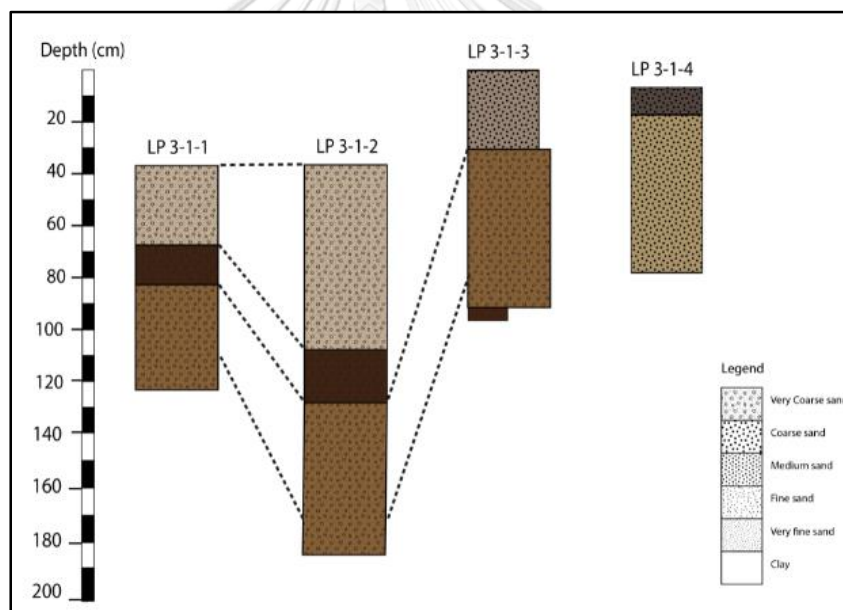


Figure 4.10 The stratigraphic correlation from station LP 3-1-1 to 3-1-4

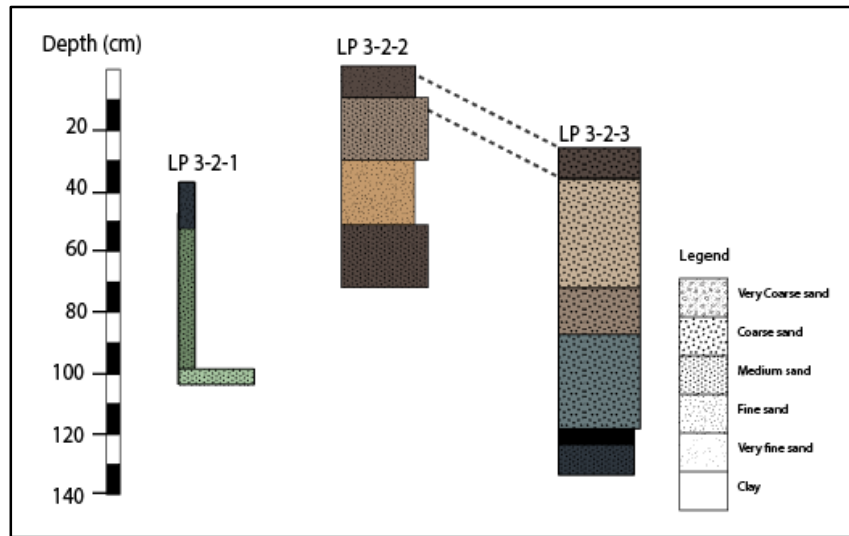


Figure 4.11 The stratigraphic correlation from station LP 3-2-1 to 3-2-3

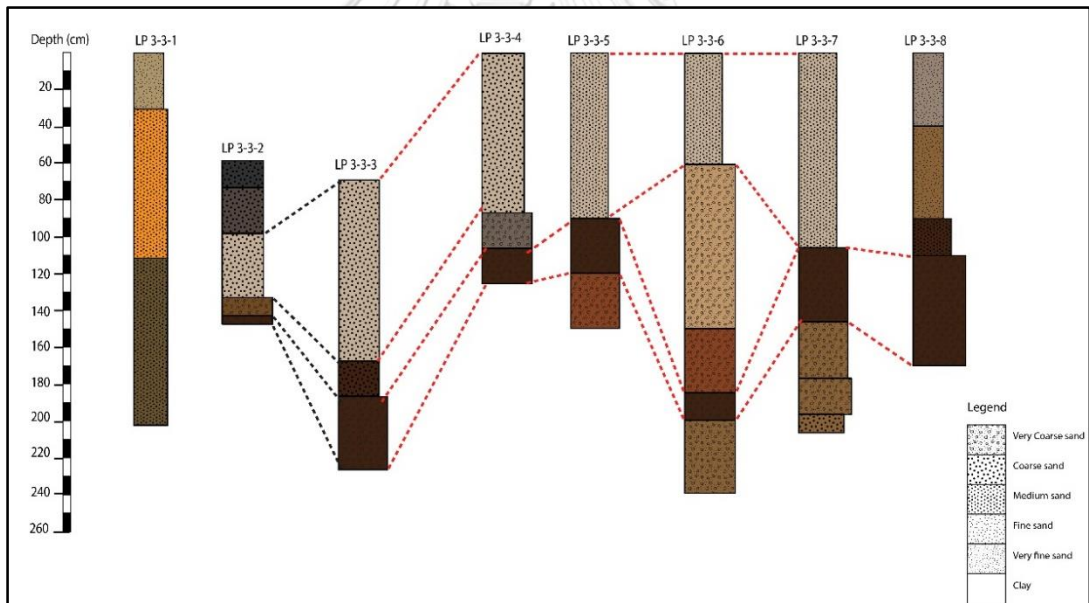


Figure 4.12 The stratigraphic correlation from station LP 3-3-1 to 3-3-8

4.4 Sedimentological analysis

4.4.1 Grain size analysis

Grain size analysis is the quantification of the size of sedimentary particles. Grain size of sediments is upon origin of sources rocks and transport agents, so that size of sediments can indicate the process of erosion and transportation. The purpose of studying in recent sediment is to determine the physical effect of the environment of these parameters for interpreting the relative timing of deposition (Folk, R. L. and Ward, 1957; Sukanraj et al., 2013).

Sieve analysis is a method for determining grain size distribution of soil. The statistics changing (mean, sorting, and skewness) were used to describe in grain size distributions which led us to understand the direction of sediment transportation (McLaren and Bowles, 1985). The characteristic of sediments texture as follows: mean, standard deviation, skewness, and kurtosis are widely used to reconstruct the depositional environments of sediments (Angusamy and Rajamanikam, 2006).

Following Lason et al. (1997), sediments were sieved with U.S. Standard sieves at 1/4-phi (ϕ) unit intervals. Phi (ϕ) is defined as the negative logarithm of the grain dimension in millimeters to the base 2. The equation for the relationship of millimeters to phi scale is:

$$\phi = -\log_2(d_{mm})$$

where

d_{mm} = particle diameter in millimeters

Grain-size analyses include of grain-size distribution tables, cumulative frequency, statistics and graphics of frequency, and probability distribution. Standard grain-size distribution statistics consist of:

- Mean grain size or average grain size
- Standard deviation or the spread of the distribution about the mean- defines the concept of sorting
- Skewness or measure of symmetry of the distribution around the mean
- Kurtosis or measure of the "tailedness" (not its peak) of the probability distribution of a real-valued random variable

These statistical parameters will give individual details on grain-size distribution and its depositional environment. The mean is the most generally used statistic to characterize the average grain size of the distribution. The sorting shows the scatter of the various grain sizes in the distribution, especially well-sorted distribution which contains a limited range of grain sizes and indicates that the depositional environment contains a narrow range of sediment sizes or a narrow band of depositional energy, whereas a poorly sorted distribution contains a wide range of grain sizes showing multiple sources of sediment or a wide range of energies of deposition. Positive skewness indicates an extreme of fine grain sizes, while negative skewness indicates an extreme of coarser grain sizes. The kurtosis indicates the ratio between the sorting in the tails of the distribution relative to the central part (sand size) of the distribution (Lason et al., 1997).

These statistical parameters are generally calculated by two different methods which are the graphic method that uses specific percentiles of a grain-size distribution and the method of moments that uses the entire grain size distribution values to mathematically create the statistical parameters and both methods were summarized by Krumbein and Pettijohn (1938).

In this study, the method of moment was brought to calculate because of it is a computational method (not graphical), more accurate, and easily to understand than graphic method. The results after plotting in each of statistic parameters were

described into 4 series of geomorphological classification which consist of outer ridges, middle ridges, inner ridges, and recent beach following figure 4.13.

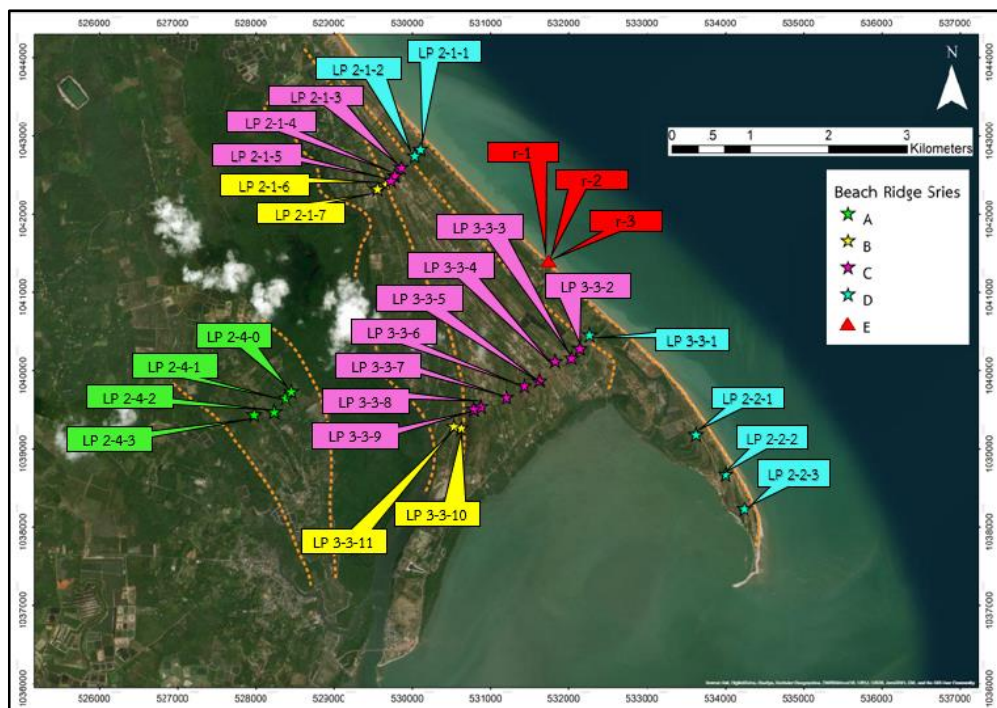


Figure 4.13 Locations of sediment sampling for studying grain size analysis in sediment from series A to E of beach ridge series.

Results of grain size analysis of sediment sampling from series A to series D of beach ridge plains and series E of recent beach are in the table 4.16 to table 4.20.

Sample No.	Mean Grain Size	Standard Deviation (Sorting)	Skewness	Kurtosis	Mean Grain Size	Standard Deviation (Sorting)	Skewness	Kurtosis	Beach Ridge Series
LP 2-4-0	1.63	1.37	-0.46	2.54	Medium sand	Poorly sorted	Very coarse-skewed	Very leptokurtic	A
LP 2-4-1	1.99	1.01	-0.47	3.26	Medium sand	Poorly sorted	Very coarse-skewed	Extremely leptokurtic	
LP 2-4-2	0.80	0.94	1.23	5.22	Coarse sand	Moderately sorted	Very fine-skewed	Extremely leptokurtic	
LP 2-4-3	1.59	0.90	0.16	3.95	Medium sand	Moderately sorted	Fine-skewed	Extremely leptokurtic	

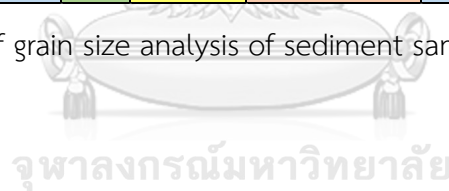
Table 4.16 Result of grain size analysis of sediment sampling from series A of beach ridge series

Sample No.	Mean Grain Size	Standard Deviation (Sorting)	Skewness	Kurtosis	Mean Grain Size	Standard Deviation (Sorting)	Skewness	Kurtosis	Beach Ridge Series
LP 2-1-6	0.81	0.78	0.17	4.14	Coarse sand	Moderately sorted	Fine-skewed	Extremely leptokurtic	B
LP 2-1-7	0.66	0.88	0.58	4.67	Coarse sand	Moderately sorted	Very fine-skewed	Extremely leptokurtic	
LP 2-3-10	1.05	1.03	-0.01	2.99	Medium sand	Poorly sorted	Near-symmetrical	Very leptokurtic	
LP 2-3-11	0.88	0.80	0.73	5.77	Coarse sand	Moderately sorted	Very fine-skewed	Extremely leptokurtic	

Table 4.17 Result of grain size analysis of sediment sampling from series B of beach ridge series

Sample No.	Mean Grain Size	Standard Deviation (Sorting)	Skewness	Kurtosis	Mean Grain Size	Standard Deviation (Sorting)	Skewness	Kurtosis	Beach Ridge Series
LP 2-1-3	0.71	0.87	0.38	3.45	Coarse sand	Moderately sorted	Very coarse-skewed	Extremely leptokurtic	C
LP 2-1-4	1.12	0.69	0.24	3.77	Medium sand	Moderately well sorted	Very coarse-skewed	Extremely leptokurtic	
LP 2-1-5	0.92	0.69	0.57	5.37	Coarse sand	Moderately well sorted	Very fine-skewed	Extremely leptokurtic	
LP 2-3-2	0.69	1.08	0.82	3.61	Coarse sand	Poorly sorted	Very fine-skewed	Extremely leptokurtic	
LP 2-3-3	1.35	0.89	0.05	3.15	Medium sand	Moderately sorted	Near-symmetrical	Extremely leptokurtic	
LP 2-3-4	0.62	0.82	0.64	4.75	Coarse sand	Moderately sorted	Very fine-skewed	Extremely leptokurtic	
LP 2-3-5	1.05	0.72	0.29	5.20	Medium sand	Moderately sorted	Fine-skewed	Extremely leptokurtic	
LP 2-3-6	1.32	0.73	0.37	4.48	Medium sand	Moderately sorted	Very fine-skewed	Extremely leptokurtic	
LP 2-3-7	1.62	0.89	0.07	3.58	Medium sand	Moderately sorted	Near-symmetrical	Extremely leptokurtic	
LP 2-3-8	1.22	0.56	0.22	7.12	Medium sand	Moderately well sorted	Fine-skewed	Extremely leptokurtic	
LP 2-3-9	1.01	0.82	0.33	4.54	Medium sand	Moderately sorted	Very fine-skewed	Extremely leptokurtic	

Table 4.18 Result of grain size analysis of sediment sampling from series C of beach ridge series



Sample No.	Mean Grain Size	Standard Deviation (Sorting)	Skewness	Kurtosis	Mean Grain Size	Standard Deviation (Sorting)	Skewness	Kurtosis	Beach Ridge Series
LP 2-1-1	1.22	0.88	-0.10	2.96	Medium sand	Moderately sorted	Coarse-skewed	Very leptokurtic	D
LP 2-1-2	0.81	0.88	0.37	4.01	Coarse sand	Moderately sorted	Very fine-skewed	Extremely leptokurtic	
LP 2-2-1	2.04	0.59	-0.22	3.43	Fine sand	Moderately well sorted	Coarse-skewed	Extremely leptokurtic	
LP 2-2-2	1.44	0.70	-0.25	3.84	Medium sand	Moderately well sorted	Coarse-skewed	Extremely leptokurtic	
LP 2-2-3	0.83	1.39	0.08	1.67	Coarse sand	Poorly sorted	Near-symmetrical	Very leptokurtic	
LP 2-3-1	1.21	0.82	-0.01	2.71	Medium sand	Moderately sorted	Near-symmetrical	Very leptokurtic	

Table 4.19 Result of grain size analysis of sediment sampling from series D of beach ridge series

Sample No.	Mean Grain Size	Standard Deviation (Sorting)	Skewness	Kurtosis	Mean Grain Size	Standard Deviation (Sorting)	Skewness	Kurtosis	Beach Ridge Series
LP r-1	1.18	0.73	-0.29	3.56	Medium sand	Moderately sorted	Coarse-skewed	Extremely leptokurtic	E
LP r-2	0.50	1.07	0.13	2.50	Coarse sand	Poorly sorted	Fine-skewed	Very leptokurtic	
LP r-3	1.90	0.72	-0.09	5.43	Medium sand	Moderately sorted	Very coarse-skewed	Extremely leptokurtic	

Table 4.20 Result of grain size analysis of sediment sampling from series E of beach ridge series

In addition, grain size parameters from series A to E of beach ridge series along with statistic parameters were summarized into table 4.21 which consist of mean grain size values, standard deviation (sorting) values, skewness values, and kurtosis values of beach ridge series A to E following detail below.

Series A

- Mean Grain Size

The mean grain size values are ranging from 0.80 ϕ (coarse sand) to 1.99 ϕ (medium sand) and the average mean grain sizes value is 1.50 ϕ (medium sand).

- Standard Deviation (Sorting)

The standard deviation values are ranging from 0.90 ϕ (moderately sorted) to 1.37 ϕ (poorly sorted) and the average standard deviation value is 1.05 ϕ (poorly sorted).

- Skewness

The skewness is for measuring the systematic of the distribution or predominance of coarse or fine-sediments. The positive value indicates more material in fine-tail (i.e. fine skewed), while the negative values indicates coarse skewed material. The skewness value ranges from -0.47 (very coarse skewed) to 1.23 (very fine-skewed) and the average skewness value is 0.12 (fine-skewed).

- Kurtosis

The kurtosis is a measure of the "tailedness" of the probability distribution of a real-valued random variable. This heaviness or lightness in the tails usually means that data looks flatter (or less flat) compared to the normal distribution. The standard normal distribution has a kurtosis of 3, so if values are close to that then the graph is nearly normal. These nearly normal distributions are called mesokurtic. If the tails are very thin compared to the normal distribution, these distributions are called platykurtic which is negative kurtosis. If the tails are fatter than the normal distribution, these distributions are called leptokurtic which is an excess positive kurtosis where the kurtosis is greater than 3 (DeCarlo, 1997). The kurtosis value ranges from 2.54 (very leptokurtic) to 5.22 (extremely leptokurtic) and the average kurtosis value is 3.74 (extremely leptokurtic).

Series B

- Mean Grain Size

The mean grain size values are from 0.66 ϕ (coarse sand) to 1.05 ϕ (medium sand) and the average mean grain sizes value is 0.85 ϕ (medium sand).

- Standard Deviation (Sorting)

The standard deviation values are from 0.78 ϕ (moderately sorted) to 1.03 ϕ (poorly sorted) and the average standard deviation value is 0.87 ϕ (poorly sorted).

- Skewness

The skewness value ranges are from -0.01 (very coarse skewed) to 0.73 (very fine- skewed) and the average skewness value is 0.37 (fine-skewed).

- Kurtosis

The kurtosis value ranges are from 2.99 (very leptokurtic) to 5.77 (extremely leptokurtic) and the average kurtosis value is 4.39 (extremely leptokurtic).

Series C

- Mean Grain Size

The mean grain size values are from 0.62 ϕ (coarse sand) to 1.62 ϕ (medium sand) and the average mean grain sizes value is 1.29 ϕ (medium sand).

- Standard Deviation (Sorting)

The standard deviation values are from 0.56 ϕ (moderately well sorted) to 1.08 ϕ (poorly sorted) and the average standard deviation value is 0.75 ϕ (moderately sorted).

- Skewness

The skewness value ranges are from 0.05 (near-symmetrical) to 0.82 (very fine-skewed) and the average skewness value is 0.25 (fine-skewed).

- Kurtosis

The kurtosis value ranges are from 3.15 (extremely leptokurtic) to 7.12 (extremely leptokurtic) and the average kurtosis value is 4.93 (extremely leptokurtic).

Series D

- Mean Grain Size

The mean grain size values are from 0.81 ϕ (coarse sand) to 2.04 ϕ (fine sand) and the average mean grain sizes value is 1.38 ϕ (medium sand).

- Standard Deviation (Sorting)

The standard deviation values are from 0.59 ϕ (moderately well sorted) to 1.39 ϕ (poorly sorted) and the average standard deviation value is 0.87 ϕ (moderately sorted).

- Skewness

The skewness value ranges are from -0.25 (coarse skewed) to 0.37 (very fine-skewed) and the average skewness value is -0.10 (coarse-skewed).

- Kurtosis

The kurtosis value ranges are from 1.67 (very leptokurtic) to 4.01 (extremely leptokurtic) and the average kurtosis value is 2.92 (extremely leptokurtic).

Series E

- Mean Grain Size

The mean grain size values are from 0.50 ϕ (coarse sand) to 1.90 ϕ (medium sand) and the average mean grain sizes value is 1.19 ϕ (medium sand).

- Standard Deviation (Sorting)

The standard deviation values are from 0.72 ϕ (moderately sorted) to 1.07 ϕ (poorly sorted) and the average standard deviation value is 0.84 ϕ (moderately sorted).

- Skewness

The skewness value ranges are from -0.29 (coarse skewed) to 0.13 (fine-skewed) and the average skewness value is -0.08 (near-symmetrical).

- Kurtosis

The kurtosis value ranges are from 2.50 (very leptokurtic) to 5.43 (extremely leptokurtic) and the average kurtosis value is 3.83 (extremely leptokurtic).

Ridge series	Functions	Mean	Sorting	Skewness	Kurtosis
Series A	Max	1.99	1.37	1.23	5.22
	Min	0.80	0.90	-0.47	2.54
	Avg	1.50	1.05	0.12	3.74
Series B	Max	1.05	1.03	0.73	5.77
	Min	0.66	0.78	-0.01	2.99
	Avg	0.85	0.87	0.37	4.39
Series C	Max	1.62	1.08	0.82	7.12
	Min	0.62	0.56	0.05	3.15
	Avg	1.29	0.75	0.25	4.93
Series D	Max	2.04	1.39	0.37	4.01
	Min	0.81	0.59	-0.25	1.67
	Avg	1.38	0.87	-0.10	2.92
Series E	Max	1.90	1.07	0.13	5.43
	Min	0.50	0.72	-0.29	2.50
	Avg	1.19	0.84	-0.08	3.83

Table 4.21 Summary of grain size parameters from series A to E of beach ridge series

The average values of grain size parameters are summarized following table 4.22 and were separated into individual analyze of each parameter among beach ridge series in form of bar chart which consist of mean grain size, standard deviation (sorting), skewness, and kurtosis.

For the mean grain size (Table 4.23), series A, C, D, and E are medium sand, whereas series B is coarse sand.

For the standard deviation (sorting) (Table 4.24), series A is poorly sorted, whereas series B, C, D, and E are moderately sorted.

For the skewness (Table 4.25), series A, and C are fine-skewed, series B is very fine-skewed, series D is coarse skewed, and series E is near-symmetrical.

For the kurtosis (Table 4.26), series A, B, C, and E are extremely leptokurtic, whereas series D is very leptokurtic.

Beach Ridge Series	Mean Grain size	Standard Deviation (Sorting)	Skewness	Kurtosis
A	Medium sand	poorly sorted	fine-skewed	extremely leptokurtic
B	Coarse sand	moderately sorted	very fine-skewed	extremely leptokurtic
C	Medium sand	moderately sorted	fine-skewed	extremely leptokurtic
D	Medium sand	moderately sorted	coarse-skewed	very leptokurtic
E	Medium sand	moderately sorted	near-symmetrical	extremely leptokurtic

Table 4.22 Summary of result of grain size analysis of sediment sampling from series E of beach ridge series

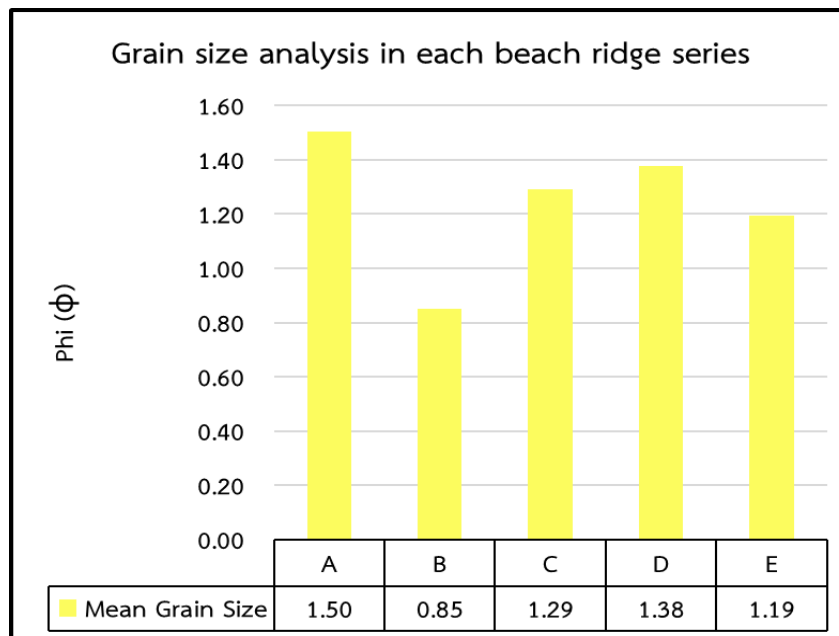


Table 4.23 Bar chart of grain size analysis from series A to E of beach ridge series. This bar graph shows the average mean grain size values of sediment sample from series A to E.

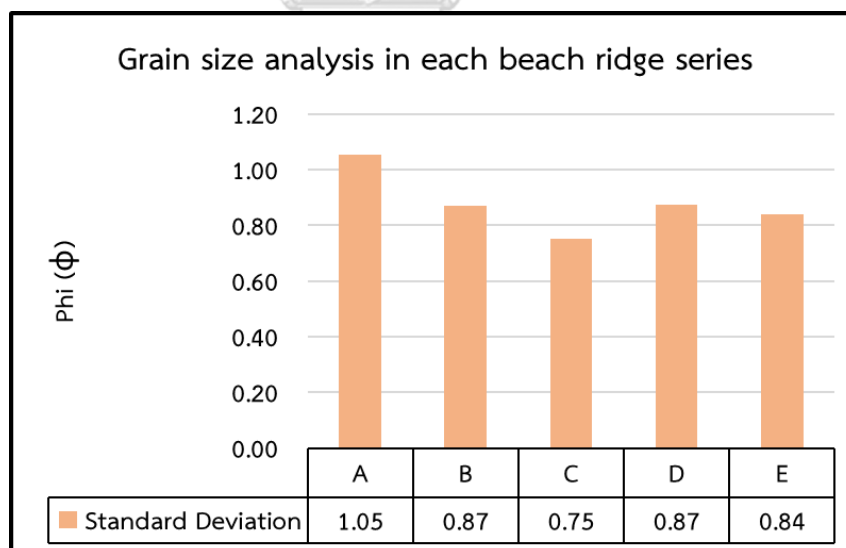


Table 4.24 Bar chart of grain size analysis from series A to E of beach ridge series. This bar graph shows the average standard deviation (sorting) values of sediment sample from series A to E.

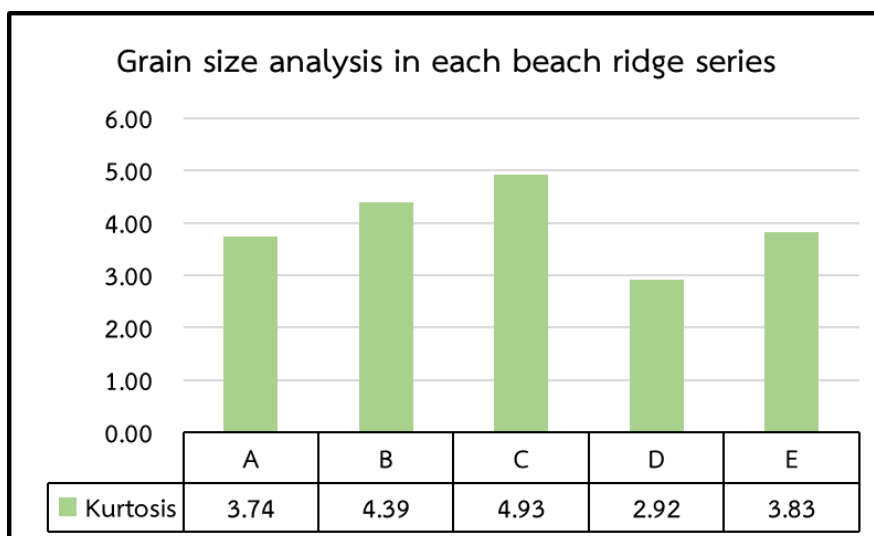


Table 4.25 Bar chart of grain size analysis from series A to E of beach ridge series. This bar graph shows the average kurtosis values of sediment sample from series A to E.

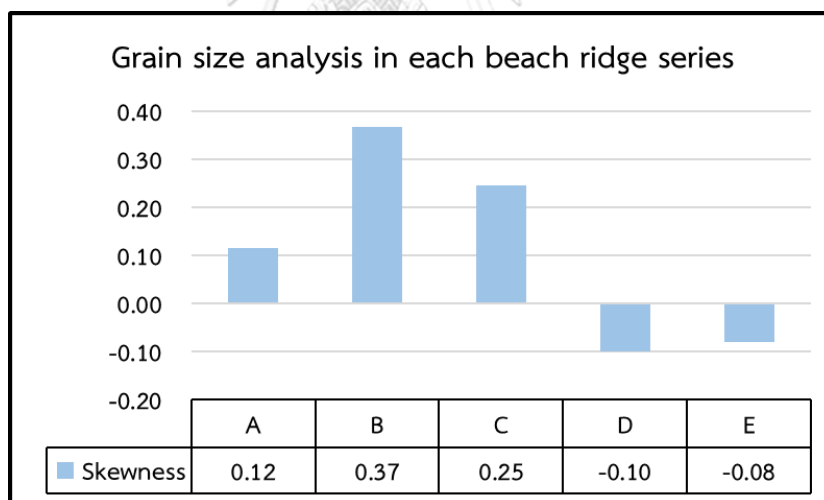


Table 4.26 Bar chart of grain size analysis from series A to E of beach ridge series. This bar graph shows the average skewness values of sediment sample from series A to E.

Sediment compositions, roundness, and sphericity

Some of sediment samples which could not describe in fieldwork were selected to analysis under microscope in laboratory in term of variation of mineral composition of beach sediments which were controlled by source rock and weathering condition. The composition of source rock and weathering condition can describe size fractional distribution. Most of resistant minerals deposit at coastal commonly are quartz and feldspars. Nevertheless, trace minerals are generally the best indicators of source rock. Moreover, heavy minerals can describe themselves of source and process and other features of geomorphic variability in the coastal zone. The clearly seasonal variations in heavy minerals may occur in sediment at beach and nearshore, and sometimes heavy minerals are lag deposits on the beach after storms (Larson et al. 1997).

In Laem Pho study area following the samples from different locations (Figure 4.13) and brought to analyze under microscope found that the compositions of beach ridges are mostly of quartz and minor of feldspar. Bioclasts are dominant only in spit part and nearshore area results in table 4.27, 4.28, 4.29, 4.30, and 4.31 then summarized into major compositions in figure 4.15 and minor composition in figure 4.16.

Sample No.	Composition							Sphericity	Roundness	Beach Ridge Series
	Quartz	Feldspar	Heavy mineral	Mica	Bioclast	Rock fragment	Organic matter			
LP 2-4-0	92.00	4.00	0.00	0.00	0.00	1.00	3.00	low	sub-angular	A
LP 2-4-1	94.00	3.00	0.00	0.00	0.00	1.00	2.00	low	sub-angular	
LP 2-4-2	88.00	8.00	0.00	0.00	0.00	2.00	2.00	low	sub-angular	
LP 2-4-3	94.00	4.00	0.00	0.00	0.00	0.00	2.00	low	sub-angular	
Average	92.00	6.00	0.00	0.00	0.00	0.50	1.50	low	sub-angular	

Table 4.27 Result of composition of sediment sampling from series A of beach ridge series.

Sample No.	Composition							Sphericity	Roundness	Beach Ridge Series
	Quartz	Feldspar	Heavy mineral	Mica	Bioclast	Rock fragment	Organic matter			
LP 2-1-6	90.00	7.00	0.00	0.00	0.00	0.00	3.00	low	sub-angular	B
LP 2-1-7	90.00	9.00	0.00	0.00	0.00	0.00	1.00	low	sub-angular	
LP 2-3-10	98.00	2.00	0.00	0.00	0.00	0.00	0.00	low	sub-angular	
LP 2-3-11	95.00	4.00	0.00	0.00	0.00	0.00	1.00	low	sub-angular	
Average	93.25	5.50	0.00	0.00	0.00	0.00	1.25	low	sub-angular	

Table 4.28 Result of composition of sediment sampling from series B of beach ridge series.

Sample No.	Composition							Sphericity	Roundness	Beach Ridge Series
	Quartz	Feldspar	Heavy mineral	Mica	Bioclast	Rock fragment	Organic matter			
LP 2-1-3	85.00	10.00	0.00	0.00	0.00	5.00	0.00	low	sub-angular	C
LP 2-1-4	90.00	8.00	0.00	0.00	0.00	1.00	1.00	low	sub-angular	
LP 2-1-5	95.00	5.00	0.00	0.00	0.00	0.00	0.00	low	sub-angular	
LP 2-3-2	85.00	10.00	0.00	0.00	0.00	2.00	3.00	low	sub-angular	
LP 2-3-3	95.00	4.00	0.00	0.00	0.00	0.00	1.00	low	sub-angular	
LP 2-3-4	88.00	7.00	0.00	0.00	0.00	2.00	3.00	low	sub-angular	
LP 2-3-5	90.00	5.00	0.00	0.00	0.00	0.00	5.00	low	sub-angular	
LP 2-3-6	80.00	10.00	0.00	0.00	0.00	0.00	10.00	low	sub-angular	
LP 2-3-7	90.00	7.00	0.00	0.00	0.00	0.00	3.00	low	sub-angular	
LP 2-3-8	95.00	4.00	1.00	0.00	0.00	0.00	0.00	low	sub-angular	
LP 2-3-9	90.00	5.00	0.00	0.00	0.00	3.00	2.00	low	sub-angular	
Average	72.13	5.40	0.00	3.33	13.33	2.33	3.47	low	sub-angular	

Table 4.29 Result of composition of sediment sampling from series C of beach ridge series.

Sample No.	Composition							Sphericity	Roundness	Beach Ridge Series
	Quartz	Feldspar	Heavy mineral	Mica	Bioclast	Rock fragment	Organic matter			
LP 2-1-1	95.00	4.00	0.00	0.00	0.00	0.00	1.00	low	sub-angular	D
LP 2-1-2	87.00	10.00	0.00	0.00	0.00	2.00	1.00	low	sub-angular	
LP 2-2-1	91.00	4.00	0.00	0.00	0.00	2.00	3.00	low	sub-angular	
LP 2-2-2	95.00	3.00	0.00	0.00	0.00	0.00	2.00	low	sub-angular	
LP 2-2-3	90.00	5.00	0.00	0.00	0.00	1.00	4.00	low	sub-angular	
LP 2-3-1	63.00	7.00	0.00	5.00	20.00	3.00	2.00	low	sub-angular	
Average	72.13	5.40	0.00	3.33	13.33	2.33	3.47	low	sub-angular	

Table 4.30 Result of composition of sediment sampling from series D of beach ridge series.

Sample No.	Composition							Sphericity	Roundness	Beach Ridge Series
	Quartz	Feldspar	Heavy mineral	Mica	Bioclast	Rock fragment	Organic matter			
LP r-1	94.0	2.0	0.0	1.0	0.0	1.0	2.0	low	sub-angular	E
LP r-2	93.0	2.0	0.0	1.0	0.0	1.0	3.0	low	sub-angular	
LP r-3	93.0	2.0	0.0	1.0	0.0	1.0	3.0	low	sub-angular	
Average	93.3	2.0	0.0	1.0	0.0	1.0	2.7	low	sub-angular	

Table 4.31 Result of composition of sediment sampling from series E of beach ridge series.

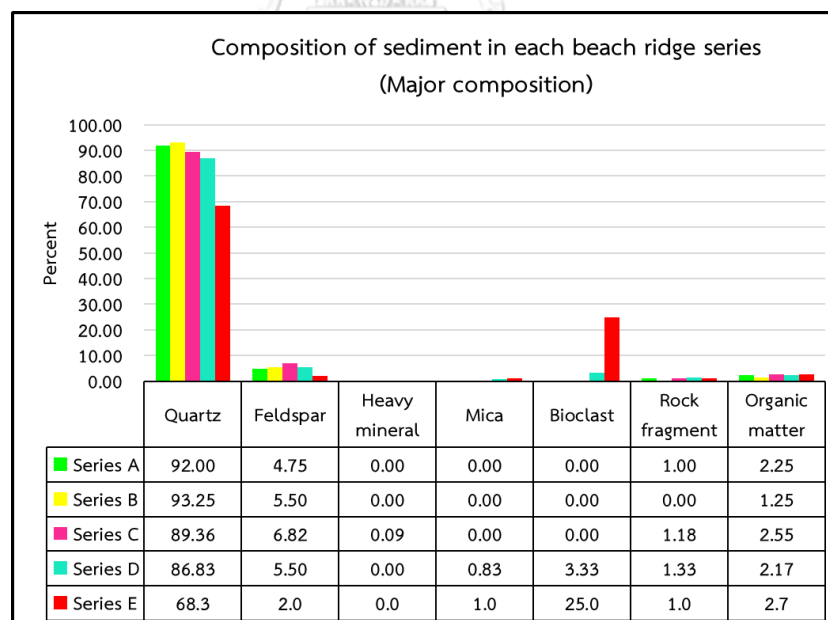


Figure 4.14 Bar graph of composition of sediment sampling from series A to E of beach ridge series. This bar graph shows the major composition of sediment sample from all of series is quartz.

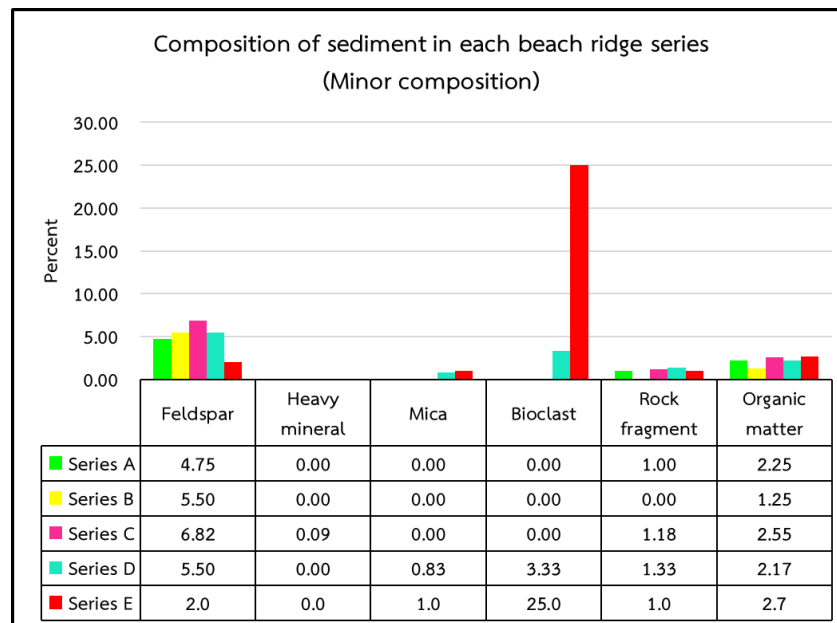


Figure 4.15 Bar graph of composition of sediment sampling from series A to E of beach ridge series. This bar graph shows the minor composition of sediment sample from all of series are feldspar and organic matter. Bioclasts are dominant only in series C and D.

4.5 Age determination by optically stimulated luminescence dating

To understand periods of sediments deposition in the study area, there needs to study in age determination first. In this study, optically stimulated luminescence dating (OSL dating) which is a kind of age determination was used to clarify ages of all sediments. Results of age determination by OSL dating were showed in tables below follow 5 series of beach ridge series (Table 4.32, 4.33, 4.34, and 4.35) and were summarized with satellite image in figure 4.17.

No.	U (ppm)	Th (ppm)	K (%)	W (%)	AD (Gy/ka)	ED (Gy)	Age (Yr)
LP2-4-1	0.19	8.16	3.00	18.87	4.84	4.63	950±30
LP2-4-2	0.00	5.27	3.43	6.75	4.51	11.17	2,470±130
LP2-4-3	0.26	2.93	2.35	4.38	2.99	9.94	3,320±200
LP2-4-4	0.06	4.86	2.46	6.60	3.56	22.34	6,270±430

Table 4.32 Results of sampling at series A of beach ridge series from OSL dating.

No.	U (ppm)	Th (ppm)	K (%)	W (%)	AD (Gy/ka)	ED (Gy)	Age (Yr)
LP2-1-5	0.07	6.54	1.62	3.50	2.03	9.50	4,680±240
LP2-1-6	0.27	4.68	1.33	4.04	1.69	10.59	6,280±450
LP2-1-7	0.33	2.61	1.42	4.16	1.63	11.68	7,170±460
LP2-3-8	0.00	4.95	0.74	4.72	2.07	7.55	3,650±160
LP2-3-9	0.00	7.01	2.08	5.42	3.75	9.67	2,570±100
LP2-3-10	0.00	5.82	1.67	4.66	3.10	9.78	3,150±150
LP2-3-11	0.44	3.28	1.92	5.35	2.70	6.78	2,510±150

Table 4.33 Results of sampling at series B of beach ridge series from OSL dating.

No.	U (ppm)	Th (ppm)	K (%)	W (%)	AD (Gy/ka)	ED (Gy)	Age (Yr)
LP2-1-3	0.00	4.23	1.98	4.39	2.15	5.93	2,750±110
LP2-1-4	0.07	5.03	1.11	3.89	1.47	6.80	4,620±280
LP2-3-2	0.13	2.41	0.51	3.83	1.26	5.15	4,090±240
LP2-3-3	0.24	3.56	0.25	4.39	1.30	5.48	4,200±410
LP2-3-4	0.00	3.11	0.89	4.21	1.76	5.56	3,160±170
LP2-3-5	0.00	6.81	1.41	3.91	3.11	4.92	1,570±60
LP2-3-6	0.61	4.31	0.00	4.38	1.27	7.39	5,830±370
LP2-3-7	0.55	2.50	2.21	5.67	2.76	8.71	3,150±140

Table 4.34 Results of sampling at series C of beach ridge series from OSL dating.

No.	U (ppm)	Th (ppm)	K (%)	W (%)	AD (Gy/ka)	ED (Gy)	Age (Yr)
LP2-1-1	0.39	4.86	2.70	4.87	2.93	1.67	570±20
LP2-1-2	0.20	4.68	1.14	4.31	1.51	2.96	1,960±160
LP2-2-1	0.79	6.84	2.10	16.32	3.72	1.65	440±10
LP2-2-2	0.23	4.10	3.89	23.52	4.63	0.72	150±5
LP2-2-3	0.09	6.29	3.95	5.80	5.22	0.62	110±4
LP2-3-1	0.08	4.93	2.03	3.98	3.19	3.06	950±30

Table 4.35 Results of sampling at series D of beach ridge series from OSL dating.

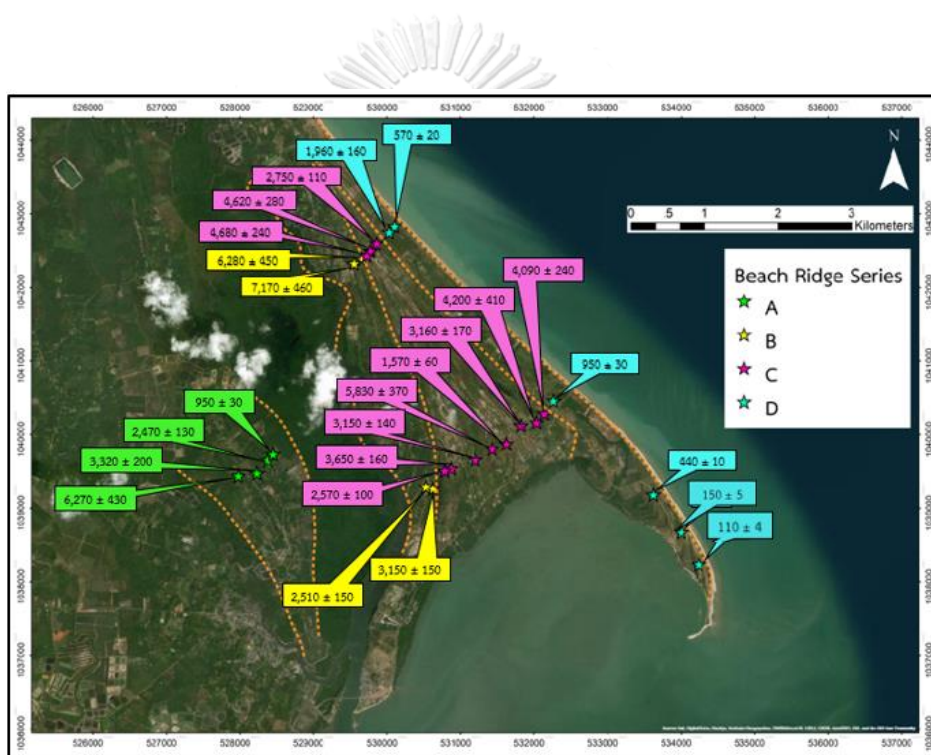


Figure 4.16 Age results from OSL dating in each of sampling locations with different star colors for different beach ridge series.

4.6 Fossil and microfossil evidence

To confirm that sediment samples are from marine sediment, some of them were studied in detailed of fossil and microfossil evidence. In this study, only sample no. LP 3-3-1 was taken to classify because there are abundant fossils. After representative sample was studied under dissecting microscope and the scanning electron microscope (SEM), it showed that fossils and microfossils which were found in this area come from marine source which include of mollusks, foraminiferas and ostracods.

Fossil of benthic foraminiferas, ostracodas, and molluscas at Laem Pho study area were found in fine to medium sand at depth 110 – 200 centimeters in the lower part of the borehole. The microfossil frequencies have been calculated for 100 grams of dried sediment. A total of selected samples were identified at least 17 species.

4.6.1 Systematic description

Chromista (Kingdom)

Harosa (Subkingdom)

Rhizaria (Infrakingdom)

Foraminifera (Phylum)

Globothalamea (Class)

Rotaliida (Order)

Rotalioidea (Superfamily)

Ammoniidae (Family)

Ammoniinae (Subfamily)

Ammonia (Genus)

Ammonia beccarii (Linné, 1758) (**Species**); Figure 4.18 (6 - 9)

Ammonia ketienziensis (Ishizaki, 1943) (**Species**); Figure 4.18 (4 - 5)

Ammonia pauciloculata (Phleger and Parker, 1951) (**Species**); Figure 4.18 (1 - 3)

Habitat: Near shore zone; Inner shelf environment; Euryhaline and tolerates water freshening; Brackish marine (Chekhovskaya et al., 2014; Nisha and Singh, 2012; Wilkinson, 2007)

Asterorotalia (**Genus**)

Asterorotalia pullchella (d'Orbigny, 1839) (**Species**); Figure 4.21 (1 - 9)

{(Synonym: *Asterorotalia trispinosa* (Thalman, 1933)

Habitat: Lagoon; Shallow; Marginal-marine ecosystem; Upper-middle neritic zone; Tropical-subtropical water; Indicator of warm water (Jingxing and Luping, 2012).

Elphidiidae (**Family**)

Elphidiinae (**Subfamily**)

Elphidium (**Genus**)

Elphidium advenum (Haynes, 1973) (**Species**); Figure 4.19 (8) - (12)

Elphidium hispidulum (Cushman, 1936b) (**Species**); Figure 4.19 (1) - (6)

Elphidium limpidum (Ho, Hu et Wang, 1965) (**Species**); Figure 4. 20 (1) - (6)

Elphidium macellum (Fichtel and Moll, 1798) (**Species**); Figure 4.19 (7)

Habitat: Shallow marine; Marginal marine; Middle and outer shelf environment; Brackish waters (El Baz and Furjany, 2018; Nisha and Singh, 2012; Troga et al., 2013)

Tubothalamea (**Class**)

Miliolida (**Order**)

Miliolina (**Suborder**)

Milioloidea (**Superfamily**)

Hauerinidae (**Family**)

Miliolina (**Genus**)

Miliolina (Quinqueloculina) bogdanowiczi (Serova, 1955) (**Species**); Figure 4.20 (7)

Habitat: Shallow and warm water of the infralittoral zone; Undersea meadows and beaches; Brackish and nearshore marine waters in the Gulf of Mexico (together with Elphidium and Rotalia); Marginal marine. (Łuczowska, 1974; Troga et al., 2013)

Foraminifera incertae sedis (**Class**)

Lagenida (**Order**)

Nodosarioidea (**Superfamily**)

Nodosariidae (**Family**)

Nodosariinae (**Subfamily**)

Nodosaria (**Genus**)

Nodosaria intermittens (Roemer, 1838) (**Species**); Figure 4.20 (8)

Habitat: Shallow infaunal foraminifera; Deposited principally during a regression of the sea; Barrier island indicate deposition in stream channels early in the subsequent transgression. (Mallory, 1959)

Animalia (**Kingdom**)

Arthropoda (**Phylum**)

Crustacea (**Subphylum**)

Oligostraca (**Superclass**)

Ostracoda (**Class**)

Podocopa (**Subclass**)

Podocopida (**Order**)

Cytherocopina (**Suborder**)

Cytheroidea (**Superfamily**)

Cytherideidae (**Family**)

Cyprideis (**Genus**)

Cyprideis ruggierii (Decima, 1964); (**Species**); Figure 4.23 (1)

Habitat: *C. ruggierii* lived in very different environments; Brackish water, saline lake; Marginal marine environment with lowered salinities; Littoral zone; Not found in deep waters; Peaks in abundance in the transitional zone from marine to freshwater conditions (Ligos and Gliozzi, 2012; Mazzini et al., 2013; Wilkinson, 2007)

Trachyleberididae (**Family**)

Keijella (**Genus**)

Keijella reticulate (Whatley & Zhao Yi-Chun, 1988) (**Species**); Figure 4.23 (2)

Keijella sp. (**Species**); Figure 4.23 (3)

Habitat: Tropical, Shallow and brackish water; Inner shelf region; Shallow marine (Mohammed Nishath et al., 2017)

Leptocytheridae (**Family**)

Callistocythere (**Genus**)

Callistocythere canaliculata (Reuss, 1850) (**Species**); Figure 4.23 (4)

Habitat: Shallow marine; Interstitial environments; Outer reef flat, The shoreline zone and the mid to high tide levels of the littoral zone, The shoreline to the sub-tidal zone. (Ha and Tsukagoshi, 2015; Whatley and Watson, 1985)

Loxoconchidae (**Family**)

Palmoconcha (**Genus**)

Palmoconcha guttata (Norman, 1865) (**Species**); Figure 4.23 (5)

Habitat: Shallow marine; From littoral to outer shelf environments (Athersuch et al., 1989; Bonaduce et al., 1975; Wilkinson, 2007)

Animalia (**Kingdom**)

Mollusca (**Phylum**)

Bivalvia (**Class**)

Heterodonta (**Subclass**)

Archiheterodonta (**Infraclass**)

Carditida (**Order**)

Carditoidea (**Superfamily**)

Condylocardiidae (**Family**)

Carditellinae (**Subfamily**)

Carditella (**Genus**)

Carditella pallida (E. A. Smith, 1881) (**Species**); Figure 4.22 (1)

Habitat: Subtropical; Intertidal (Bernard, 1983)



Antalis entalis (Linné, 1758) (**Species**); Figure 4.22 (2)

Habitat: Offshore in sand; Coastal; Subtropical; Subtidal; Intertidal or littoral. (Hayward et al., 1995)

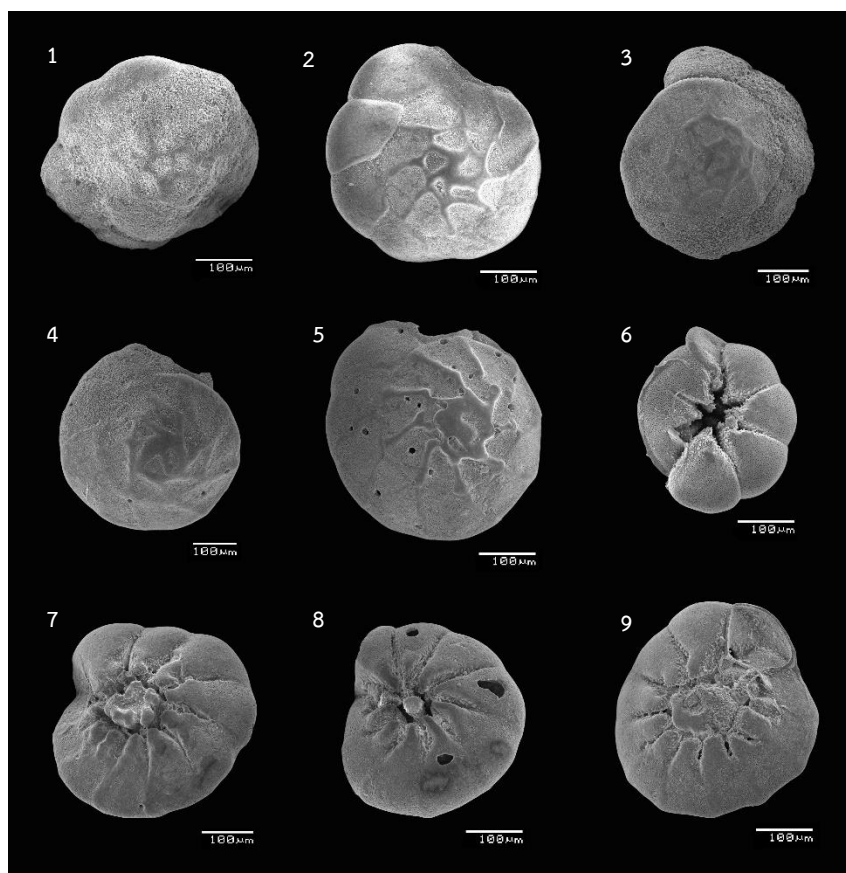


Figure 4.17 Foraminifera: (1 - 3) *Ammonia pauciloculata* (Phleger and Parker, 1951); (4,5) *Ammonia ketienziensis* (Ishizaki, 1943); (6 - 9) *Ammonia beccarii* (Linné, 1758).

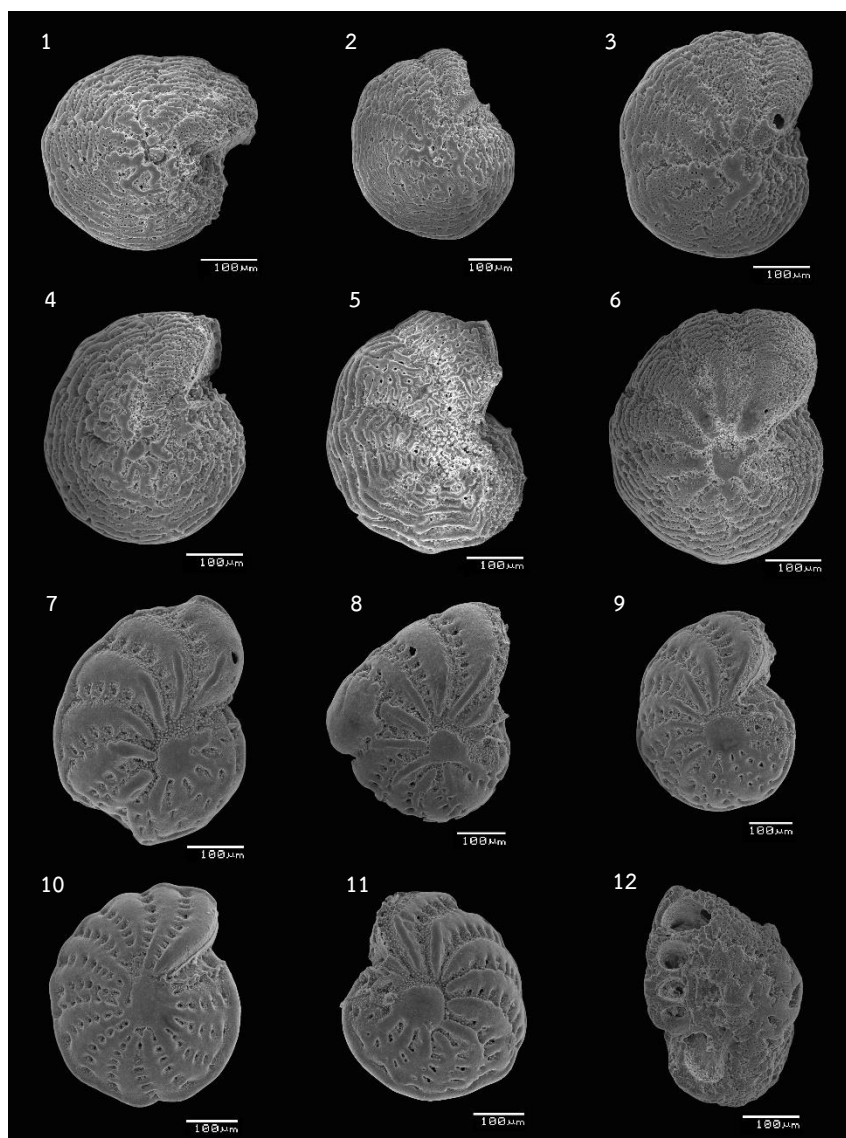


Figure 4.18 Foraminifera: (1 - 6) *Elphidium hispidulum* (Cushman, 1936b); (7) *Elphidium macellum* (Fichtel and Moll, 1798); (8 - 12) *Elphidium advenum* - lateral (Haynes, 1973).

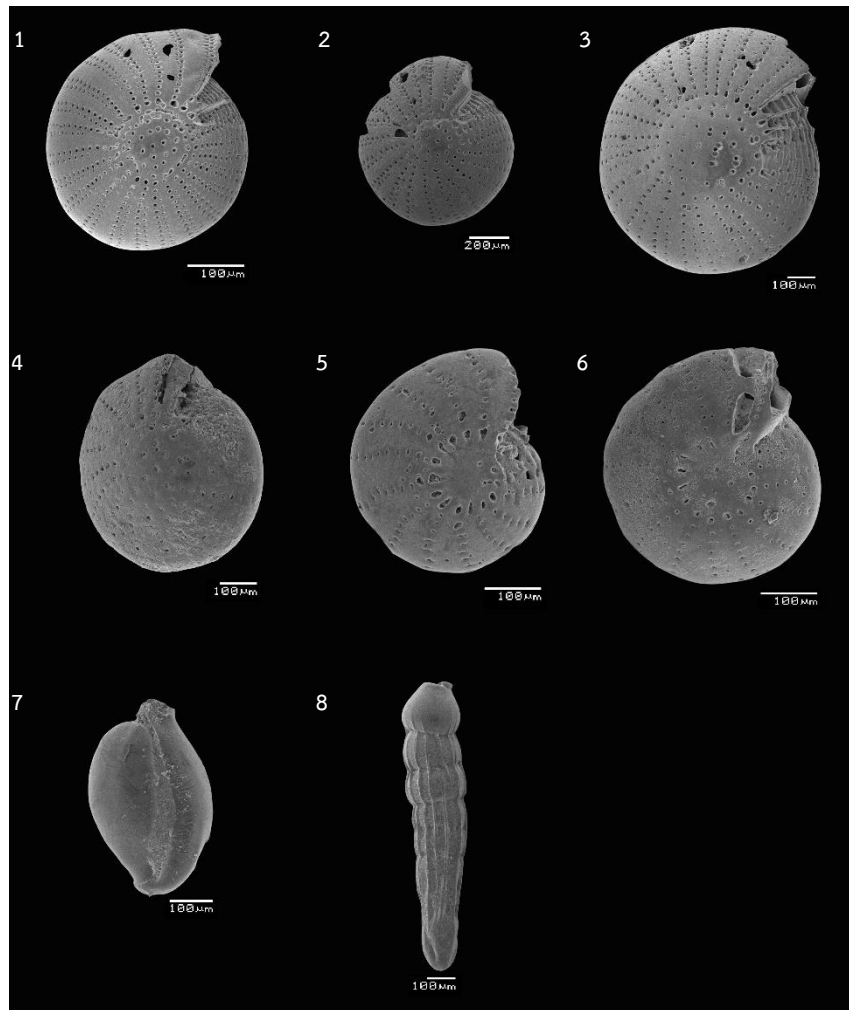


Figure 4.19 Foraminifera: (1 - 6) *Elphidium limpidum* (Ho, Hu et Wang, 1965); (7) *Miliolina (Quinqueloculina) bogdanowiczi* (Serova, 1955) and (8) *Nodosaria intermittens* (Roemer, 1838).

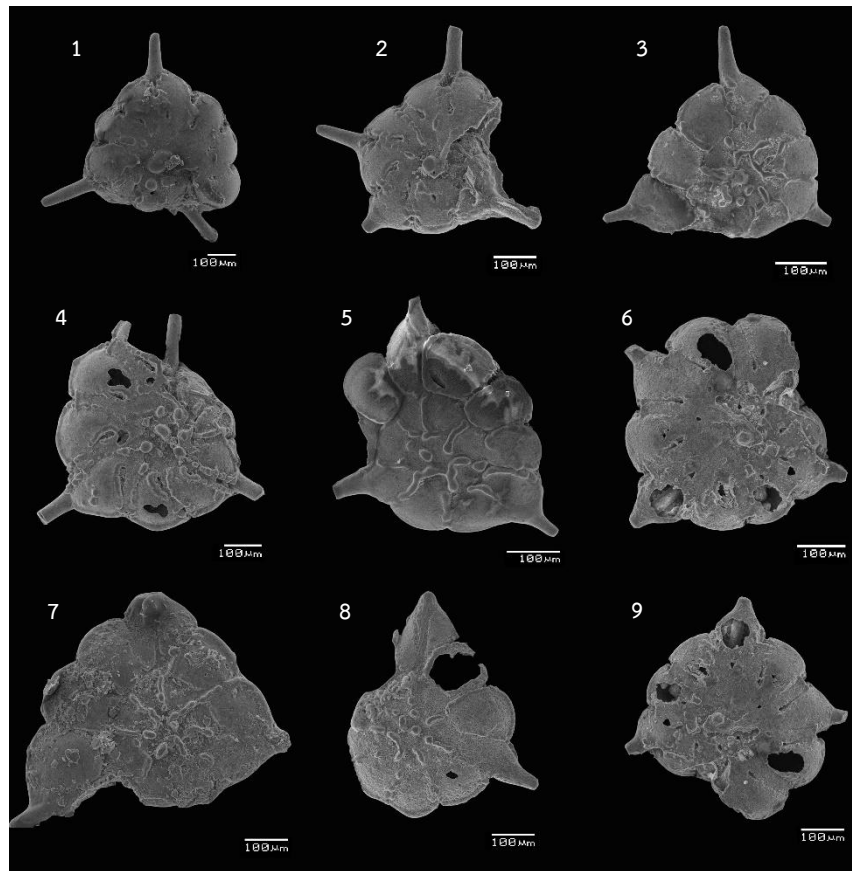


Figure 4.20 Foraminifera: (1 - 9) *Asterorotalia pullchella* (d'Orbigny, 1839) (Synonym: *Asterorotalia trispinosa* (Thalman, 1933).

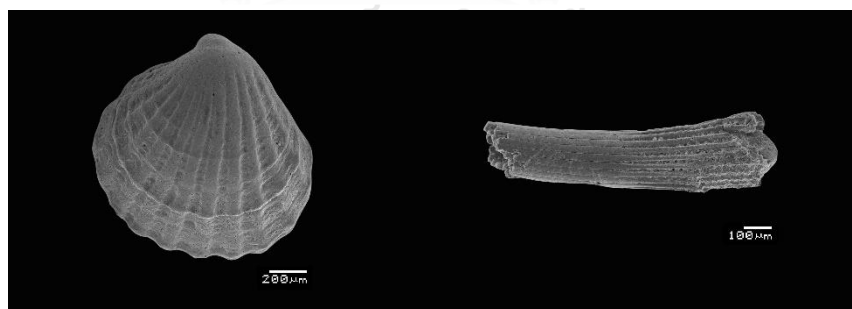


Figure 4.21 Mollusk: (1) *Carditella pallida* (E. A. Smith, 1881) and (2) *Antalis entalis* (Linnaeus, 1758).

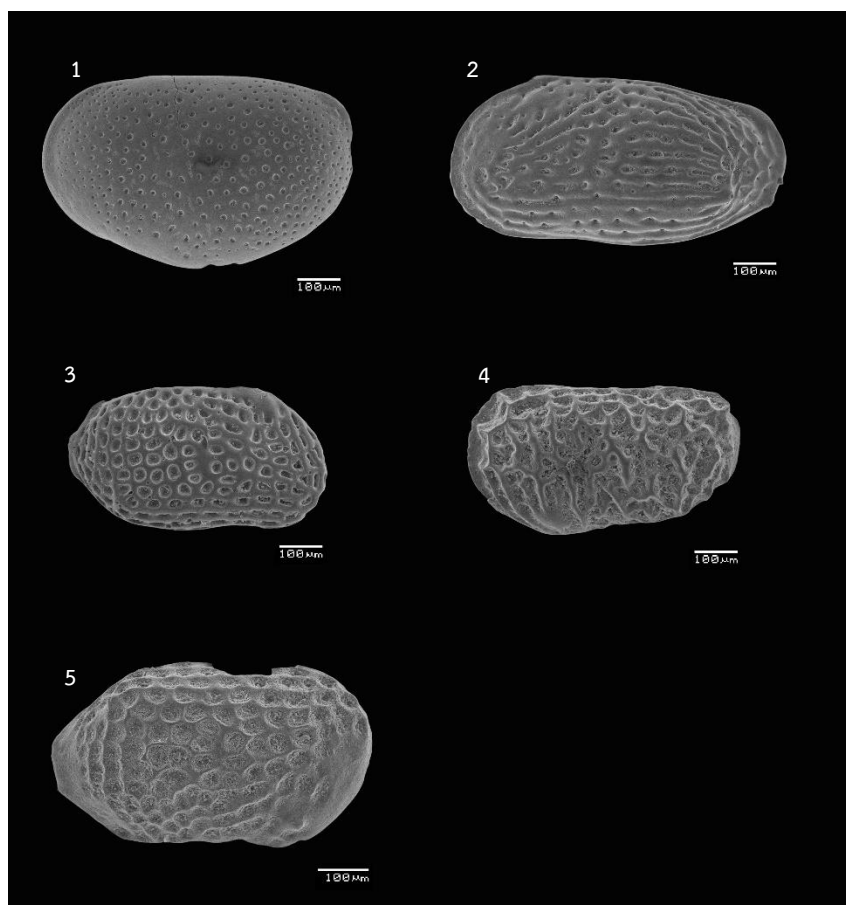


Figure 4.22 Ostracod: (1) *Cyprideis ruggierii*. (Decima, 1964); (2) *Keijella reticulata* (Whatley & Zhao (Yi-Chun), 1988); (3) *Keijella* sp. (Sars, 1866); (4) *Callistocythere canaliculata* (Reuss, 1850); and (5) *Palmoconcha guttata* (Norman, 1865).

CHAPTER 5

DISCUSSIONS

5.1 Boundary of paleo-shoreline from satellite image interpretation

The analysis of paleoshorelines together with the most recent highstands can be observed by satellite images and during field investigations (Liu et al., 2013). However, most observable paleoshorelines provide a biased record since they tend to be the product of recent regressive phases, with older shorelines more likely to have been erased during repeated transgressive–regressive lake level fluctuations. Moreover, satellite images can indicate many sets of beach ridges in the form of groups (Li et al., 2009). Beach ridges are dominant landforms of a Quaternary coastal plains and other coastal landforms, therefore, they are indicator of the position of ancient seashores and associated sea-levels. Beach ridges clearly have an origin by wave-built and also indicator of ancient higher sea-levels than present sea-levels (Otvos, 2000). Beach ridges are dominated by wave deposition (Johnson, 1919), or by the combination of both wave and aeolian deposition (Hesp, P., 2005; Otvos, 2000).

Laem Pho study area has dominant landforms of beach ridge plains and active sand spit at southern part that prograding into the sea by recent longshore current. However, the orientations of beach ridges in this area have individual characteristic that can be classified into 5 series. Series A which locates at the most inner part of the study area, then following by series B, C, D which separate from series A by Phum Rieng canal. Series B, C, and D locate at the middle part of study area which can be grouped as a large beach ridge plain. Series E, recent beach, locates next to the shoreline. Due to the present of innermost beach ridge (series A), it can be used to indicate paleo-shoreline of this study area as covering approximately 4.5 kilometers from present shoreline (Figure 5.1). Based on the orientation, elevation, and morphology of beach ridges, they were possibly reflected their relationship with sea-level fluctuation, wave

height, and sediment supply. In this area, beach ridges prograde seaward at the foreshore, and longshore currents supply more material to the beach than local wave activity can remove. Naturally, if the environmental conditions change, previous ridge features will under interruptions, truncations, or erosion, so that the younger beach ridges may be deposit in different orientations or shapes (Taylor and Stone, 1996).

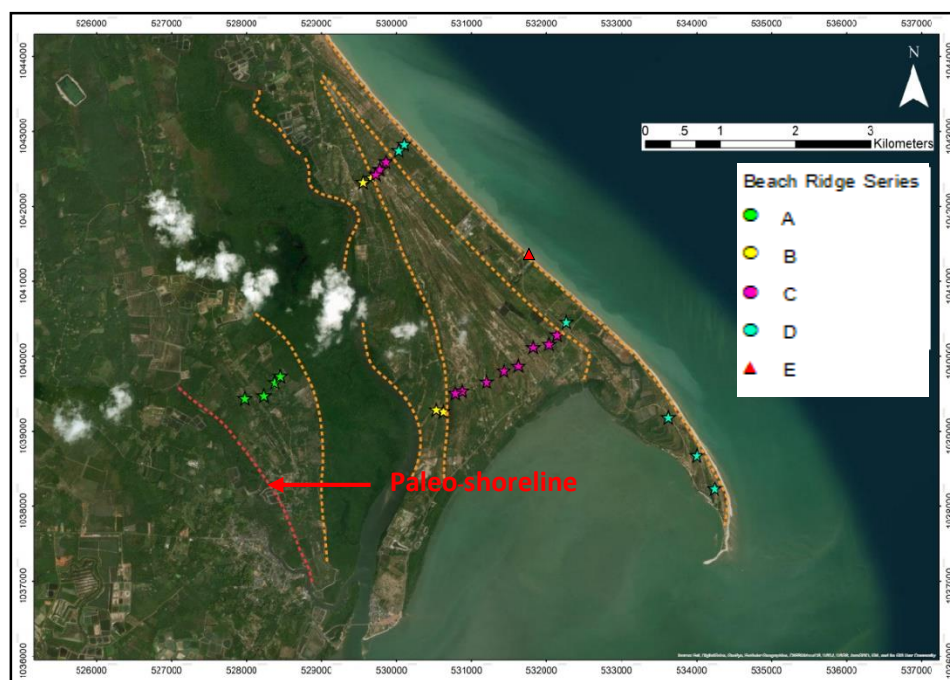


Figure 5.1 Geomorphology of study area from satellite image and the red dash line shows paleo-shoreline boundary.

5.2 Stratigraphic correlation

Stratigraphic data were carried out from coring, outcrop, or road cuts for matching up continuous sequences. The study of the facies changes is important because of they may show some can indications of the changes in sea-level. A rising of sea-level indicates a transgression phase which normally produces a vertical sequence of finer-grained facies overlying coarser-grained facies (fining-upward sequence) which indicates gradually deeper water environments. The fining upward sequences indicate sediments were deposited under decreasing energy conditions

(Murali Krishana et al., 2017), while a dropping of sea-level indicates a regression phase which usually produces a sequence of coarser-grained facies overlying finer-grained facies (coarsening-upward) which indicates gradually shallower water environments. Facies associations in both vertical and lateral allow the study of sedimentary facies in space and time, and their relationship with longer-term cycles, such as relative sea-level changes or tectonic phases, and subsequent accumulation in sedimentary basins (Friedman, G.M. et al., 1992).

The color of soils or sediments usually depends on the content of organic matter and ferric oxide. The thicker of organic matter causes the soil darker and ferric oxide coating the sediment grains as red grains (Rapp and Hill, 2006). Black and dark gray coloration in sediment generally indicates the presence of organic carbon and/or iron. Organic carbon in sediment requires anoxic environmental conditions (lacking free oxygen), which might be found in calm water marine environments such as deep lakes and estuaries. While red and brown coloration in sediment indicates the presence of iron oxides. For well-oxygenated continental sedimentary environments, the iron in the sediments is oxidized to form hematite or ferric iron oxide (Fe_2O_3), which colors the sediment red, brown, or purple. Furthermore, red and brown sediment can indicate marine environments (due to oxidation of the iron in the sediment after deposition), while the oxidation condition developed as a result of exposure to the atmosphere during a time of greatly lowered sea-level (Levin, 2006).

From the study of the relation of color to environment by Stanley (1969). The sediment color depends on many factors consist of:

- 1) Natural colors of the minerals or rock fragments of sample.
- 2) Secondary effects of rock destruction process, climatic conditions, and patterns of sediment transportation on the natural colors of the mineral and rock fragments.
- 3) Size of sediment grains and the closeness of their packing.

4) Conditions at the area while deposit, including the content and kind of organic matter and the degree of oxidation or reduction of pigment at the sediment-water interface.

5) Degree of hydration of iron mixtures and the state of iron in clay minerals.

6) Diagenesis during and following deposition of sediments.

7) More superficially, the conditions under that the sample is examined, including index of refraction of the surrounding medium, polarization, diffraction, and scattering.

In Laem Pho study area, the very dark brown sand layer which found at station LP 3-1-1 to 3-1-3 and LP 3-3-2 to 3-3-8. For LP 3-2-1 to 3-2-3 which located on the spit part of study area has an outstanding geomorphology of old lagoon and swale, so there is no evidence of very dark brown sequence. On the other hand, there is a dominant in black layer of organic matter rich sequence instead. The present of very dark brown sand layer found in the shallow depth at Laem Pho study area may represent the conditions at the site of deposition, including the content of organic matter and the degree of oxidation or reduction of pigment at the sediment-water interface. It is also possibly due to the degree of hydration of iron compounds and the state of iron in clay minerals in the layer which coated the sediment grains during wetter interval which possibly linked to the high water table. In addition, the presence of high organic matter in the environment of deposition can lead the reduction of the oxides to non-red colors (dark brown color in this area).

5.3 Grain size analysis

The study of relationship between size parameters and distance of transportation and depositional processes of beach sediments is necessary for understanding the paleo environment of deposition from sediments in the study area

as the studied by many researchers Lason et al. (1997); McLaren and Bowles (1985); Muzuka and W (2000); Rajmohan et al. (2012); Rashedi and Siad (2016); Sukanraj et al. (2013) The grain size statistical parameters (mean grain size, sorting, skewness, and kurtosis) were calculated by using the moment method (Friedman, G.M. and Sanders, 1978).

The mean grain size values of the beach sediments were influenced by source of sediments, mode of transportation and environment of deposition (Folk, R.L., 1966). The grain size of the sediments was controlled by the mode and also reveals the distance of transportation which is the longer of transportation distance, the finer of grain size deposit. While skewness and kurtosis parameters were used to analyze sediments which occur in the same environment (Martins, L. R. and Barboza, 2005). Most of the sediments in Laem Pho study area are exhibited the size of coarse to medium sand which indicates the depositional environment is under the moderately high energy condition. Naturally, the increasing of energy while transporting has an ability to carry coarse grain sediment to deposit (Folk and Ward, 1957). Sandy loam and sandy clay are founded dominantly in swale (old lagoon) which commonly characterize as a low energy environment. However, the factor that control the difference in grain size distribution of beach sediments is not only the distance, but also the time.

The sorting is a measurement of the uniformity of grain-size distribution within the sediment samples. It depends on the size range in the source rock, extent of weathering, distance of transportation and the energy variation of the depositing medium (Amaral and Prayor, 1977; Folk, R. L. and Ward, 1957). Moreover, there is a little selection of grains during transportation or deposition which might be explained as the result of highly variable energy, turbulent conditions, and lack of constant energy in any one direction, while good sorting indicates smooth, stable currents (Amaral and Prayor, 1977). On the other hand, the poor sorting of sediments probably due to the lack of any effective hydrodynamic factor or sorting agent. Thus, they reflect

the low energy conditions which result in the appearance of the biogenic materials with different growth stages. In addition, the origin and the production of the volume of sedimentary materials were linked to the high rate of sedimentation, so the chances for the sediments to get sorted are very little (Hamouda et al., 2014). In this area, sorting of beach sediments indicate low to fairly high energy current.

Skewness and kurtosis are indicators of the selective action of the transporting agent which can compare of sediments from the same environment but different in occurring (Krumbein and Pettijohn, 1938; Martins and Barboza, 2005). They also considered extremely important by Folk and Ward (1957) for analyzing the bimodality of grain-size distribution (Martins, L.R., 1965). The positive skewness values indicate the finer grain sizes and the negative skewness values indicate the coarser grain sizes (Ameral and Pryor, 1997). From the result, 80 percent of sediment at Laem Pho study area samples presented the fine skewness value which indicate calm environment to storm environment as Friedman, G.M. (1961); Mason and Folk (1958) mentioned that dune sands are generally positively-skewed, whether the dunes are barrier island, coastal, lake, river, or desert dunes, while beach sands were found to be negatively skewed. The rest of 20 percent of sediment samples in this area which showed the coarse-skewed value, therefore, interpreted as a high energy deposition environment. In various studies it has been demonstrated that dune sands are better sorted and finer grain than beach sands (Abuodha, 2003). Moreover, Duane (1964) suggested that the winnowing action by waves and tidal currents produces the negative skewness in sands of the littoral, beach, and tidal inlet environments. Besides, the negative skewness can be interpreted as evidence of a high energy shoal area resembling modern shallow shelves. From the studied of Wigley (1961), the negative skewness of the shoal sands can indicate the intense winnowing of tidal currents and storm waves. In conclusion, the kurtosis value of Laem Pho beach sand samples is mostly extremely leptokurtic which can describe that the central portions are better sorted at the tails.

The methods identification the using for sedimentary environment by grain size distribution data is usually analyzed together with other evidences (i.e. roundness, sphericity, texture of grains, biogenic components, and mineral compositions) which can indicate the depositional processes. In Laem Pho study area, mostly sediments in beach ridge are composed of quartz and minor of feldspar. Texture of sediments is sub-angular which indicated a short-time of transportation and a distance does not far from source rock. While the presence of clay-size materials in sand layer especially in the sand spit part of the area, are due to the characteristic of swale (old lagoon) depositional environment which located in the low energy area and clam environment.

5.4 Fossils evidence

The fossil evidences found in beach ridge series D (sample 3-3-1 at depth 110 - 200 centimeters) of Laem Pho study area, showed the abundant of microfossils (benthic foraminiferas and ostracodas) and shell fragments. Most of marine fossils (bivalvia and Scaphopoda) were found as a fragment. The broken shell fragments indicate that they live in shallow marine environment under influenced of tidal and wave processes (Valia and Cameron, 1997). Moreover, the presence of fossil and microfossil including Foraminiferas (Ammonia, Elphidium, Miliolina, Nodosaria, and Asterorotalia), Ostracoda (Cyprideis, Keijella, Callistocythere, Palmoconcha), Bivalvia (Carditella), and Scaphopoda (Antalis) found in the study area indicated the living habitats in shallow marine environment in intertidal zone (or littoral zone, marginal marine) and warm water condition.

5.5 Ages of sand deposit by optically stimulated luminescence dating

From the study of coastal evolution of the Greater Surat Thani city area, Southern Thailand by Chaimanee (2001), he suggested that the arriving time of transgression into Surat Thani coast at about 8,000 years BP from the results of C-14

dating. Subsequently, due to the rapid sea-level rise during the early Holocene, the transgression has a maximum height at more than 5 meters about 5,000 years BP. Furthermore, because of an influx of upland sediments into the sea, the coastal plain has prograded rapidly. As far as about 1,000 years BP., the sediments supplied to the sea decreased and affected to the fluvial dominant delta transforming into the tide-dominated delta. The Surat Thani and Chaiya coasts have possible been in still-stand phase since that time with the mudflat and beach barrier forming respectively. The age results of Laem Pho study area were conformed to the studied by Chaimanee (2001) which have an age during that time. Finally, the younger ages in series D especially in the sand spit part, which the ages ranging from 440 ± 10 to 110 years BP are representing the modern process of sediments progradation from the longshore current.

The discontinue of age dating results in the central part of the study area which consist of beach ridge series B, C, and D is possibly influenced from typhoon strikes in the Gulf of Thailand. Williams et al. (2016) released that there are eleven typhoon strikes at Cha-am area with the ages ranging from 1,952 to 7,575 years BP and eight typhoon strikes at Kui Buri area with the ages ranging from 4,075 to 7,740 years BP. The frequency of typhoon strikes was 2-5 times greater from 3,900 to 7,800 years BP. Relatively, the age of beach ridge in central part of Laem Pho ranging from 1,570 to 5,830 years BP can be compared with frequency of typhoon strikes approximately 12 typhoons proposed by Williams, H. et al. (2016) (Figure 5.2). However, the coring samples in swale or old lagoon would be recommended. One of the obvious evidence of typhoon strikes is the sharp contact of sand sheets intercalated between mud layer. According to the environmental deposition of normal lagoon is clay or mud sediments, so that the presence of sand layers is categorized to unusual condition (Phantu Wongraj, S. et al., 2010). The extreme occurrence of typhoons in mid-Holocene associated with the climate changes in the Mid-Holocene Warm Period in Southeast Asia and a

changing of landscape occurred due to the mid-Holocene sea-level highstand. Moreover, the progradation in two directions which are southwestward and eastward direction of beach ridge series in the central part may cause a reworking process and repeating of sediment deposit and this is another interesting assumption of the age discontinuity in this area.

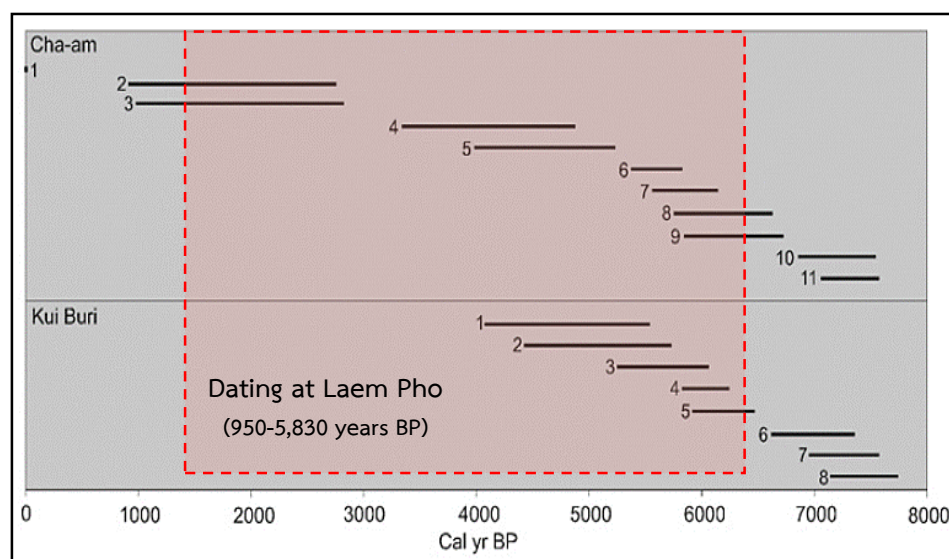


Figure 5.2 Frequency of typhoons recorded at Cha-am and Kui Buri (modified after Williams et al. 2016). Red square indicate age of beach ridge from Laem Pho.)

5.6 sea-level curves

Sea-level curve is the best tool for understanding the relationship between sea-level change and time. In Southeast Asia coastal regions, sea-level curve records (Figure 5.3). have developed at first by Geyh et al. (1979) from the studied of Malacca Strait. revealed the sea-level curve indicating a maximum mid-Holocene sea-level of +5 meters which showing a smoothly falling sea-level but they could not determine whether sea-level fell smoothly or in an oscillatory trend. The first sea-level curve in Thailand was proposed by Sinsakul et al. (1985) on which sea-level fluctuated with 2 highstands at approximately 6,000 years BP with +5.0 meters and 4,000 years BP with

+ 3 meters. Sinsakul et al (1985) also suggested the rebound phase of marine transgression occurred approximately 4,700 years BP before stable at the present mean sea-level. As a similar trend as the studied of Thai-Malay Peninsula by Tjia (1987) and Tjia and Fujii (1992) which showed the 3 rebound phases in the curves during the Mid to Late Holocene with highstands at 6, 4, and 2.7 ka and two sea-level highstand at approximately 4,500 and 2,500 years BP. The first high sea-level was up to 3-4 metres above present sea-level (Sinsakul, S. , 1992). Although, the curve by Sinsakul et al. (1985) represents a complex sea-level history, it is a basis for the present investigation of the Holocene period in Thailand. Nevertheless, the studied of Singapore sea-level curve by Hesp et al. (1998) plotted against the Geyh et al. (1979), Sinsakul et al. 1985, Tjia (1987) and Tjia and Fujii (1992). A rapid post glacial marine transgression rising to present mean sea-level at 6,500 BP, sea-level rose to approximately 3 meters. Then around 2,000 to 1,000 years BP, sea-level was reached to present sea-level. After that Choowong et al. (2004) proposed a revised sea-level envelope for the Gulf of Thailand which corresponded well with the sea-level curves at the Thai-Malay Peninsula by Horton et al. (2005). The curves show an upward trend of rising Holocene sea-level to a Mid-Holocene highstand with the average rate at approximately 5 millimeters per year and fall from highstand at approximately 1.1 millimeters per year, then sea-level slightly fall to the present with no evidence of second highstand. Moreover, Nimnate et al. (2015) presented additional sea-level curve for the Gulf of Thailand, the area of studied at Pak Nam Chumphon which locates northern of Laem Pho study area. The highest level of transgression approximately 4-5 meters at last 7,600 years BP.

From the results of topographic survey and OSL dating at Laem Pho study area, the alignment of former beach ridge plains at Laem Pho study area has an elevation of the oldest beach ridges approximately 4 meters from mean sea-level at last $7,170 \pm 460$ years BP which indicates the highest marine transgression of this study area. After that sea-level tended to prograde into seaward direction and slightly drop to mean sea-level (Figure 5.4).

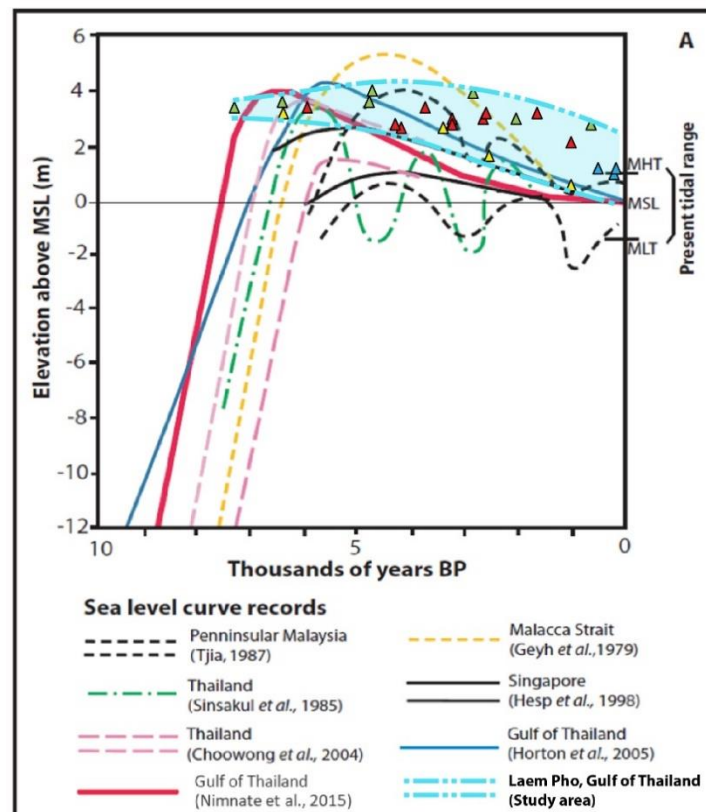


Figure 5.3 The summary of sea-level curves in Southeast Asia including Malacca Strait (Geyh *et al.*, 1979), Peninsular Malaysia (Tjia, 1987), Singapore (Hesp *et al.*, 1998), Gulf of Thailand (Sinsakul *et al.*, 1985; Choowong *et al.*, 2004; Horton *et al.*, 2005; Nimnate *et al.*, 2015).

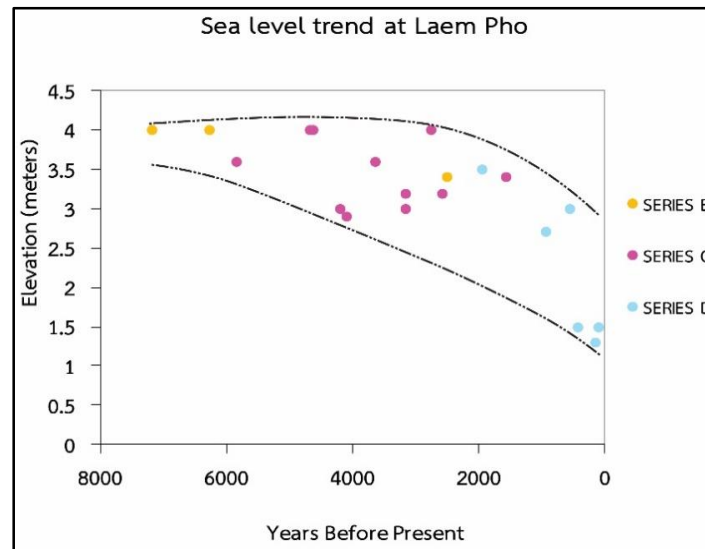


Figure 5.4 Sea-level envelop at Laem Pho study area from the data only in series B, C, and D (series A is lack of topographic profile data and series E is recent beach).

5.7 Model of coastal geomorphological evolution

The results of geomorphological survey, sediments analysis, and age determination were evaluated and summarized to construct the model of coastal evolution for understanding paleo-environmental change of Laem Pho study area. In addition, fossil interpretation is also applied as one of additional parameters for understanding of wave action to this area.

During the Late Pleistocene, a glaciation period, there was a drastic effect in sea-level drop worldwide. Also as Southeast Asia, sea-level dropped more than 50 meters in the Gulf of Thailand and for the Sunda shelf, it presented as a continental (Bisward, 1973). Until the end of the Late Pleistocene, the climate turned to warm and humid leading to sea-level rapidly rose worldwide due to the melting of ice mass. The rising of sea-level caused of the marine transgression in the coastal plain of Thailand. In Surat Thani area, there is an evidence of marine transgression approximately 35 kilometers from present shoreline at Khian Sa town where series of beach ridges can

be used to indicate paleo-shoreline of the area. The results of C-14 dating the period of sea-level arriving was at approximately 8,000 years BP (Chaimanee, 2001).

During Early Holocene, there was a rapid sea-level rise which might cause some parts of transgression sequence eroded. At 5,500 year BP, the marine transgression was reached the peak at approximately 5 meters, after that the paleo-shoreline presented between Pre-Holocene outcrop at approximately 1 to -2 meters at mean sea-level. The inundation of marine transgression covered the area of Chaiya, Thachang, Phunphin and Surat Thani city areas (Chaimanee, 2001).

After Middle Holocene period, the marine regression was started and caused the seaward prograding of sediments along the coast. The coastal plain of Surat Thani area developed at approximately 5,000 years BP through the forming of tidal flat and beach ridge along the Surat Thani and the Chaiya coasts. One large canal in the middle part of the area suggested that the coastal plain rapidly prograded by the supply of abundant terrestrial sediments during marine regression. The decreasing of sediments supplied to the sea started at approximately 1,000 years ago and left an effect to the fluvial dominant delta transforming to tide dominant delta. It is indicated by the forming of mud flat at Surat Thani coast and beach barrier at Chaiya coasts since that time. It is possible that they were developed in the still-stand phase (Chaimanee, 2001).

Laem Pho study area is a part of Chaiya coast which has a dominant landform of beach ridge plains and sand spit. From the studied of sediment facies by Chaimanee (2001), Chaiya coast (northwestern rim of Surat Thani basin) were formed under an influence of the last Quaternary marine transgression and regression phases as a represent in vertical sequence of coastal and shelf facies units including Beach Ridges Sand facies, Shallow Marine sand facies, Shallow Marine Clay facies, Lagoonal Clay facies, and Tidal Flat Sand facies.

In term of the orientation of beach ridge sets in the study area, sea-level changes did not seem to indicate beach-ridge growth, but likely represent orientation and elevation of beach-ridge sets in a beach ridge plain. Basically, bench ridges are progradational landforms occurring in the foreshore and considered the product of wave and wind deposition which present at the upper limit of wave run up. A different in orientations and shape, interruption, truncation, erosion of beach ridges and deposition of younger beach ridges may be under influence of climate, and sea-level or sediment supply fluctuations. Therefore, beach ridges are the evidence which can use to understand the reconstruction of sea-level, climate, and sediment record (Taylor and Stone, 1996).

The orientations of beach ridges of Laem Pho study area (Figure 5.5) indicate southward direction of paleo-longshore currents, but still owns the difference in the tail of orientation which changed the direction into southwestward direction (inland area). In present, sediment transportation in this area which is a part of the Gulf of Thailand mostly under influence of northeast monsoon (NE monsoon) during November to February (Figure 5.7) which transport abundant of sediments to deposit along the shoreline. In addition, the dominance of sand spit in the southern part of study area which prograding in westward at the recent shoreline can be well described itself of the direction of wind and wave current in this area. However, the orientation in the tail of ridge or spit is often with a recurved end (in this area recurved in southwestward), due to the dominant current slows and weakens to produce an extended finger of depositional materials (Department of Marine and Coastal Resource, 2014).

From the interpretation of the orientation, it indicates the sources of sediments deposition in this area mostly from north to south which may come from far away source in the upper part of study area by the shoreline current. In addition, the sediments may come from the barrier beach in front of the Chaiya coast. Especially, sand spit may under influence of Phum Riang canal which carry an abundant of

sediments in to the sea, then, wave current carry sediments to supply to form the spit together with the longshore current. Moreover, from the results of sorting in grain size analysis which series of beach ridges A and B are in the poorly sorted indicates that the energy of source may be strong in the short-time period which can be an evidence of strong waves and current and for series C to E are in the moderately sorted indicates that the energy of source may be in moderately calm which wave current is rather moderate waves and currents. The outer beach ridge series are better sorted than inner ridge. It can be interpreted that waves and currents are more stable may be due to the influence of northeast monsoon current is weaker.

Trend of geomorphological evolution at Laem Pho study area prograde from west to east. However, model of coastal geomorphological evolution (Figure 5.6) can clearly describe the evolution as divided into 3 phases (6 units) upon the period of deposition and orientation. Phase 1 is between 7,500 – 6,000 year BP, consists of unit 1A and 2A (green color). Unit 1A locates continuing from alluvial plain which locate in innermost part of the study area. Unit 2A might be paleo-barrier island parallel to shoreline then beach ridge in phase 2 which started forming by depositing along barrier island as beach ridge plain between 6,000 – 2,000 year BP (pink color). Unit 1B is composed a short period of shoreline retreat in the south and 2B deposited with high progradation in eastward. Phase 3 is between 2,000 years BP to present (orange color) consisting of unit 1C and 2C which has highly deposit and prograding into southwestward due to wave current. Rate of sand spit progradation in unit 2C can be categorized into 2 phases, consisting of phase 1 (from 440 to 150 years BP) which has a rate of progradation at 2.22 meters/year. Phase 2 (from 150 to 110 years BP) has a rate of progradation at 12 meters/year. However, rate of progradation at phase 2 is high possible influenced from storm or intense monsoon during 150 to 110 years BP.

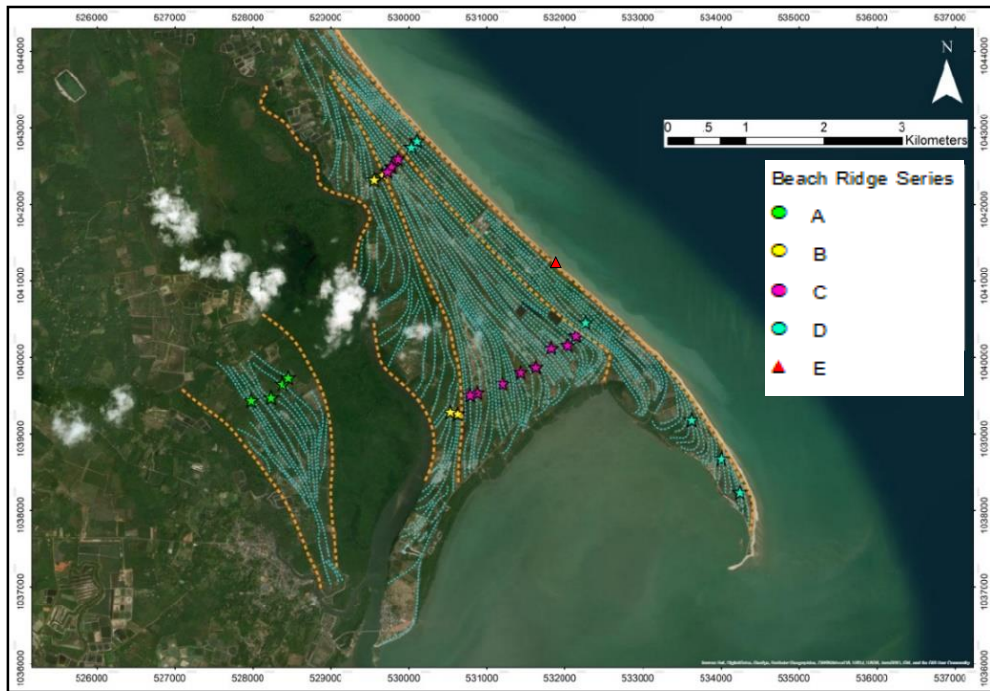


Figure 5.5 Geomorphological of study area from satellite image with the dash lines of beach ridges orientations in each of series.

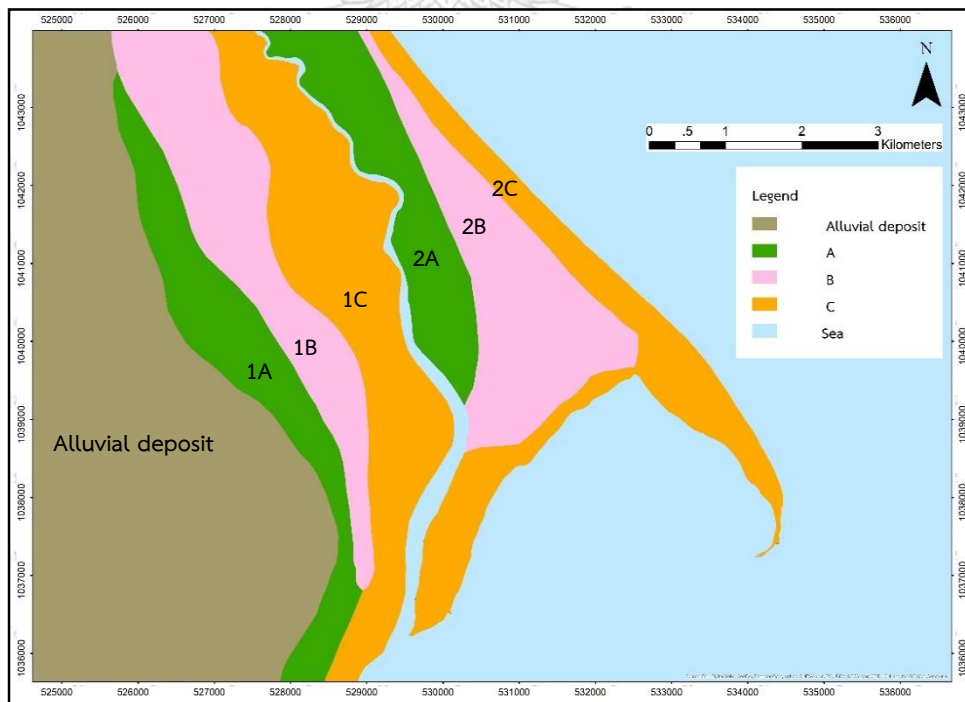


Figure 5.6 Model of coastal geomorphological evolution of Laem Pho study area.

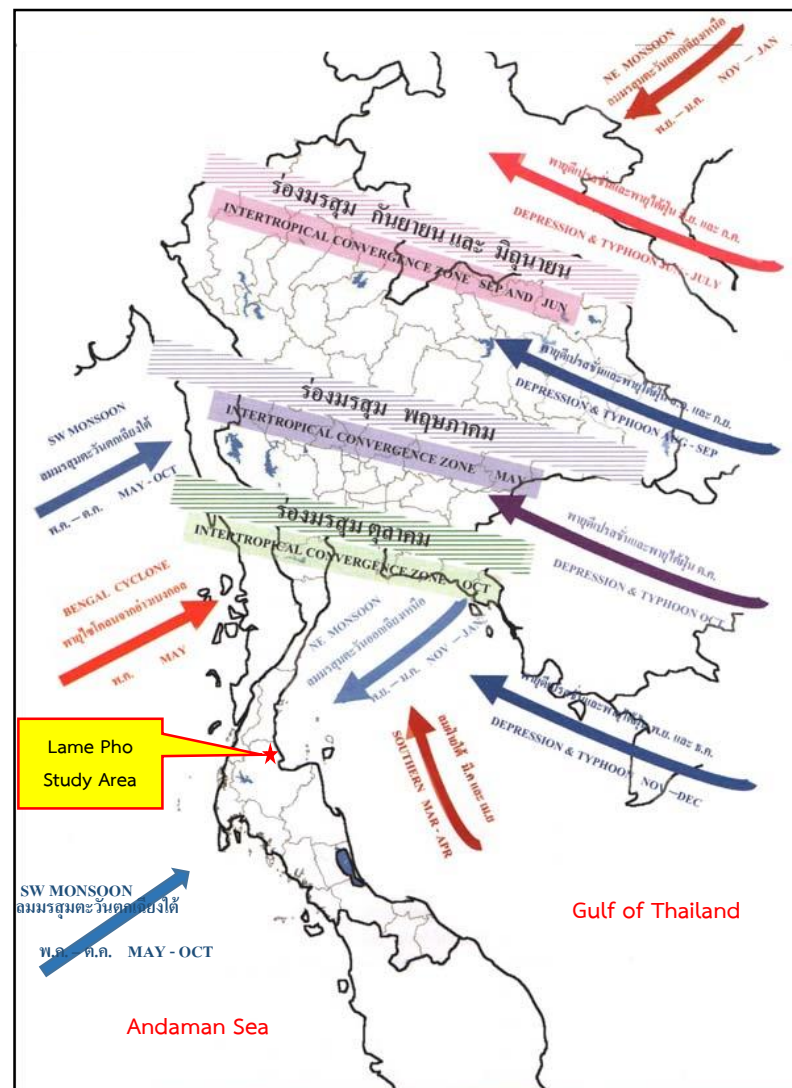


Figure 5.7 Monsoon direction of Thailand

(Source: <http://tumsikwae.blogspot.com/2016/05/journey-of-wind-story.html>)

5.8 Sea-level change and vulnerability of the coastal zone

Study of sea-level curves at Laem Pho area illustrated that the sea-level has trended to gradually fall about 2-4 meters in mid-Holocene period as well as Southeast Asia. However, the fluctuation of sea-level in regional scale can occur in the future that it always influences to environmental changes, especially shoreline and estuary area. At the present day, the shoreline area is occupied for habitation and cultivation such as beach ridge and sand spit. Moreover, some parts remain unchanged due to the conservation of mangrove. The growth of mangrove forests suggests the change in

space that can be managed with the balance to shrimp pond. Therefore, understanding in sea-level change is necessary for this area.

5.8.1 Mangrove as an indicator of sea-level changes

To understand the paleo-environment of mangrove at Laem Pho, the growth of mangrove forests should be explained. Generally, the rates of accumulation of sediments have an influence on the growth of mangrove forests. Mangrove with high productivity could adapt to the rising of sea-level of 5 millimeters/year and move to landward (Miyaki et al., 1995). Moreover, Fujimoto et al. (1999) suggested that mangrove sediments are the indicator for paleo-shoreline interpretation by pollen analysis (Ellison, 1989), mangrove peat (Khan et al., 2017), as well as stratigraphic records (Ellison and Stoddart, 1991). The growth of mangrove which apparently cover the most of shoreline in many coasts may affect from the erosion of shoreline while sea-level rises or wave is intense. Moreover, the lack of sediment supply and longshore current transport took the erosion from sea-level rise gets worse (Mimura and Yokoki, 2008). Pollen analysis at the Southwestern coast of Thailand indicated that the mangrove forests expanded seaward when sea-level fall, in contrast, they retreated landward when sea-level rise (Fujimoto et al., 1999). Thus, mangrove habitat dynamics are related to the sea-level changes in the Holocene that it proposes the important prediction based on the influence of an anticipated sea-level rise. Mangrove in this area is limited its boundary in Phum Rieng canal in the middle part and at the canal mouth. This mangrove zone can be used to bound the shoreline as well.

5.8.2 Vulnerability assessment in study area from sea-level changes

To assess the impact from sea-level changes at Laem Pho, the prediction in sea-level rise to the area is important. Most of residence and cultivated area are nearby shoreline that may be directly affected from the rising of sea-level. At the study area, this area is occupied by shrimp ponds and 6 villages following Ban Phum Rieng, Ban Laem Pho, Ban Laem Sai, Ban Laem Thong, Ban Nuea Nam, and Ban Takrop.

The distal part of sand spit settled by Ban Laem Sai and Ban Laem Pho is located in low elevation at 1-2 meters from mean sea-level that it is different from Ban Phum Rieng and Ban Takrop located on the land closed to the channel. Therefore, the villages closed to distal sand spit are vulnerable from sea-level rise, especially the

shrimp ponds and oysters. Figure 5.8 illustrates the sea level rises scenario up to 3-4 meters that it influences to distal part of sand spit and tidal flat or mangrove forests. Most residences, however, are located on beach ridge of sand spit or paleo-shoreline. They are safe from sea-level change in 1-4 meters. In contrast, if the sea level may rise up to 5 meters, these villages can be at risk. Remarkably, the area along the channel and stream is not inundated because it is protected by banks which are higher.

The vulnerable map (figure 5.8) is studied in regional scale. Therefore, the more precise topographic survey and land use will be recommended for modeling the accurate vulnerable map. Finally, these data are integrated to predict the risk area, and then, the planning of land-use, evacuation, and the preventing approach will be guided in the future.



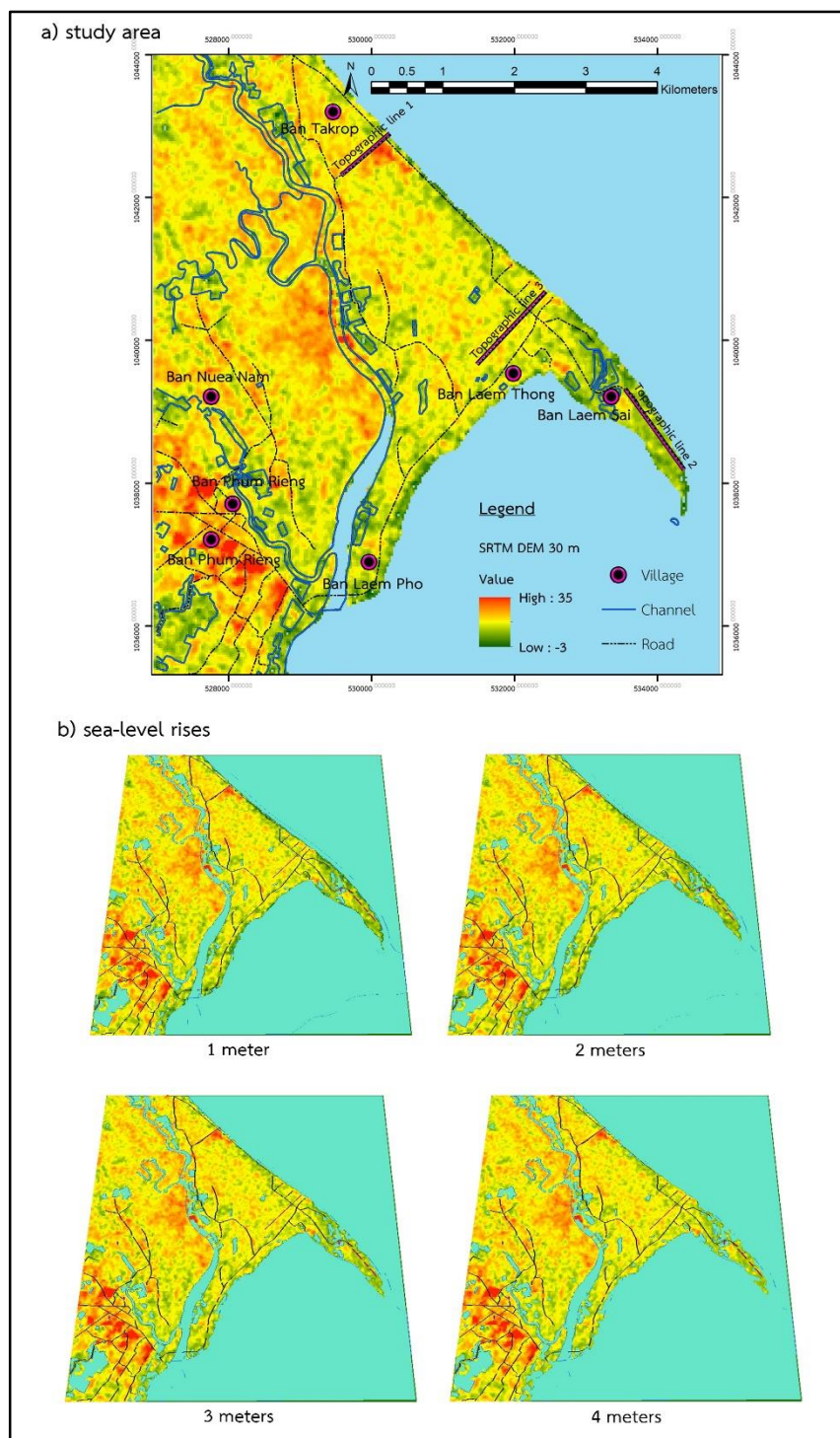


Figure 5.8 Map of study area with SRTM-DEM 30 m. following: a) study area showing location of villages and channels and b) sea-level rises showing flood area at 1-4 meters from mean sea level.

CHAPTER 6

CONCLUSION

This study is aimed to investigate coastal geomorphology and sedimentology of beach ridge plain from the area where its formation might be related to the history of the Holocene sea level changes at Laem Pho, Amphoe Chaiya, Changwat Surat Thani. According to satellite image interpretation, Laem Pho area has dominant landforms of beach ridge plains and active sand spit at southern part. Trend of their formations show seaward and eastward progradation as a result from longshore current flowing from the north to the south. The orientations of each beach ridge set in this area shows individual characteristic that can be classified into 5 series (A, B, C, D, and E). Series A locates at the most inner part, then following by series B, C, D which separate from series A by Phum Rieng canal. Series B, C, and D can be grouped as a large beach ridge plain locating at the central part of study area, while series E represents recent beach at the present shoreline. The innermost beach ridge (series A) can be used to indicate that the paleo-shoreline was at approximately 4.5 kilometers far inland from the present shoreline.

The formation of beach ridge plains here showed the relationship with sea-level fluctuation during the Holocene. Topographic survey of ridges reveals former level of sea level in particular wave height. The orientation of ridges, elevation from present mean sea level and morphology of beach ridges indicate possible source of sediment supply from northern part by southward longshore current. In conclusion, the evidences of sea level change in the study area include the present geomorphological landforms which were divided into 3 units consisting of old sandy beach, young sandy beach, and old lagoon.

In the study area, major sediments in beach ridge are composed of quartz and minor of feldspar while the deposition in swale is composed of sand with clay and

broken shell fragments. Roundness and sphericity of beach sediment is sub-angular indicating local source in which abundant sediments were transported from northern part of study area along Phum Rieng cana. Bioclasts are dominant only in sand spit and nearshore area. While the presence of clay-size materials in swale (old lagoon) depositional environment indicates low energy area and calm environment. Swale between spit ridges in the southern part of study area contains dominant black layer of organic matter rich sequence.

Statistic parameters (mean, sorting, skewness, and kurtosis) derived from grain size analysis were used to qualitatively describe the characteristics of beach ridges. Most of the sediments in Laem Pho study area exhibited the mean grain size of coarse to medium sand which indicates the moderately high energy condition of depositional environment. Sorting value of sediments is poorly to moderately sorted which indicates the low to fairly high energy current. About 80 percent of sediment samples at the study area was characterized by fine-skewed which indicate calm to storm environment and the rest 20 percent of sediment samples in this area showed the coarse-skewed value which indicates a high energy deposition environment. Kurtosis value of this study area is mostly extremely leptokurtic which indicates that the central portions are better sorted at the tails.

Fossils and microfossils were found at LP 3-3-1 which located in nearshore confirmed shallow marine environment in intertidal zone (or littoral zone) and warm water condition. They include 10 species of foraminiferas, 5 species of ostracods, 1 species of bivalvia and scaphopoda. Foraminiferas includes species of *Ammonia beccarii*, *Ammonia ketienziensis*, *Ammonia pauciloculata*, *Elphidium advenum*, *Elphidium hispidulum*, *Elphidium limpidum*, *Elphidium macellum*, *Miliolina (Quinqueloculina) bogdanowiczii*, *Nodosaria intermittens*, and *Asterorotalia pullchella* (Synonym: *Asterorotalia trispinosa*). Ostracoda includes species of *Cyprideis ruggierii*, *Keijella reticulate*, *Keijella sp.*, *Callistocythere canaliculata*, and *Palmoconcha guttata*. Bivalvia by the presents of *Carditella pallida*. Scaphopoda includes *Antalis*

entalis. The broken shell fragments showed that their living habitats are not only under shallow marine environment with the influence from tidal and wave processes. However, there are no evidence of any fossils found in sediments which deposited for thousand years ago. It may be due to the CaCO_3 in fossil's structure was dissolved by the solution from the sea.

Optically Stimulated Luminescence (OSL) ages of sandy beach ridge in the study area can be summarized in relation to their formation history as follows: Inner part of beach ridge set started its formation in the early Holocene to mid Holocene ($7,170 \pm 460$ years BP). Three profiles of topography survey indicate the continuation of beach progradation in eastward direction. The maximum elevation of beach ridge plain is 4 m above present mean sea level and the elevation relief of beach ridge and swale on beach ridge plain is less than 1 meter.

Model of coastal geomorphological evolution can be described into 3 phases (6 units) following the period of deposition and orientation. Phase 1 (unit 1A and 2A) occurred between 7,500 – 6,000 years BP including unit 1A located in innermost part of the study area, continuing from alluvial plain and unit 2A that might be paleo-barrier island parallel to shoreline. Beach ridge in phase 2 (unit 1B and 2B) started deposition along barrier island as beach ridge plain between 6,000 – 2,000 years BP. Unit 1B is composed of a short period of shoreline retreat in the south and unit 2B deposited with high progradation in eastward direction. Phase 3 (unit 1C and 2C) formed between 2,000 years BP with the deposition and prograding into southwestward direction.

REFERENCES

- Abuodha, J. O. Z. 2003. Grain size distribution and composition of modern dune and beach sediments, Malindi Bay coast, Kenya. Journal of African Earth Sciences, 36: 41-54.
- Aitken, M. J. 1985. Thermoluminescence dating. London: Academic Press
- Aitken, M. J. 1998. An Introduction to Optical Dating. Oxford, UK: Oxford Science Publications
- Amaral, E. J., and Prayor, W. A. 1977. Depositional environment of the St. Peter sandstone deduced by textural analysis. J.Sediment.Petrol., 47: 32-52.
- Angusamy, N. G., and Rajamanikam, V. 2006. Depositional environment of sediments along the southern coast of Tamil Nadu, India. Oceanologia, 48(1): 87-102.
- Athersuch, J., Horne, D. J., and J.E., W. 1989. Marine and brackish water ostracods. In D. M. a. B. Kermack, R.S.K. (Ed.), Synopses of the British Fauna (New Series) (Vol. 43, pp. 345)
- Bateman, M. D., Boulter, C. H., Carr, A. S., Frederick, C. D., Peter, D., and Wilder, M. 2006. Preserving the paleoenvironmental record in drylands: bioturbation and its significance for luminescence derived chronologies. Sedimentary Geology, 195(2007): 5-19.
- Bates, R. L., and Jackson, J. A. 1980. Glossary of Geology (2 ed.). Virginia: American Geological Institute
- Bernard, F. R. 1983. Catalogue of the Living Bivalvia of the Eastern Pacific Ocean: Bering Strait to Cape Horn. Canadian Special Publication of Fisheries and Aquatic Science 61: 34.
- Bird, E. 2008. Coastal Geomorphology (2 ed.). United Kingdom: John Wiley&Sons
- Bisward, B. 1973. Quaternary change in sea level in South China sea. . Geol.Socl. Malaysia 6: 224-256.
- Bonaduce, G., Ciampo, G., and Masoli, M. 1975. Distribution of Ostracoda in the Adriatic Sea. Pubblicazioni della Stazione zoologica di Napoli 40: 1-305.

- Botter- Jensen, L. , McKeever, S. , and Wintle, A. 2003. Optically Stimulated Luminescence Dosimetry. Amsterdam: Elsevier
- British Geological Survey. Sea Level and Coastal Changes. 2016. Available from <http://www.bgs.ac.uk/discoveringGeology/climateChange/general/coastal.html?src=topNav>
- Chaimanee, N. 2001. COASTAL EVOLUTION OF THE GREATER SURAT THANI CITY AREA, SOUTHERN THAILAND. Paper presented at the Academic symposium, Geology division, Department of Mineral Resource.
- Chaimanee, N. Quaternary Geology and coastal Evolution of the Greater Surat Thani City Area, Southern Thailand. Paper presented at the The Symposium on Geology of Thailand, Bangkok, Thailand. (2002, 26-31 August 2002)
- Chekhovskaya, M. P., Stepanova, A. Y., Khusid, T. A., Matul, A. S., and Rakowski, A. Z. 2014. Late Pleistocene–Holocene Ostracod Assemblages of the Northern Caspian Sea Shelf. Oceanology, 54(2): 212-221.
- Choowong, M. 2002. Isostatic models and Holocene relative changes in sea level from the coastal lowland area in the Gulf of Thailand Journal of Scientific Research, Chulalongkorn University, 27(1): 83-92.
- Choowong, M., Ugai, H., Charoentitirat, T., Charusiri, P., Daorerk, V., Songmuang, R., and Ladachart, R. 2004. Holocene Biostratigraphical Records in Coastal Deposits from Sam Roi Yod National Park, Prachuap Khiri Khan, Western Thailand. The Natural History Journal of Chulalongkorn University 4(2): 1-18.
- DeCarlo, L. 1997. On the Meaning and Use of Kurtosis. Psychological Methods, 2(3): 292-307.
- Department of Marine and Coastal Resource. 2014. Littoral cell categories in Thailand for coastal management. In Coastal situation and the resolution of coastal erosion from the past to present (pp. 75-76). Bangkok: Visuddhi Consultants Company Limited
- Duane, D. B. 1964. Significance of skewness in recent sediments, western Pamlico Sound, North Carolina. Journal of Sedimentary Petrology 34(4): 864-874.

- El Baz, S. M., and Furjany, A. A. 2018. Middle Miocene benthic foraminifera from the Al Khums area, northwestern Libya. Journal of African Earth Sciences 138: 112-123.
- Ellison, J. C. 1989. Pollen Analysis of Mangrove Sediments As A Sea-Level Indicator: Assessment from Tongtapu, Tonga. Paleogeography, Paleoclimatology, Palaeoecology, 74: 327-341.
- Ellison, J. C., and Stoddart, D. R. 1991. Mangrove Ecosystem Collapse During Predicted Sea-Level Rise: Holocene Analogues and Implications. Journal of Coastal Research, 7(1): 151-165.
- Fenoglio-Marc, L., Schöne, T., Illigner, J., Becker, M., Manurung, P., and Khafid. 2012. Sea Level Change and Vertical Motion from Satellite Altimetry, Tide Gauges and GPS in the Indonesian Region. Marine Geodesy 35(S1): 137-150.
- Folk, R. L. 1966. A review of grain-size parameters. Sedimentology, 6: 73-93.
- Folk, R. L., and Ward, C. W. 1957. Brazos river bar: a study in the significance of grain size parameters. Journal of Sedimentary Petrology, 27(1): 3-26.
- Friedman, G. M. 1961. Distinction between dune, beach, and river sands from the textural characteristics. Journal of Sedimentary Petrology, 31(4): 514-529.
- Friedman, G. M., and Sanders, J. E. 1978. Principles of Sedimentology. New York: John Wiley & Sons
- Friedman, G. M., Sanders, J. E., and Kopaska-Merkel, D. C. 1992. Principles of Sedimentary Deposits: Stratigraphy and Sedimentology. New York: Macmillan
- Fujimoto, K., Miyaki, T., Murofushi, Y., Mochida, Y., Umitsu, M., Adachi, H., and Promojanee, P. 1999. Mangrove habitat dynamics and Holocene sea-level changes in the Southwestern coast of Thailand. Tropics, 8(3): 239-255.
- García-Gaines, R. A., and Frankenstein, S. 2015. USCS and the USDA Soil Classification System. Retrieved from
- Geyh, M. A., Kudhass, H. R., and Streif, H. 1979. Sea level changes in the late Pleistocene and Holocene in the Strait of Malacca. Nature, 278(5703): 441-443.
- Ha, T. M., and Tsukagoshi, A. 2015. First records of interstitial leptocytherids (Crustacea, Ostracoda) : two new species and a redescription of Callistocythere

- ventricostata Ruan & Hao, 1988 collected from the Okinawa Islands, southern Japan. Zootaxa, 4006(1): 83-102.
- Hamouda, A., El-Gharabawy, S., Awad, M., Shata, M., and Badawi, A. 2014. Characteristic properties of seabed fluvial-marine sediments in front of Damietta promontory, Nile Delta, Egypt. Egyptian Journal of Aquatic Research 40: 373-383.
- Hanebuth, T., Stattegger, K., and Grootes, P.M. . 2000. Rapid flooding of the Sunda shelf: A late-glacial sea-level record. Science, 288(5468): 1033–1035.
- Hayward, P. J., Wingham, G. D., and Yonow, N. 1995. Molluscs (Phylum Mollusca). In P. J. a. R. Hayward, J.S. (Ed.), Handbook of the Marine Fauna of North-West Europe (pp. 490). New York: Oxford University Press
- Hesp, P. 2005. Beach ridges, foredunes or transgressive dunefields? Definitions and an examination of the Torres to Tramandaí barrier system, Southern Brazil. An. Acad. Bras. Ciênc, 77(3): 493-508.
- Hesp, P. A., Hung, C. C., Hilton, M., Ming, C. L., and Turner, I. M. 1998. A First Tentative Holocene SeaLevel Curve for Singapore. Journal of Coastal Research, 14(1): 308-314.
- Horton, B. P., Gibbard, P. L., Milne, G. M., Morley, R. J., and Purintavaragul, C. 2005. Holocene sea levels and palaeoenvironments, Malay-Thai Peninsula, Southeast Asia. The Holocene, 15(8): 1199–1213.
- Jingxing, L., and Luping, D. 2012. Quaternary marine transgressions in eastern China. Journal of Palaeogeography, 1(2): 105-125.
- Johnson, D. W. 1919. Shore Processes and Shoreline Development. New York: John Wiley & Sons
- Khan, N. S. et al. 2017. Driver of Holocene sea-level change in the Caribbean. Quaternary Science Reviews, 155: 13-36.
- Khawdee, P. 2008. Geophysical Study of the Geothermal Resources in Kanchanadit and Ban Na Doem District, Surat Thani Province. (Master), Prince of Songkla University,
- Krumbein, W. C., and Pettijohn, F. J. 1938. Manual of sedimentary petrography. New York: D. Appleton- Century

- Lambeck, K., and Chappell, J. 2001. Sea level change through the last glacial cycle. Science, 292: 679-686.
- Lason, R., Morang, A., and Gorman, L. 1997. Monitoring the Coastal Environment; Part II: Sediment Sampling and Geotechnical Methods. Journal of Coastal Research, 13(2): 308-330.
- Levin, H. L. 2006. The Sedimentary Archives. In The Earth Through Time (8 ed.). United State of America: John Wiley & Sons, Inc
- Li, D. W., Li, Y. K., Ma, B. Q., Dong, G. C., Wang, L. Q., and Zhao, J. X. 2009. Lake-level fluctuations since the last Glaciation in Selin Co (lake) , Central Tibet, investigated using optically stimulated luminescence dating of beach ridges. Environmental Research Letters, 4: 1-10.
- Lian, O. B. 2007. Luminescence Dating. In S. A. Elias (Ed.), Encyclopedia of Quaternary Science (Second ed.): Elsevier
- Ligios, S., and Gliozzi, E. 2012. The genus *Cyprideis* Jones, 1857 (Crustacea, Ostracoda) in the Neogene of Italy: A geometric morphometric approach. Revue de Micropaléontologie 55(4): 171-207.
- Liu, X. J., Lai, Z. P., Zeng, F. M., Madsen, D. B., and E, C. Y. 2013. Holocene lake level variations on the Qinghai-Tibetan Plateau. International Journal of Earth Sciences 102(7): 2007-2016.
- Łuczowska, E. 1974. Miliolidae (Foraminiferida) from the Miocene of Poland Part II. Biostratigraphy, palaeoecology and systematics. Acta Palaeontologica Polonica 19(1): 3-176.
- Luu, Q. H., Tkalich, P., and Tay, T. W. 2005. Sea level trend and variability around Peninsular Malaysia. Ocean Science 11: 617-628.
- Mallory, J. A. 1959. Nodosaria Sand Environments in Eastern Counties of Texas Gulf Coast. American Association of Petroleum Geologists Bulletins, 43(10): 2514.
- Martins, L. R. 1965. Significance of skewness and kurtosis in environmental interpretation. Journal of Sedimentary Petrology, 35(3): 768-770.
- Martins, L. R., and Barboza, E. G. 2005. Sand-Gravel Marine Deposit and Grain Size Properties. Gravel, 33: 59-70.

- Mason, C. C., and Folk, R. L. 1958. Differentiation of beach, dune, and aeolian flat environments by size analysis, Mustang Island, Texas. Journal of Sedimentary Petrology 28: 211-226.
- Mazzini, I. et al. 2013. Palaeoenvironmental and chronological constraints on the Tuğlu Formation (Çankırı Basin, Central Anatolia, Turkey). Turkish Journal of Earth Sciences, 22: 747-777.
- McLaren, P., and Bowles, D. 1985. The effect of sediment transport on grain-size distributions. Journal of Sedimentary Petrology 55(4): 457-470.
- Mimura, N., and Yokoki, H. 2008. Sea-Level Change and Vulnerability of the Coastal Zone in Change in the Human-Monsoon System of East Asia in the Context of Global Change. In C. Fu, J. R. Freney, & J. W. B. Steward (Eds.), Monsoon Asia integrate Regional Study on Global Change (Vol. 1). Singapore: World Scientific Publishing Co. Pet. Ltd.
- Miyaki, T., Kiluchi, T., and Fujimoto, K. 1995. Late Holocene sea-level changes and mangrove peat accumulation/habitat dynamics in the western Pacific area. In T. Kikuchi (Ed.), Rapid sea-level rise and mangrove habitat dynamics. Gifu University: Institute of Basin Ecosystems studies
- Mohammed Nishath, N., S.M., H., Neelavnnan, K., Thejasino, S., Saalim, S., and Rajkumar, A. 2017. Ostracod biodiversity from shelf to slope oceanic conditions, off centralBay of Bengal, India. Palaeogeography, Palaeoclimatology, Palaeoecology 483: 70-82.
- Murali Krishana, K. N., Reddy, K. S. N., Ravi Sekhar, c., Ganapathi Rao, P., and Bangaku Naidu, K. 2017. Textural studies on red sediments of Bhimunipatnam, Andhra Pradesh, east coast of India. Journal of the Geological Society of India, 90(1): 111-117.
- Muzuka, A. N. N., and W, S. Y. 2000. Grain size distribution along the Msasani Beach, north of Dar es Salaam Harbour. Journal of African Earth Sciences 30(2): 417-426.
- Nicholls, R. J. et al. 2007. Coastal systems and low-lying areas. In M. L. Parry, Canziani, O.F., Palutikof, J.P., van der Linden, P.J. and Hanson, C.E (Ed.), Climate Change

2007: Impacts, Adaptation and Vulnerability. Contribution of Working Group II to the Fourth

Assessment Report of the Intergovernmental Panel on Climate Change (pp. 315-356).

Cambridge: Cambridge University Press

Nimnate, P., Chutakositkanon, V., Choowong, M., Pailoplee, S., and Phantuwoongraj, S.

2015. Evidence of Holocene sea level regression from Chumphon coast of the Gulf of Thailand. ScienceAsia, 41: 55-63.

Nisha, N. R., and Singh, A. D. 2012. Benthic Foraminiferal Biofacies on the Shelf and Upper Continental Slope off North Kerala (Southwest India). Journal of the Geological Society of India, 80: 783-801.

Otvos, E. G. 2000. Beach ridges-definitions and significance. Geomorphology, 32: 83-108.

Phantuwoongraj, S. 2006. Shoreline change after the 26 December 2004 Tsunami between Leam Prakarang-Kho Lak area, Changwat Pang-nga, Thailand. (Master), Chulalongkorn University,

Phantuwoongraj, S. 2012. Sedimentological Characteristics of Storm-Induced Washover Deposits Along the Coastal Zone of Changwat Prachuap Khiri Khan to Nakorn Si Thammarat, Thailand. (Doctor of Philosophy's), Chulalongkorn University,

Phantuwoongraj, S., Choowong, M., and Silapanth, P. Geological evidence of sea-level change: a preliminary investigation at Panang Tak area, Chumphon province, Thailand. Paper presented at the The 117th Annual Meeting of the Geological Society of Japan, Toyama, Japan. (2010, 18-20 September 2010)

Preusser, F. et al. 2008. Luminescence dating: basics, methods and application. Eiszeitalter und Gegenwart Quaternary Science Journal, 57(1-2): 95-149.

Rabineau, M., Berné, S., Olivet, J. L., Aslanian, D., Guillocheau, F., and Joseph, P. 2006. Paleo sea levels reconsidered from direct observation of paleoshoreline position during Glacial Maxima (for the last 500,000 yr). Earth and Planetary Science Letters, 252: 119-137.

Rajmohan, S., Singarasubramainian, S. R., Suganraj, K., Sathya, A., and Sundararajan, M. 2012. Grain size distribution and depositional environment of coastal sediments

- at Ponnaiyar and Gadilam estuary, east coast of India. International Journal of Recent Scientific Research, 3(11): 919-922.
- Rapp, G. R., and Hill, C. L. 2006. Sediments, Soils, and Environment Interpretations. In Geoarchaeology: The Earth-Science Approach to Archaeological Interpretation. United State of America: Yale University Press
- Rashedi, S. A., and Siad, A. 2016. Grain size analysis and depositional environment for beach sediments along Abu Dhabi coast, United Arab Emirates. International Journal of Scientific & Technology Research, 5(7): 106-115.
- Silapanth, P. 2005. Geoarcheology of Thungsetthi, Tambon Nayang, Amphoe Cha-Am, Changwat Phetchaburi. (Master), Chulalongkorn University,
- Sinsakul, S. 1992. Evidence of quaternary sea level changes in the coastal areas of Thailand: a review. Journal of Southeast Asian Earth Science 7: 23-37.
- Sinsakul, S. 2000. Late Quaternary geology of the Lower Central Plain, Thailand. Journal of Asian Earth Sciences, 18: 415-426.
- Sinsakul, S., Sonsuk, M., and Hasting, P. J. 1985. Holocene sea levels in Thailand: evidence and basis for interpretation. Geol. Soc. Thailand, 8: 1-12.
- Sinsakul, S., Tantiyapirat, S., Chaimanee, N., and Aramprayoon, B. 2002. Academic report of The Changing coastal areas of the Gulf of Thailand (1 ed.). Bangkok: Modern Film Center Company Ltd
- Songmuang, R. 2005. Seasonal Shoreline Changes of the Prachuap Khiri Khan Coast. (Master), Chulalongkorn University,
- Stanley, D. J. 1969. Atlantic Continental Shelf and Slope of the United States - Color of Marine Sediments. Retrieved from Washington:
- Sukanraj, K., Singarasubramainian, S. R., Rajmohan, S., A., S., and Sundararajan, M. 2013. Grain Size Statistical Parameters of Coastal Sediments at Kameswaram, Nagapattinam District, East Coast of Tamilnadu, India. International Journal of Recent Sciencetific Research, 4(2): 102-106.
- Tatong, T., Magane, A., Kunthasup, P., and Chartprasert, S. 2001. Technical Report No.30 of Hydrogeology of the Surat Thani Greater City Area. Retrieved from
- Taylor, M., and Stone, G. W. 1996. Beach ridges: a review. Journal of Coastal Research, 12: 612-621.

- Tjia, H. D. 1987. Change of sea level in the southern South China Sea area during Quaternary times. Retrieved from
- Tjia, H. D., and Fujii, S. 1992. Late Quaternary shorelines in Peninsular Malaysia. In H. D. a. A. Tjia, S.M.S (Ed.), The Coastal Zone of Peninsular Malaysia (pp. 28-41). Bangi, Malaysia: Universiti Kebangsaan Malaysia
- Trisirisatayawong, I., Naeije, M., Simons, W., and Fenoglio-Marc, L. 2011. Sea level change in the Gulf of Thailand from GPS-corrected tide gauge data and multi-satellite altimetry. Global and Planetary Change, 76: 137-151.
- Troga, C., Höfera, D., Frenzelb, P., Camachoc, S., Schneidera, H., and Mäusbacher, R. 2013. A multi-proxy reconstruction and comparison of Holocenepalaeoenvironmental changes in the Alvor and Alcantarilha estuaries (southern Portugal). Revue de micropaléontologie, 56: 131-158.
- United States Department of Agriculture (USDA). 1987. Soil mechanics level 1, Module 3. Retrieved from Washington, DC:
- Valia, H. S., and Cameron, B. 1997. Skewness as a Paleoenvironment Indicator. Journal of Sedimentary Petrology, 47(2): 784-793.
- Whatley, R. C., and Watson, K. "A preliminary account of the distribution of ostracoda in recent reef and reef associated environments in the Pulau Seribu or Thousand Island Group, Java Sea" in Evolutionary Biology of Ostracoda. Paper presented at the The Ninth International Symposium on Ostracoda, Development in Paleontology and Stratigraphy, Japan. (1985)
- Wigley, R. L. 1961. Bottom sediments of Georges Bank. Journal of Sedimentary Petrology, 31: 165-188.
- Wilkinson, I. P. 2007. Foraminifera and Ostracoda in the St Andrew's Bay Member (Forth Formation; Holocene), offshore Montrose. Retrieved from
- Williams, H., Choowong, M., Phantuwongraj, S., Surakietchai, P., Thongkhao, T., Kongsan, S., and Simon, E. 2016. Geologic records of Holocene typhoon strikes on the Gulf of Thailand coast. Marine geology 372: 66-78.
- Williams, M., Dunkerley, D., Deckker, P. D., Kershaw, P., and Chappell, J. 1998. Quaternary Environments (2 ed.). New York: Arnold

Wisconsin Department of Transportation. 2017. Wisconsin Soil Development and Distribution – Soil Classification Systems. In Geotechnical Manual (pp. 1-3)

Woodroffe, S. A., and Horton, B. P. 2005. Holocene sea-level changes in Indo-Pacific. Journal of Asian Earth Sciences, 25(1): 29-43.



APPENDIX



จุฬาลงกรณ์มหาวิทยาลัย
CHULALONGKORN UNIVERSITY

VITA

Miss Sinenard Polwichai was born on April, 19th 1991 in Surat Thani, Thailand. She finished her high school from Suratthani school and attended to the Geoscience Program, Mahidol University. She got Bachelor's Degree of Science in 2013 with the research study in Lithostratigraphy and faunal assemblages at Ban Tha Kra Dan area, Si Sawat District, Kanchanaburi Province. After that she interested in Environmental science, so she decided to get a master degree at Interdisciplinary Program of Environmental Science, Graduate School, Chulalongkorn University in 2015. However, she would like to applied her geology with environmental science, so she decided to do a research with Department of Geology, Faculty of Science, Chulalongkorn University in the topic of Paleo Sea-Level Change of Laem Pho, Amphoe Chaiya, Changwat Surat Thani. Besides, her research got financial supports from the 90th Anniversary of Chulalongkorn University Fund (Ratchadapiseksomphot Endowment Fund) and the Thailand Research Fund (MRG5780008).

